1992-06

A study of Nusselt number distributions in a curved channel.

Schallert, Anthony R.

Monterey, California. Naval Postgraduate School

Unclassified
SECURITY CLASSIFICATION OF THIS PAGE

REPORT DOCUMENTATION PAGE

Form Approved
OMB No 0704-0188

1a REPORT SECURITY CLASSIFICATION
Unclassified

1b RESTRICTIVE MARKINGS

2a SECURITY CLASSIFICATION AUTHORITY

2b DECLASSIFICATION / DOWNGRADING SCHEDULE

3 DISTRIBUTION / AVAILABILITY OF REPORT
Approved for public realease: Distribution is unlimited

4 PERFORMING ORGANIZATION REPORT NUMBER(S)

5 MONITORING ORGANIZATION REPORT NUMBER(S)

6a NAME OF PERFORMING ORGANIZATION
Naval Postgraduate School

6b OFFICE SYMBOL (If applicable)
ME

7a NAME OF MONITORING ORGANIZATION
Naval Postgraduate School

6c ADDRESS (City, State, and ZIP Code)
Monterey, CA 93943-5000

7b ADDRESS (City, State, and ZIP Code)
Monterey, CA 93943-5000

8a NAME OF FUNDING / SPONSORING ORGANIZATION

8b OFFICE SYMBOL (If applicable)

9 PROCUREMENT INSTRUMENT IDENTIFICATION NUMBER
MIPR-No. C-800019-F

8c ADDRESS (City, State, and ZIP Code)
U.S. Army Aviation Res. & Tech Activity
AVSCOM
NASA-Lewis Res. Center Cleveland Ohio

10 SOURCE OF FUNDING NUMBERS

PROGRAM ELEMENT NO	PROJECT NO	TASK NO	WORK UNIT ACCESSION NO

11 TITLE (Include Security Classification)
A Study of Nusselt Number Distributions In A Curved Channel

12 PERSONAL AUTHOR(S)
Anthony R. Schallert

13a TYPE OF REPORT	13b TIME COVERED	14 DATE OF REPORT (Year, Month, Day)	15 PAGE COUNT
Master's Thesis	FROM _____ TO _____	June 1992	155

16 SUPPLEMENTARY NOTATION
The views expressed are those of the autor and do not reflect the official policy or position of the Department of Defense or the U.S. Government

17 COSATI CODES		
FIELD	GROUP	SUB-GROUP

18 SUBJECT TERMS (Continue on reverse if necessary and identify by block number)
curved heating channel, heat transfer coefficients, Nusselt numbers, Dean vortices, centrifugal instabilities

19 ABSTRACT (Continue on reverse if necessary and identify by block number)

The effects of curvature and the resulting centrifugal instabilities on local heat transfer distributions are studied in a curved channel with a rectangular cross section and a 40 to 1 aspect ratio at Dean numbers from 100 to 278. The experimental conditions are identified for which forced convection with weak buoyancy, and forced convection with strong buoyancy are present. With weak buoyancy effects present ($Re^2/Gr > 50 \times 10^{-6}$) a new method is developed to deduce forced convection Nusselt numbers without the influence of natural convection. Resulting data provide information on the influence of Dean vortex pair and their secondary flows. For a Dean number of 275, Nusselt numbers measured on the concave surface are higher than the ones on the convex surface through out the curved portion, for X/D from 130 to 230, where X is the distance from the start of the heated section, and D is the width of the channel. For Dean numbers from 175 to 250, Nusselt numbers are higher on the concave surface than on the convex surface for X/D from 160 to 230, such that differences increase with Dean number.

20 DISTRIBUTION / AVAILABILITY OF ABSTRACT
☒ UNCLASSIFIED/UNLIMITED ☐ SAME AS RPT ☐ DTIC USERS

21 ABSTRACT SECURITY CLASSIFICATION
unclassified

22a NAME OF RESPONSIBLE INDIVIDUAL
Phillip M. Ligrani

22b TELEPHONE (Include Area Code)
(408) 646-3382

22c OFFICE SYMBOL
ME/Li

DD Form 1473, JUN 86 Previous editions are obsolete

S/N 0102-LF-014-6603

SECURITY CLASSIFICATION OF THIS PAGE
Unclassified

Approved for public release; distribution is unlimited

A Study Of Nusselt Number Distributions In A Curved Channel

by

Anthony R. Schallert
Lieutenant, United States Navy
B.S., University of South Carolina, 1983

Submitted in partial fulfillment of the
requirements for the degree of

MASTER OF SCIENCE IN MECHANICAL ENGINEERING

from the

ABSTRACT

The effects of curvature and the resulting centrifugal instabilities on local heat transfer distributions are studied in a curved channel with a rectangular cross section and a 40 to 1 aspect ratio at Dean numbers from 100 to 278. The experimental conditions are identified for which forced convection with weak buoyancy, and forced convection with strong buoyancy are present. With weak buoyancy effects present ($Re^2/Gr > 50 \times 10^{-6}$) a new method is developed to deduce forced convection Nusselt numbers without the influence of natural convection. Resulting data provide information on the influence of Dean vortex pair and their secondary flows. For a Dean number of 275, Nusselt numbers measured on the concave surface are higher than the ones on the convex surface through out the curved portion, for X/D from 130 to 230, where X is the distance from the start of the heated section, and D is the width of the channel. For Dean numbers from 175 to 250, Nusselt numbers are higher on the concave surface than on the convex surface for X/D from 160 to 230, such that differences increase with Dean number.

TABLE OF CONTENTS

LIST OF FIGURES

I. INTRODUCTION

A. DESCRIPTION OF THE PROBLEM

Local and spanwise averaged heat transfer distributions from the surfaces of a curved channel are measured and studied. The aspect ratio of the channel is 40 and δ / r_i = 0.011 in the curved section, which indicates mild curvature. Results are presented for Dean numbers ranging from 52 to 278, which corresponds to a variety of different flow regimes which make up a sequence of transition events. As Dean number increases at one streamwise location, Dean vortex pairs first develope from curved channel Poiseuille flow. Vortex pairs subsequently split and merge, and develope wavy modes. The twisting wavy mode then inspires the initiation of local turbulence regions, which eventually increase in magnitude and spatial extent to ultimately form into a fully turbulent flow.

Some work in this area addresses the development of vortex flows due to centrifugal instabilities and the effects of these secondary flows on transition from laminar to turbulent behavior without considering heat transfer. Ghia and Sokhey [Ref. 1], Komiyama [Ref. 2], and Iacovides et al. [Ref. 3] used different numerical analyses of flow in curved rectangular channels to predict the formation of counter-rotating vortices. Humphrey et al. [Ref. 4] describe velocity measurements from a curved square duct which are in good agreement with a numerical solution. Ligrani and Niver [Ref. 5], and Ligrani et al. [Ref. 6], [Ref. 7], [Ref. 8] present experimental results showing the development of counter-rotating vortex pairs in a curved channel with the same aspect ratio and internal geometry employed in the present study.

Several other studies focus on heat transfer in channels with turbulent flows. Yee et al. [Ref. 9], and Iacovides and Launder [Ref. 10] used different numerical techniques to predict heat transfer characteristics in a variety of duct geometries. Mori et al. [Ref. 11] and Johnson and Launder [Ref. 12] present local heat transfer results from a channel with a 180 degree bend and a square cross section. They describe complex secondary flows which develope from the instabilities from curvature. Additional studies are described by Chang et al. [Ref. 13], who employ a channel with a 180 degree bend and square cross section, and by Brinch and Graham [Ref. 14], who use a curved channel with an aspect ratio of 6. Studies dealing with the effects of heat transfer on turbulent boundary layers developing on curved surfaces include ones described by Gibson et al. [Ref. 15], Simon and Moffat [Ref. 16] and Chang et al. [Ref. 17] and Iacovides and Launder [Ref. 18]. Cheng and Akiyama [Ref. 19] use a numerical technique to predict velocity and temperature profiles in a curved, rectangular channel with laminar flow. Chilukuri and Humphrey [Ref. 20] use a numerical analysis to study the effects of buoyant forces, aligned with, and opposed to, laminar flow in a curved rectangular channel.

Skogerboe [Ref. 21] provides some preliminary heat transfer data from a channel with similar internal dimensions as the present facility. The facility used by Skogerboe [Ref. 21] is also described by Hughes [Ref. 22]. Development of the present facility is described by Payne [Ref. 23]. His study, as well as the present one, and ones by Hughes [Ref. 22] and Skogerboe [Ref. 21] were and are undertaken to obtain improved understanding of the effects of concave curvature on flows in devices such as heat exchangers and gas turbine blades.

B. OBJECTIVES

The objective of this thesis is to provide new experimental information on the effects of curvature on heat transfer distributions from the surfaces of a curved channel for Dean numbers from 52 to 278. This is accomplished by: (1) qualifying experimental procedures, measurement techniques and channel facilities by conducting several baseline comparisons on the straight and curved portions of the channel, and (2) by presenting new Nusselt number data for the concave and convex surfaces of the 180 degree curved channel to provide information as to how centrifugal instabilities and the resulting vortex pairs affect local and spanwise averaged heat transfer distributions.

C. ORGANIZATION

Subsequent to this introduction, Chapter II details the design and construction of the curved heated channel. Chapter III discusses the experimental procedures and measurement techniques. The Nusselt number measurements are presented in Chapter IV. Chapter V presents conclusions and recommendations.

II EXPERIMENTAL FACILITIES

A. CURVED HEATED CHANNEL

The rectangular cross-section curved channel used in this study is shown in Figure 1. Within this facility, local surface temperatures and other quantities are measured so that local Nusselt numbers can be determined and then investigated regarding the influence of concave and convex curvature. This channel is oriented to minimize the influence of seams prior to the first heaters, and to minimize the influences of buoyancy and body forces on the flow. The channel is dimensionally identical to the channels employed by Ligrani and Niver [Ref. 5], Ligrani et al. [Refs. 6,7,8], Fuqua [Ref. 24], Fields [Ref. 25], Kendal [Ref. 26], Baun [Ref. 27], Longest [Ref. 28], Niver [Ref. 29], Skogerboe [Ref. 21], and Payne [Ref. 23]. The channel has an interior rectangular cross section of 1.27 cm (1/2 inch) by 50.1 cm (20 inches), giving an aspect ratio of 40. The present heat transfer channel and the heat transfer channel described in References 21 and 23 is different from the transparent channel described in References 5 through 8, and 24 through 29 since it allows for the thermal expansion which results from heating. This is accomplished by non-rigid securing of channel surfaces and by constructing much of the channel on skids to allow for longitudinal expansion. A detailed description of the design and construction of the channel is presented by Hughes [Ref. 22] and by Payne [Ref. 23]. A brief summary of design and construction details is also given here.

1. Channel Construction

A photograph of the channel for heat transfer measurements is shown in Figure 1. Details of the inlet section are shown in Figure 2 and details of the blower are shown in Figures 3 and 4. The lip of the nozzle inlet is constructed of quarter sections of 15.2 cm outside diameter Lexan pipe. Lexan is the commercial name of a polycarbonate material. The flow enters the rectangular duct inlet section which contains an aluminum honeycomb and three wire screens all placed normal to the flow direction. These devices reduce spatial non-uniformities in the flow. As the air exits the 25.4 cm by 50.8 cm rectangular duct inlet, it enters a 20 to 1 contraction ratio nozzle. The shape of the nozzle is designed using a fifth order polynomial with respect to streamwise distance to ensure that the flow remains laminar and un-separated as it enters the channel. The nozzle was originally constructed from the same two continuous pieces of lexan as used for the straight and curved test section walls. The heated portion was replaced by Payne [Ref. 23] to eliminate irregularities and small protrusions at the seams. The concave wall has since been shortened to help insure that, after thermal expansion, the concave and convex walls of the channel remain against the wall spacer so that no leaks are present.

The procedure used to join the wall was identical to the procedure used by Payne [Ref. 23]. The concave wall was first cut upstream of the first heater, and the ends were then squared. To insure correct dimensions after the repair, C-clamps were then installed around the curved section of the channel. The Lexan segment from the concave wall plus 1/4 inch extra were then removed and the ends were again squared. A T-shaped backing plate, manufactured out of plexiglass, was subsequently bonded to the Lexan channel walls using Weldon 16 (a commercial material). Once bonded, gaps were filled in using a cyano acrylate adhesive, HST-4 Gap filling instant glue, whose curing

time can be accelerated using HST-4 KICK IT Power Cure Accelerator. Once filled, the seams were sanded smooth with sand paper of grits ranging from 100 to 400. To remove any remaining sandpaper scratches, methyl chloride was quickly swiped over the sanded area to produce a chemical reaction on the Lexan that causes the sanding marks to disappear.

After exiting the inlet nozzle, air first enters a straight section, 2.44 m (96 inches) in length, of which the last 1.52 m is heated, with interior dimensions of 1.27 cm by 50.8 cm (.5 inches by 20 inches). The straight section allows hydrodynamically and thermally fully developed channel flow to develop before the flow enters the curved section. The equations for hydrodynamic and thermal entry length given in Incropera and Dewitt [Ref. 30] show that the flow entering the curved section is hydrodynamically fully developed for Dean numbers less than 560 and thermally fully developed for Dean numbers less than 500. The flow is hydrodanymically fully developed entering the heated section for Dean numbers less than 210. The fluid then enters a 180 degree curved channel section with a convex surface radius of 59.69 cm (23.5 inches) and a concave surface radius of 60.96 cm (24 inches). The interior walls of the heated section are made of two continuous pieces of 0.08 cm thick Lexan. Upon exiting the curved section, air then enters a second straight section with a length of 2.44 m (96 inches).

On the convex surface of the second straight section, a 5.08 cm (2.0 inches) wide slot is present which allows insertion of a probe into the channel to measure outlet mixed mean temperatures. The slot is located approximately 57.1 cm (22.5 inches) from the trailing edge of the heater on the curved convex wall, or 19.05 cm (7.5 inches) downstream of the end of curvature. A support block was constructed to support the area around the slot. Brass inserts are placed just inside the slot to allow insertion

of two thin foam strips which adhere to the brass to provide an air tight seal between the channel interior and exterior as the probe is traversed. As flow leaves the second straight portion, it passes through four screens, a honeycomb, a diffuser with a total angle of 3 degrees, and finally into Plenum #1.

The channel is designed to allow for thermal expansion in longitudinal and transverse directions which occurs as test surfaces are heated. As is illustrated in Reference 21, the surfaces of the channel are not rigidly secured, but are clamped onto the sidewalls to allow for motion in these two directions. As the test conditions are set-up the channel is heated to thermal equilibrium during which, channel surfaces expand to the sizes they assume as measurements are made. After reaching thermal equilibrium, C-clamps are installed along the curved section to ensure that no leakage occurs from the exterior to the interior of the channel. In addition, both the inlet and outlet sections, including Plenum #1 and all inlet flow management apparatus, are constructed on two plexiglass skids to allow for longitudinal expansion.

2. Blower Assembly

The blower and piping connecting it to the channel are shown schematically in Figure 3 and pictured in Figure 4. The blower itself is an ILG Industries 10P type, capable of producing 10.2 cm of water vacuum at 4.82 m^3/min volumetric flow rate. It is used to depressurize outlet Plenum #2 to pressures just below atmospheric pressure. In doing so, air is then drawn from Plenum #1 through a globe valve and a 5.08 cm inside diameter PVC pipe. With this system, flow rates can be varied to produce Dean numbers from 10 to 435. Flow rates are measured by means of a pressure drop across a 3.51 cm (1.5 inch) orifice plate. Details concerning the orifice plate are given in Hughes [Ref. 22] and also discussed in Chapter III.

To reduce vibrations from the blower to the test section and to minimize disturbances to the flow, an air tight rubber flexible coupling is used to connect the suction side of the blower to Plenum #2 and a second flexible coupling is used to connect Plenum #2 to the orifice plate. The second flexible coupling consists of a thin sheet of plastic wrapped around the piping and attached at both ends with standard hose clamps in order to prevent any leaks. In addition, rubber mounts are used to mount the blower and blower frame to further reduce vibrations. A schematic of the blower assembly is in Figure 3 and a photograph is shown in Figure 4.

3. Heaters

Four etched foil heaters, manufactured by the Electrofilm Corporation, are installed on each of the two Lexan surfaces, as shown in Reference 26. In the present study, these heaters provide the means to heat both the concave and convex surfaces of the channel, all at the same power dissipation rates, to produce uniform heat flux boundary conditions at the channel walls. The dimensions of each heater are 38.1 cm by 152.4 cm (15.0 inches by 60.0 inches), and maximum power capacity is 2 KW. Drawings showing how the heaters are attached are presented in Figure 5 and in Reference 21 and are discussed further by Schwartz [Ref. 31]. CC1 and CV1 are used to designate the two heaters on the concave and convex surfaces of the straight section, respectively, and CC2 and CV2 used to designate the heaters on the concave and convex surfaces of the curved section, respectively. The leading edge of the CC1 and CV1 heaters are 88.4 cm from the channel inlet. The trailing edges of the CC2 and CV2 heaters end approximately 38.1 cm (15.0 inches) from the completion of channel curvature. This is about 57.15 cm (22.5 inches) upstream of the location of the temperature traverse probe.

Each heater is powered by a Superior Electric type 136B variac. With each variac, the voltage to a heater may be adjusted between 0 and 115 volts, and the current may be adjusted from 0 to 10 amps. A detailed schematic of the heater circuitry is given by Hughes [Ref. 22] and also shown in Figure 6. Power inputs to each heater are determined by measuring voltage drops across 50 mv, 10 amp shunt resistors, as well as across each heater. The shunt resistance measurement allows for the heater current to be determined. Details in adjusting desired heat input levels are given in Chapter III.

4. Insulation

To minimize heat conducted from the heaters, and maximize convected heat into the channel airstream, the outside of the channel from just upstream of the heaters CC1 and CV1 to the traverse slot downstream of heaters CC2 and CV2 is insulated with black foam insulation manufactured by the Halstead Company. A detailed drawing showing how various layers of insulation are attached to the channel to produce a total thickness of 6.98 cm (2.75 inches) on each side is illustrated in Figure 7.

5. Thermocouples

100 copper-constantan thermocouples (TC's) are placed on channel surfaces to allow spatially resolved surface temperature measurements to be made. Twenty-five thermocouples are placed on the Lexan channel surfaces which are not exposed to the airstream beneath each of the CC1, CV1, CC2, and CV2 heater surfaces. The 25 thermocouples beneath each heater are place in 5 spanwise rows of 5 per row. Heater CC1 is located above TC's 1 through 25, which are connected to the Data Acquisition Unit (DAU) channels 1 through 25. Heater CV1 is above TC's 26 through 50 which are connected to DAU channels 26 through 50. Heater CC2 is above TC's 51 through 75 which are connected to DAU channels 51 through 75. Heater CV2 is associated with TC's 76 through 79 which are connected to DAU channels 76 through 79 and with TC's 80

through 100 which are connected to DAU channels 100 through 120. The first row of thermocouples is located 103.64 cm (40.8 inches) from the inlet or 15.24 cm (6 inches) from the leading edge of the first heater. Each additional row is spaced 30.48 cm (12 inches) apart in the X direction. The thermocouples are placed over a spanwise length of approximately 10.16 cm (4.0 inches) on each side of the centerline. A detailed drawing of the installation of these thermocouples is shown in Figure 8. The purpose of these thermocouples is to provide sufficient data to determine accurate spanwise averaged local Nusselt numbers.

Forty more thermocouples, TC's 101 through 140 are connected to DAU channels 121 through 160, and are placed in the insulation to determine conduction heat loss. These thermocouples are placed in pairs along the channel centerline behind each row of thermocouples. The first thermocouple is separated from the back of the heater by 1.9 cm (0.75 inches) of insulation. The second thermocouple is separated from the first, and from the ambient air, by 2.54 cm (1 inch) of insulation. This arrangement allows the temperature drop through the insulation to be measured, and the conduction loss through the insulation to be calculated provided the insulation thermal conductivity is known.

Two additional thermocouples are used to measure mixed mean temperature at the channel inlet and mixed mean temperature at the channel outlet. Thermocouple (TC) #141 is placed just in front of the inlet for this purpose. TC #142 is used in the temperature traverse probe to provide measurement of local temperatures used to calculate outlet mixed mean temperatures downstream of the heaters.

B. DATA ACQUISITION

1. Surface Temperature Measurement

Voltages from the 142 thermocouples are read by Hewlett-Packard type T20 relay multiplexer card assemblies for T type thermocouples. These assemblies are installed in a HP3497A low-speed Data Acquisition / Control Unit and a HP3498A Extender. This system provides thermocouple compensation electronically such that voltages for type T thermocouples are given relative to 0° C. This system is connected to a Hewlett-Packard 9836A computer which processes voltages from the 142 thermocouples which are then recorded into data files along with corresponding temperatures. A schematic of this system is shown in Figure 9.

2. Outlet Mixed Mean Temperature Measurement

The acquisition system used for exit mixed-mean temperature measurements is illustrated in Figure 10. To calculate the mixed mean temperature at the exit of the heated test section for one Dean number, a survey of velocity and a survey of temperature are needed. The thermocouple probe used to measure the temperatures consists of a thermocouple attached to a metal rod. This rod is then secured to a traversing block which is also used to mount the miniature five hole pressure probe [Ref. 6] used for the velocity measurements. The automated two-dimensional traversing device, shown in Figure 10, is used to traverse the temperature probe and the five hole pressure probe. The movements of the motors on the traversing devise allow both spanwise and radial movement and are controlled by signals from the HP9836A computer, which are sent to a Modulynx Mitas PMS085-C2AR Drive Controller and then to a Modulynx Mitas PMS085-D0J0 Motion Drive. The motor Drive sends signals to each of the Superior Electric M092-FD310 stepping motors, which rotate drive

screws which then move two traversing blocks. The threads of the drive screws are such that one rotation gives a vertical or lateral probe movement of .127 cm (.05 inches). For each traverse, 320 local temperatures are recorded over a channel cross section area of 5.08 cm (2.0 inches) in the spanwise direction by 1.02 cm (.4 inches) in the radial direction in increments of 0.127 cm (.05 inches). Upon completion of the traverse, the controller is programmed to return the probe to its original position. Voltage readings from the traversing thermocouple are processed in the same manner as the channel surface thermocouples.

III. EXPERIMENTAL PROCEDURES

The procedure to obtain data consists of several steps: (1) flow is induced in the channel, (2) heater power levels are adjusted to provide a constant surface heat flux boundary condition, (3) sufficient time is allowed for the heated channel to reach thermal equilibrium, and (4) voltages from thermocouples along with other data are read and recorded by the computer. From these raw data, surface temperatures are determined, and Nusselt numbers are calculated. Flow is laminar for all tests. Pairs of counter rotating Dean vortices are present in the channel for most of the Dean numbers studied, where the initial streamwise location of the vortices moves upstream with increasing Dean number.

The experimental procedures are discussed in three parts. In part one, flowrate and Dean number settings are discussed along with details on the adjustment of thermal boundary conditions. In part two, processing of surface temperature measurements and the determination of local Nusselt numbers. Finally, part three discusses the use of the temperature traverse probe, as well as the method used to determine local and exit mixed-mean temperatures.

A. CHANNEL PREPARATION

1. Flowrate and Dean Number Adjustments

Local Nusselt numbers are measured in the channel at Dean numbers ranging from 50 to 278. The software program **Dean15** is employed to aid the experimenter in setting the Dean number at a particular value. The first step of the program is to determine the mass flowrate, $\dot{m}$, which corresponds to a particular Dean number using the equation given by:

$$\dot{m} = De\left[\rho A_{ch}\left[\frac{\nu}{d}\right]\sqrt{\frac{r_i}{d}}\right.$$

where:

De = Dean Number

ρ = Air density

A_{ch} = Channel area

r_i = Inside radius of channel curvature

d = Channel height

ν = Kinematic viscosity

The pipe Reynolds number, Re_P, is then calculated from the mass flowrate, $\dot{m}$, using the equation:

$$Re_p = \frac{\dot{m} d_p}{\rho \nu A_p}$$

where:

d_P = Pipe diameter

A_P = Pipe cross-sectional area

The next step requires the adjustment of the channel mass flow rate to the desired value. The actual flowrate is determined from a measurement of the pressure drop across a 3.81 cm (1.5 in) standard ASME orifice plate, located in piping between the two exit plenums. The initial value of this pressure drop is estimated using results such as the ones presented in Figure 11. The pressure drop, in inches of water, is then measured using a Meriam inclined manometer (with full scale range of 0.5 inches of water) for Dean numbers

less than 225, or a Validyne digital manometer (with a full scale range of 2.0 inches of water) for Dean numbers greater than 220. Mass flowrate is calculated using the equation given by:

$$\dot{m} = KA_{OR}Y\sqrt{2\rho\Delta P}$$

where:

K = Flow coefficient (A function of Reynolds number which is interpolated from the ASME Tables [Ref. 32])

Y = Expansion coefficient (Calculated from Holman and Gajda [Ref. 33]

A_{OR} = Orifice Area

ΔP = Pressure drop across orifice

Because K is dependent on Rep, an iterative procedure is required to determine $\dot{m}$. This iterative process is continued until the mass flowrate converges to within one percent for two successive calculations. This true mass flow is then employed to give the final Dean number using the equation given by:

$$De = \frac{\dot{m}}{\rho A_{ch}}\left[\frac{d}{\nu}\right]\sqrt{\frac{d}{r_i}}$$

2. Heat Flux Level Adjustments

The four heaters, CC1, CC2, CV1, and CV2 are employed to provide a constant heat flux boundary condition on the concave, convex, and straight channel surfaces. As mentioned earlier, each heater is designed to uniformly dissipate heat over its area. The magnitude of the heat flux employed on each heater is set according to three constraints. First, heat fluxes must be large enough to obtain significant differences between surface

temperatures and local mixed mean fluid temperatures. Second, maximum surface temperatures are limited to 60 Deg. C for any location in the channel because the bonding agent used to attach Lexan sheets to cross beams is not dependable at higher temperature levels. (For most runs, the maximum temperature occurs at thermocouple 98, which is located in the final spanwise row of the convex wall of the curved section.) Third, the convected power from the heaters in the curved portion of the channel must be the same as the convected power from the heaters in the straight portion of the channel. This was achieved by adjusting slightly higher overall power to the heaters on the curved portion of the channel to account for slightly higher conduction losses. Such conduction losses also result in convective loss variations on each individual heater because the surface temperature of the wall increases along the length of the heater which drives the conducted power loss up and the convected power down. The power levels required for each heater versus Dean number are shown in Figure 12.

To determine the power into each heater, the voltage drops across each shunt and across each heater are measured using a Hewlett-Packard digital volt-ohm meter and are entered into a program called **Temcurv**. Figure 13 shows voltage drops across shunt resistors ΔV_S which are needed to produce different power levels in each heater. With this voltage drop, heater current is given by:

$$I = \Delta V_S / R$$

The power to each heater then follows using an equation of the form:

$$P = \Delta V_H \times I$$

where:

I = Current (amps)

P = Power (watts)

ΔV_S = Voltage drop across the shunt (volts)

ΔV_H = Voltage drop across the heater (volts)

R = Shunt resistance (ohms)

B. SURFACE HEAT TRANSFER DISTRIBUTION MEASUREMENTS

1. Temperature Measurements

To insure that thermal equilibrium exists the system is heated for approximately 8-9 hours prior to data acquisition. As this is done, temperatures are monitored using the temperature acquisition program, **Tcheck**, to insure that maximum surface temperatures never exceed 60 Deg. C. When steady state conditions are reached, voltage readings from each thermocouple are recorded using **Temcurv** and converted into Deg. C using calibration equations determined by Payne [Ref. 23]. For thermocouples 1 through 100, which measure the channel surface temperature, voltages are converted into Deg. C using the equation given by:

$$T = 1.8558 + 24037\ V - 125550\ V^2 - 26437000\ V^3$$

For thermocouples 101 to 140, which are used to determine the conduction power loss, the conversion equation is given by:

$$T = 0.22585 + 25594\ V - 430030\ V^2 - 31234000\ V^3$$

For thermocouple 141, which measures the inlet temperature, the equation is given by:

$$T = 1.7188 + 21227\ V - 203750\ V^2 - 16567000\ V^3$$

For thermocouple 142, which is mounted on the traverse to measure the air stream temperature in the slot, the equation is given by:

$$T = -.57326 + 27873\ V - 2338500\ V^2 - 461950000\ V^3$$

where:

T = Temperature Deg. C

V = Thermocouple voltage (volts)

2. Nusselt Number Calculations

The program **Nucurv2** is used to determine local Nusselt numbers from the output provided by the **Temcurv** program. The program analyzes the energy from each heater in 5 strips such that a row of thermocouples is centered in each strip. The process begins by determining the convective power transfer at each strip of the heater using an equation of the form:

$$\dot{q}_{conv} = \dot{q}_{in} - \dot{q}_{cond} - \dot{q}_{rad}$$

where:

$\dot{q}_{conv}$ = Power convected to the channel air flow

$\dot{q}_{in}$ = Power to the heaters (V x I)

$\dot{q}_{cond}$ = Power loss by conduction

$\dot{q}_{rad}$ = Power loss by radiation, set equal to zero

Power loss by conduction is given by

$$\dot{q}_{cond} = A_{strip} K (T_{in} - T_{out}) / \Delta y$$

where:

A_{strip} = The area of each strip of the heater

T_{in} = The temperature of the thermocouple in the conduction insulation closest to the heater

T_{out} = The temperature of the thermocouple in the conduction insulation furthest away from the heater

K = The thermal conductivity of the insulation = .04 W / m C

Δy = The distance between the inner and outer thermocouples = 2.54 cm

The heat flux for each strip is then determined using:

$$\dot{q}''_{conv} = \dot{q}_{conv} / A_{strip}$$

With the convective heat flux known, the local mixed mean temperature at any streamwise channel location is determined using the equation given by:

$$t_{mm}(x) = t_{mmin} + [\dot{q}''_{conv}(x) b x] / Cp (\dot{m})$$

where:

$t_{mm}(x)$ = Local mixed mean Temperature

t_{mmin} = Inlet mixed mean temperature

b = Spanwise width of the heated surface

x = Streamwise distance from the beginning of the heating to the streamwise station of interest

$\dot{q}''_{conv}$ = Heat flux over streamwise distance x

C_P = Specific heat of air

$\dot{m}$ = Air mass flow rate

The convective heat flux is also used to find the corrected wall temperature, T_{wcorr}. This correction is required because the thermocouples used for surface temperature determination are attached behind the Lexan surfaces exposed to the flow field. Consequently, there is a thermal contact resistance between thermocouples and convective Lexan surfaces as well as thermal resistance through the Lexan surface. The temperature difference, ΔT_{wcorr}, between the actual surface and that measured by the thermocouple (to account for these resistances) is given by the equation:

$$\Delta T_{wcorr} = q''_{conv} \ (CR)$$

where:

q''_{conv} = Convected heat flux per heater area

CR = Thermal contact resistance ($^{o}C\ m^2$ / watt)

Experimental procedures used to determine CR are described by Bella [Ref. 33]. From his work, CR equals $3.4 \times 10^{-3}\ ^{o}C\ m^2$ / watt. Corrected wall temperatures are then given by:

$$T_{wcorr} = T_w - \Delta T_{wcorr}$$

With corrected wall temperatures in hand, local heat transfer coefficients are determined using the equation given by:

$$h = \dot{q}''_{conv} / (T_{wcorr} - t_{mm})$$

Finally, the local Nusselt number, Nu, is calculated from an equation having the form:

$$Nu = h (D_H) / k$$

where:

D_H = Hydraulic diameter (2 x channel width = .0254 m)

k = Thermal conductivity of air at 20^{O} Celsius (.02563 W / m K)

C. EXIT MIXED MEAN TEMPERATURE MEASUREMENTS AND DETERMINATION

The mixed mean temperature is determined from measurements of mean temperature and mean velocity at the location of the slot on the convex wall, which is 57.1 cm from the downstream edge of heater CV2. This accomplished by traversing a thermocouple and the miniature five hole pressure probe over a two dimensional plane, after each is inserted into the slot. The temperature measurements are made after the channel is at thermal equilibrium using TC #142 set in the traversing carriage. Using the program **Temtrav**, 320 voltage readings are taken over a 5.08 cm (2.0 inch) by 1.02 cm (0.4 inch) area as the probe moves in the traverse slot. Voltage readings are transformed into Deg. C using the equation

described in the previous section. The same traverse is employed at a separate time for the miniature five hole pressure probe. Procedures to determine streamwise velocities from the miniature five hole probe are described by Baun [Ref. 27] and by Ligrani et al. [Ref. 6] and [Ref.7]. The mixed mean temperature is then given by:

$$t_m = \frac{1}{A_{ch}U}\int utdA$$

where:

t_m = Mixed mean temperature

A_{ch} = Channel traversed cross section area

U = Bulk velocity (spatially averaged)

u = Local mean streamwise velocity

t = Local mean temperature

The software program **Tmxdm** is used to determine the mixed-mean temperature. This is accomplished using an approach which assumes that the area corresponding to each temperature measurement is the same:

$$t_m = \frac{1}{320}\sum_{i=1}^{320}\frac{u_i}{v}t_i$$

Since the temperature and velocity traverses cover only 75 per cent of the channel estimation of the influences of regions near the wall on t_m is required. The final t_m is then equal to 0.75 times the value from the above equation plus 0.25 times the contribution estimated from the near wall regions.

The mixed mean temperature at the slot location is also estimated from the amount of convected energy into the channel. The procedures employed to do this are described in the previous section.

IV. RESULTS AND DISCUSSION

The results are presented in two major sections. The first section presents the results of the velocity and vorticity surveys. The second section presents the spanwise averaged and the local heat transfer results. For this discussion a right hand coordinate system is used where X is the streamwise distance from the beginning of the heated section, Y is the distance across the channel from the concave wall, D is the width of the channel, and Z is in the spanwise distance from the center of the channel.

A. VELOCITY AND VORTICITY SURVEYS

The velocity and vorticity surveys were taken in a spanwise normal plane located from -2.54 cm (1 inch) to +2.54 cm (1 inch) from the spanwise centerline. This plane is located 57.1 cm (22.5 inches) downstream of the end of the last heater, and 19.05 cm (7.5 inches) from the end of the curvature. Summaries of the results of the surveys are presented in Figures 14 through 23. Figures 24 through 39 then present examples of selected individual graphs for Dean numbers of 80, 146, 175, and 247.9. In all of these graphs Z/D = 0 at the channel spanwise centerline, Y/D = 0 at the concave wall, and Y/D = 1 at the convex wall, where D is the width of the channel. The data presented include streamwise velocity is normalized by the bulk mean velocity, $\bar{U}$, $P_{ambient} - P_{total}$ normalized by $(P_{ambient} - P_{total})^*$ where $(P_{ambient} - P_{total})^*$ is the average of the minimum and maximum measured pressure differences, streamwise vorticity, radial vorticity, and spanwise vorticity.

1. Streamwise Velocity and Total Pressure Surveys

Streamwise velocity results are presented in Figures 14 and 15, and total pressure results are given in Figures 16 and 17. Even though there are quantitative differences

because of the different quantities, surveys of total pressure and streamwise velocity for each Dean number are qualitatively very similar. Consequently only streamwise velocity results are discussed.

Streamwise velocity surveys in Figures 14 and 15 for Dean numbers 51.8 through 247.9 show significant differences at different Dean numbers. At the lowest Dean number investigated, 51.8, some spanwise periodicity is evident near the concave wall due to velocity deficits evident at several spanwise locations. These deficits are separated by regions of higher velocity located near the center portion of the channel. At Dean numbers from 80 to 175.8 velocity deficits cover larger portions of the spanwise / radial plane.

2. Vorticity Surveys

Streamwise vorticity surveys are presented in Figures 18 and 19, radial vorticity surveys are presented in Figures 20 and 21, and spanwise vorticity surveys are presented in Figures 22 and 23. Vorticity data are also given in Figures 28 through 39. Results at Dean numbers of 146, 175, and 199 provide evidence that Dean vortices are located near the convex surface. This is shown by opposite signs streamwise vorticity regions near the convex surface, and by significant spanwise periodic streamwise velocity deficits present near the convex surface. Such behavior occurs after the vortices have left the curved portion of the channel because of their angular momentum. Radial vorticity distributions are consistent with these trends since spanwise periodic regions of positive and negative vorticity are evident near the convex wall which correspond to the location of the vortices. Regions of positive and negative vorticity are also present near the concave surface which are located on either side of velocity deficits. Spanwise vorticity distributions in Figures 22 and 23 show regions of negative vorticity at the same locations as the streamwise velocity deficits.

B. SPANWISE-AVERAGED AND LOCAL HEAT TRANSFER RESULTS

1. Mixed Convection Nusselt Number Results

Spanwise-averaged Nusselt numbers are presented in Figures 40 and 41 as dependent on X/D. Locally measured Nusselt numbers are presented in Figures 42 through 53 as dependent on Z/D and X/D. These results were obtained with mixed convection in the channel for $\beta\Delta T$ values ranging from .0487 to .0789. $\beta\Delta T$ is employed as a measure of the influence of natural convection since it is proportional to the Grashof and to the square of the convection velocity for buoyancy.

Figure 40 presents Nusselt numbers measured on the concave surface at Dean numbers of 100, 125, 153, 179, 200, 225, and 250 and 278. Nusselt numbers at the same Dean numbers are then given in Figure 46 which were measured on the convex surface. At a given Dean number, Nusselt numbers decrease with streamwise distance in the straight portion of the channel at X/D from 0 to 120. At larger X/D in the curved portion of the channel, the Nusselt numbers from the concave surface are then fairly constant with X/D at a particular Dean number. Exceptions to this are evident for Dean numbers of 278 and 225 where Nusselt numbers from the concave and convex surfaces show small local maxima. Nusselt numbers from the convex surface for Dean numbers less than or equal to 200 decrease with streamwise distance over the curved portion of the channel. The results for a Dean number 250 are believed to be somewhat in error and inconsistent with data trends at other Dean numbers. These data were included on Figures 40 and 41 for the sake of completeness.

Local Nusselt number measurements as dependent on normalized spanwise distance and normalized streamwise distance are presented in Figures 42 through 53. These results generally evidence spanwise uniform behavior along the surface, except for slight increases as Z/D decreases from 8 to -8 as a consequence of the influences of natural convection on the flow in addition to the effects of forced convection. The minimal influence of natural

convection at the higher Dean numbers is evidenced by Nusselt number variations with Z/D at a particular X/D and Dean number which are barely discernible.

2. Energy Balance Checks

In order to provide a check on the energy placed into the flow, energy balance tests were conducted at Dean numbers of 200 and 250. The results of these tests are presented in Figures 54 through 61. In Figures 54 and 58, local mixed mean temperatures are presented as a function of X/D. These local mixed mean temperatures were determined from energy balances on different segments of the curved channel accounting for convective heat transfer from the walls into the channel air from the streamwise location where heating begins to the streamwise location of interest. Downstream of the heated portion of the channel at X/D from 240 up to 280, the mixed mean temperature is constant with X/D. The location X/D = 280 corresponds to the location of the slot where mixed mean temperature is determined directly from temperature and velocity distributions measured in the plane normal to the flow direction. The results in Figure 54 for a Dean number of 200, and in Figure 58 for a Dean number of 250, show that the value of the mixed mean temperature from the direct measurement matches the value of mixed mean temperature from the energy balance, which provides confirmation of the validity of the energy balance procedures employed. The surveys of temperature and velocity used for the direct measurements of mixed mean temperature are presented in Figures 55 through 57 for Dean number of 203, and in Figures 59 through 61 for Dean numbers of 250.

3. Variation of Nusselt Number With Respect to $\beta\Delta T$ and Grashof Number

Figures 62 through 84 present Nusselt number variations with $\beta\Delta T$ for a given streamwise location and Dean number. Figures 85 through 88 present Nusselt number variations with Grashof number, Gr, for a given streamwise location and Dean number.

All of these results show the same general trends, and therefore, the only results for a Dean number of 275 in Figure 62 are discussed.

Figure 62 shows that Nusselt numbers for X/D = 108 at a of Dean number of 275 vary linearly with $\beta\Delta T$ such that Nusselt numbers increase as $\beta\Delta T$ decreases. Nusselt numbers at $\beta\Delta T = 0$ are near 8.24, which is sensible since this value corresponds to the forced convection solution for this particular flow. Nusselt numbers extrapolated to $\beta\Delta T = 0$ thus gives the values of the Nusselt numbers with forced convection only in the channel and zero natural convection. This is because natural convection effective velocity, which is proportional to $\beta\Delta T$, is zero. This approach is valid only for Dean numbers of 175 and greater because the influences of natural convection are minimal. These experimental conditions correspond to values of the Reynolds number squared divided by the Grashof number (Re^2/Gr) greater than about 50×10^{-6}. At smaller values of Re^2/Gr (which corresponds to Dean numbers lower than 175) natural convection effects are more significant and the extrapolation procedure employed at higher Dean numbers cannot be used. This is because data are expected to show a non-linear trend as $\beta\Delta T$ decreases from the range of the present data to 0.0.

4. Spanwise Averaged Nusselt Numbers for $\beta\Delta T = 0.06$

Spanwise averaged Nusselt numbers for $\beta\Delta T = 0.06$ for the concave surface are presented in Figure 89, and for the convex surface in Figure 90. These figures show that Nusselt numbers generally decrease with X/D at a particular Dean number through the straight portion of the channel. Values are then fairly constant with streamwise distance with X/D through the curved potion of the channel. At a given X/D, Nusselt numbers generally increase with Dean number. Spanwise averaged Nusselt numbers from the convex surface are somewhat lower than the ones measured on the concave surface at the same Dean number and X/D.

5. Spanwise Averaged Nusselt Numbers for $\beta\Delta T = 0.0$

Spanwise averaged Nusselt numbers measured on the concave surface for $\beta\Delta T$ = 0 are presented in Figure 91 and values measured on the convex surface for $\beta\Delta T = 0$ are presented in Figure 92. Figures 93 through 96 show the same data but plotted for individual Dean numbers. For Dean numbers of 275, 250, 200 and 175, these figures show that Nusselt numbers are the same on the convex surface and the concave surface at the same Dean number and X/D. Results from the straight portion of the channel for Dean numbers of 200 and 175 are additionally consistent with predictions made using the Stan5 boundary layer program, [Ref. 34], as shown in Figures 97 and 98. Nusselt numbers decrease with X/D through the straight portion of the channel $0 \leq X/D \leq 120$ and are then fairly constant through the curved portion of the channel $120 \leq X/D \leq 280$. Values of the Nusselt number for X/D from 80 to 130 are slightly lower than 8.24 on the convex and concave surfaces, however the fact that they are near 8.24 shows that the data are consistent with the forced convection solution for this flow. Data for Dean numbers of 154 and 102 are lower than the other data for all X/D because natural convection is not minimal and the extrapolation procedure described earlier does not give valid results.

Results from the concave surface are generally different than the ones on the convex surface for most X/D and for all four Dean numbers. For a Dean number of 275, results from the concave surface are higher than ones from the convex surface throughout the curved section for X/D from 130 to 230. For a Dean number of 250, results from the convex surface are higher than ones from the concave surface for X/D from 110 to 160, and are lower for X/D from 160 to 230. For a Dean number of 200, Nusselt numbers from the convex surface are higher than ones from the concave surface for X/D from 110 to 160, and are lower for X/D from 160 to 230. For a Dean number of 175, the convex surface Nusselt numbers are slightly higher than concave surface Nusselt numbers for X/D from

110 to 160. Nusselt numbers from the convex surface at this Dean number are lower than Nusselt numbers measured for the concave surface for X/D from 160 to 230.

V. CONCLUSIONS

The effects of curvature and the resulting centrifugal instabilities on local heat transfer distributions are studied in a curved channel at Dean numbers ranging from 100 to 275. The channel is designed with a rectangular cross section of 1.27 cm by 50.1 cm giving an aspect ratio of 40. These interior dimensions coincide with those of another channel which is transparent and used for flow visualization. In the channel used for thermal studies, the flow is heated in a 2.44 m straight portion, located just prior to the curved portion to obtain flow which is hydrodynamically and thermally fully developed at the entrance of the curved portion. The flow then enters a 180 degree heated curved section with a convex surface radius of 59.69 cm and a concave surface radius of 60.96 cm. Surface temperatures and ambient temperatures are measured using 142 thermocouples, whose outputs are used to determine local Nusselt numbers.

Several baseline comparisons qualify flow behavior as well as the experimental procedures and measurement techniques. In the first of these, spanwise-averaged Nusselt numbers from the two walls of the straight portion of the channel match with each other very well. As thermal entry length effects disappear, dimensional Nusselt numbers approach 8.24 as expected from the theory for thermally fully developed flow between two parallel infinite plates with constant heat flux boundary conditions. In the thermally developing region, measured Nusselt numbers match results from numerical predictions. Finally, measured mixed-mean temperatures at the exit of the curved section match values determined from energy balances. These baseline comparisons thus validate experimental procedures, the measurement approach and the facilities used, and provide confidence of the accuracy of measurements from the curved portion of the channel.

The experimental conditions are identified for which forced convection with weak buoyancy, and forced convection with strong buoyancy are present. With weak buoyancy effects present ($Re^2/Gr > 50 \times 10^{-6}$) a new method is developed to deduce forced convection Nusselt numbers without the influence of natural convection. Resulting data provide information on the influence of Dean vortex pair and their secondary flows. For a Dean number of 275, Nusselt numbers measured on the concave surface are higher than the ones on the convex surface through out the curved portion, for X/D from 130 to 230, where X is the distance from the start of the heated section, and D is the width of the channel. For Dean numbers from 175 to 250, Nusselt numbers are higher on the concave surface than on the convex surface for X/D from 160 to 230, such that differences increase with Dean number. Forced convection Nusselt numbers decrease through the straight portion of the channel and then approach a constant value for a given Dean number. Through the curved portion of the channel, Nusselt numbers then remain fairly constant on the concave surface, but continue to decrease with X/D on the convex surface. At a given X/D, Nusselt numbers for a particular surface generally increase with Dean number.

APPENDIX A
FIGURES

The following pages contain the figures used in the development of this thesis.

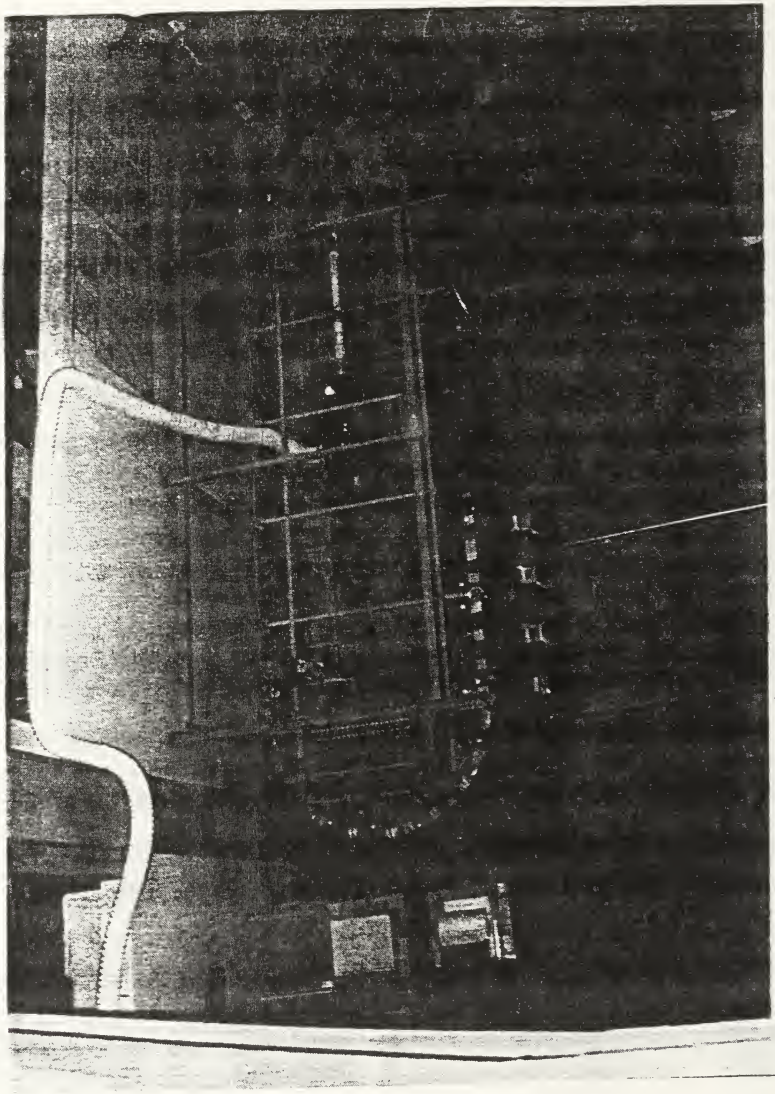

Figure 1. Curved Heat Transfer Channel

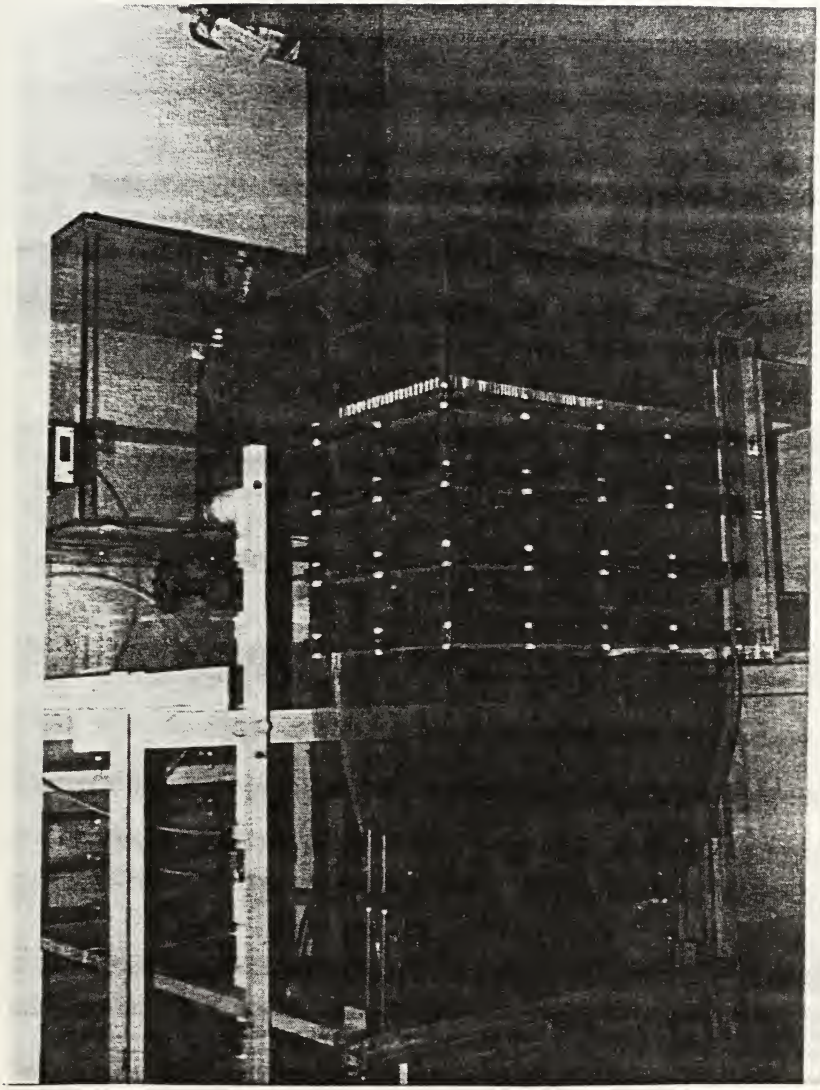

Figure 2. Channel Inlet Section

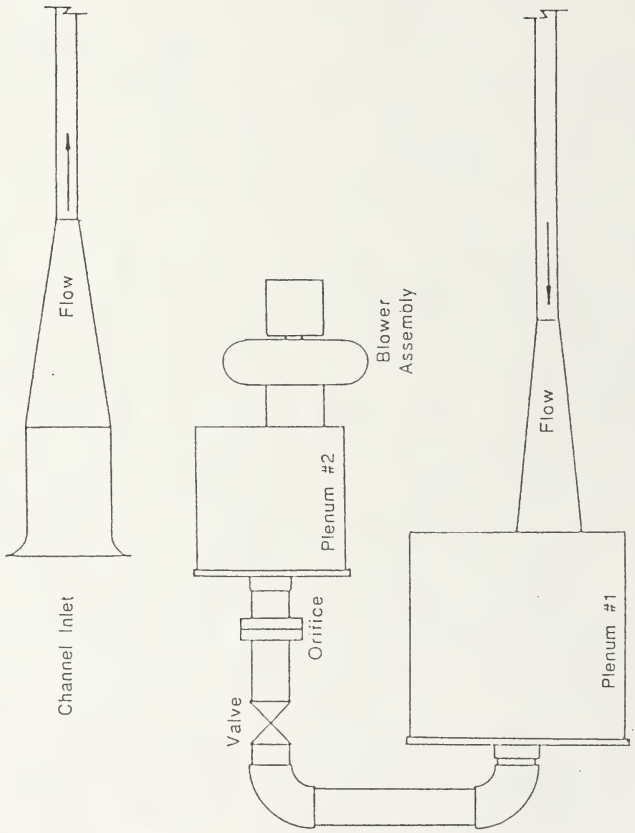

Figure 3. Schematic of Blower Assembly

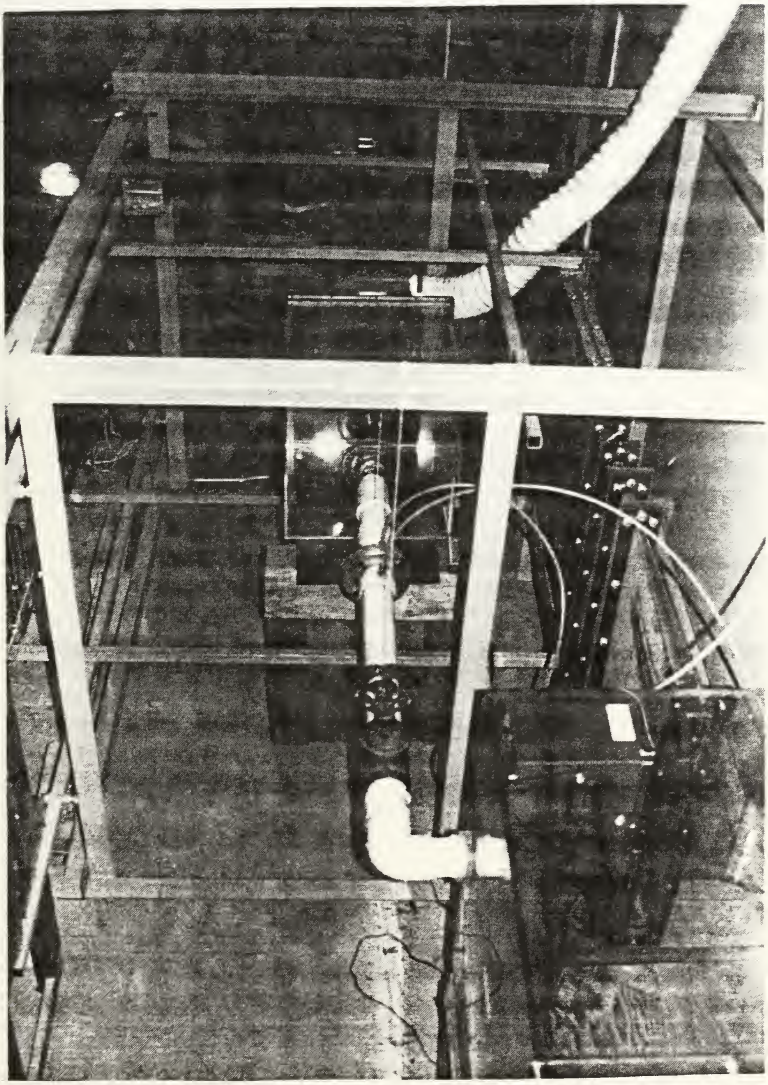

Figure 4. Photograph of Blower Assembly

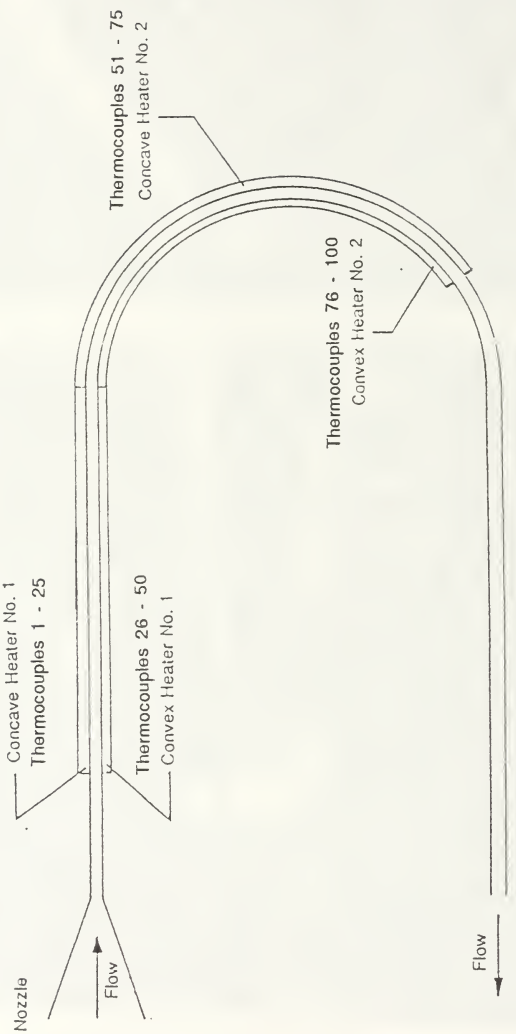

Figure 5. Channel Heater Identification

Figure 6. Heater and Control Circuit Wiring Diagram

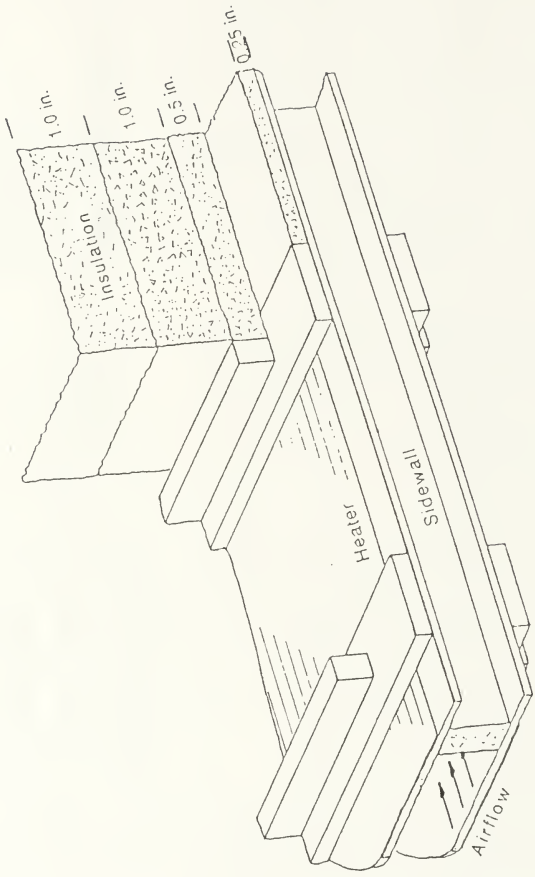

Figure 7. Channel Insulation Drawing

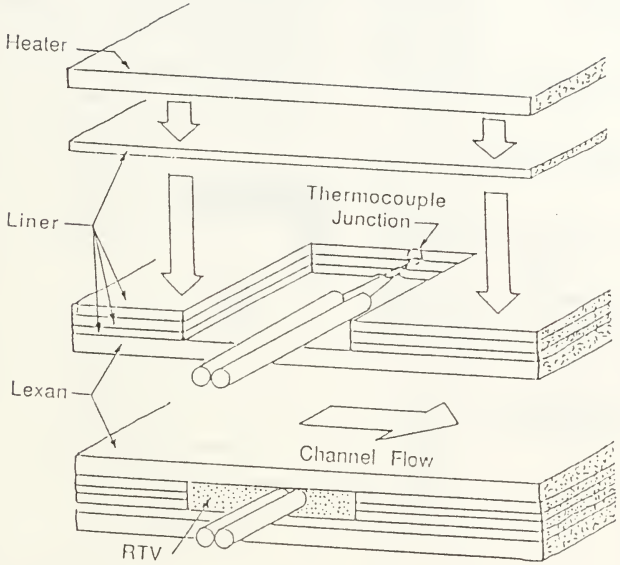

Figure 8. Channel Thermocouple Installation

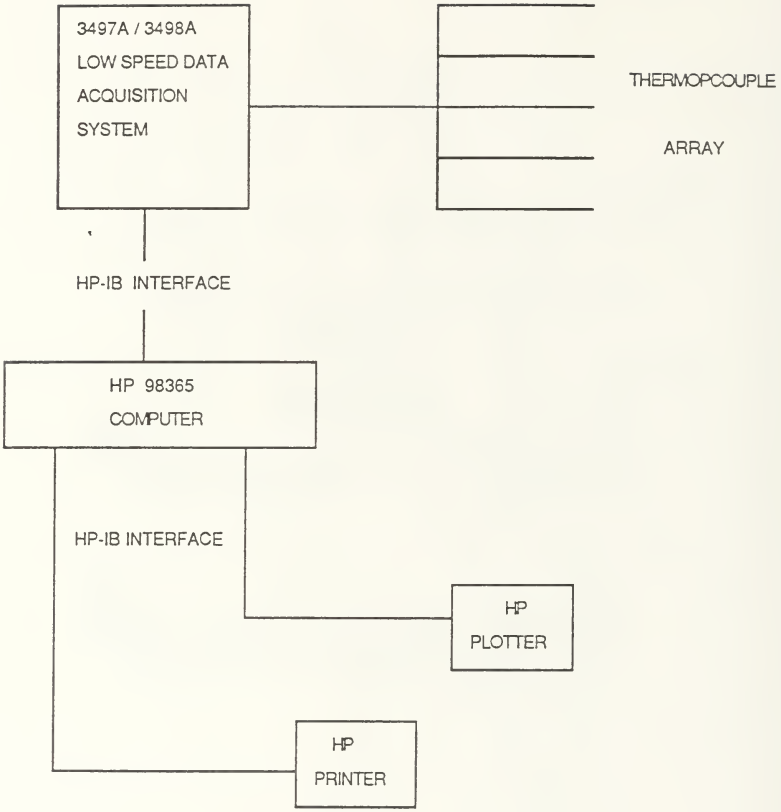

Figure 9. Data Acquisition System For Temperature Measurement

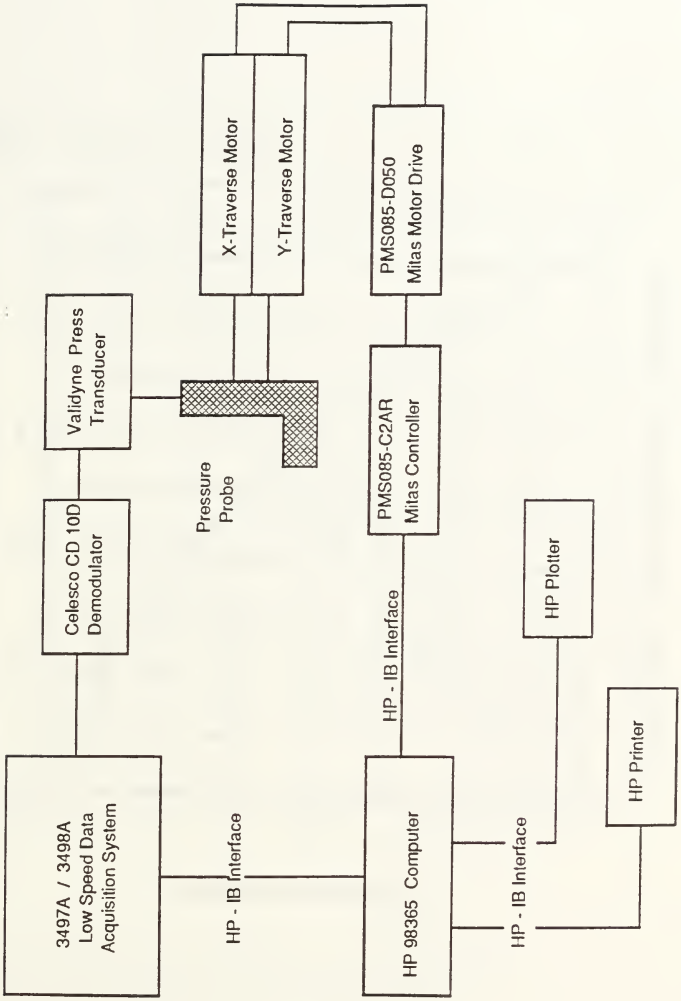

Figure 10. Traversing Mechanism

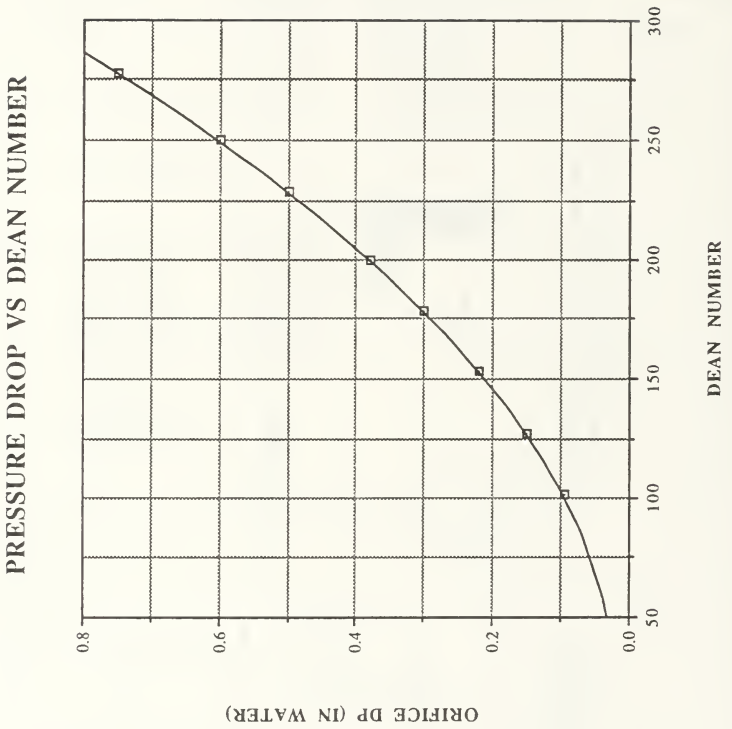

Figure 11. Dean Number Versus Pressure Drop Across Orifice Plate

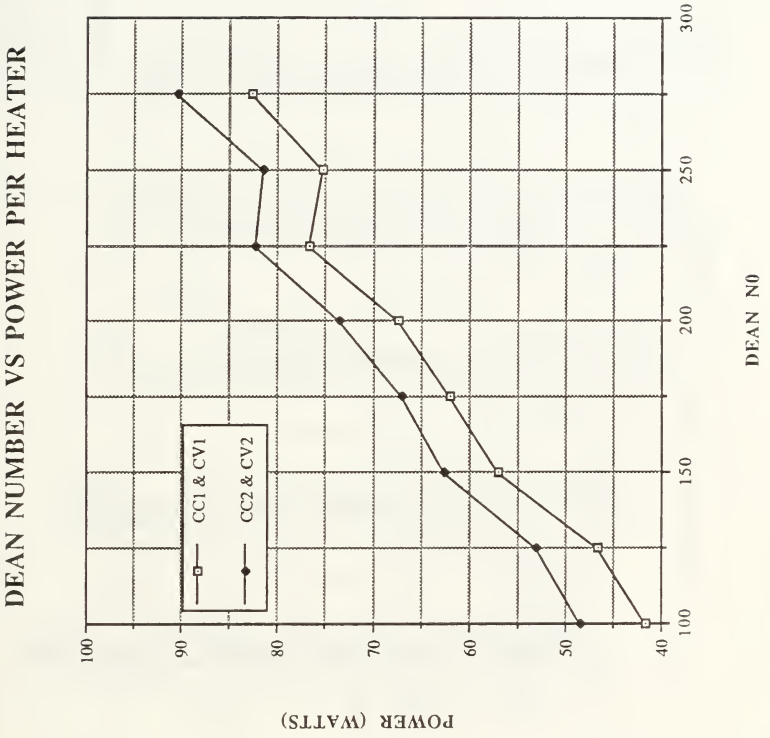

Figure 12. Dean Number Versus Power Input Per Heater

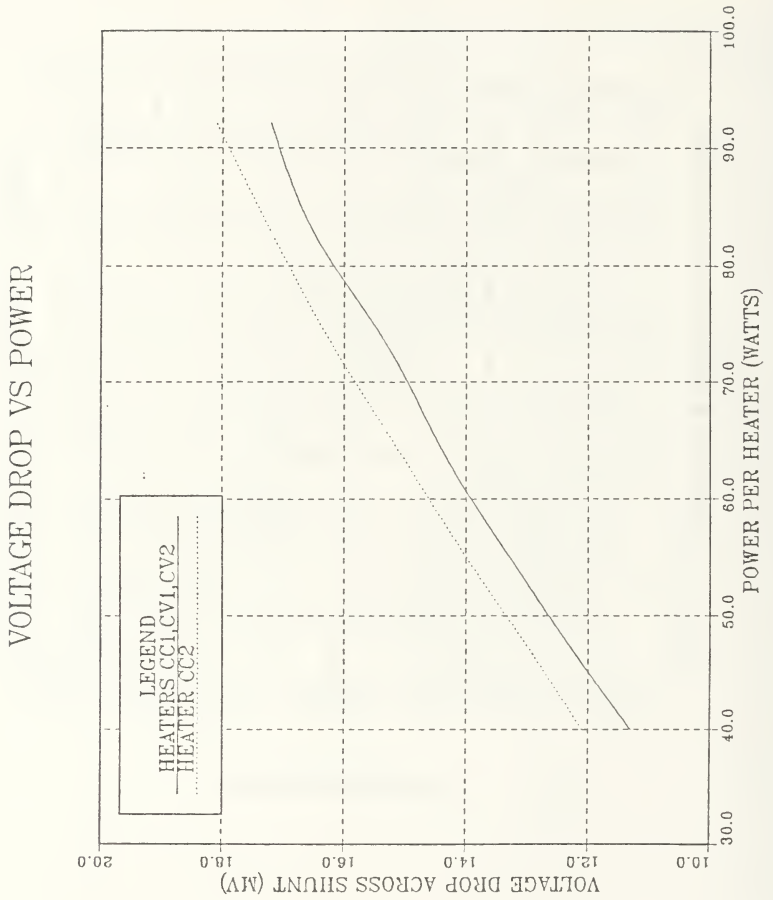

Figure 13. Voltage Drop Across Shunt Versus Heat Flux

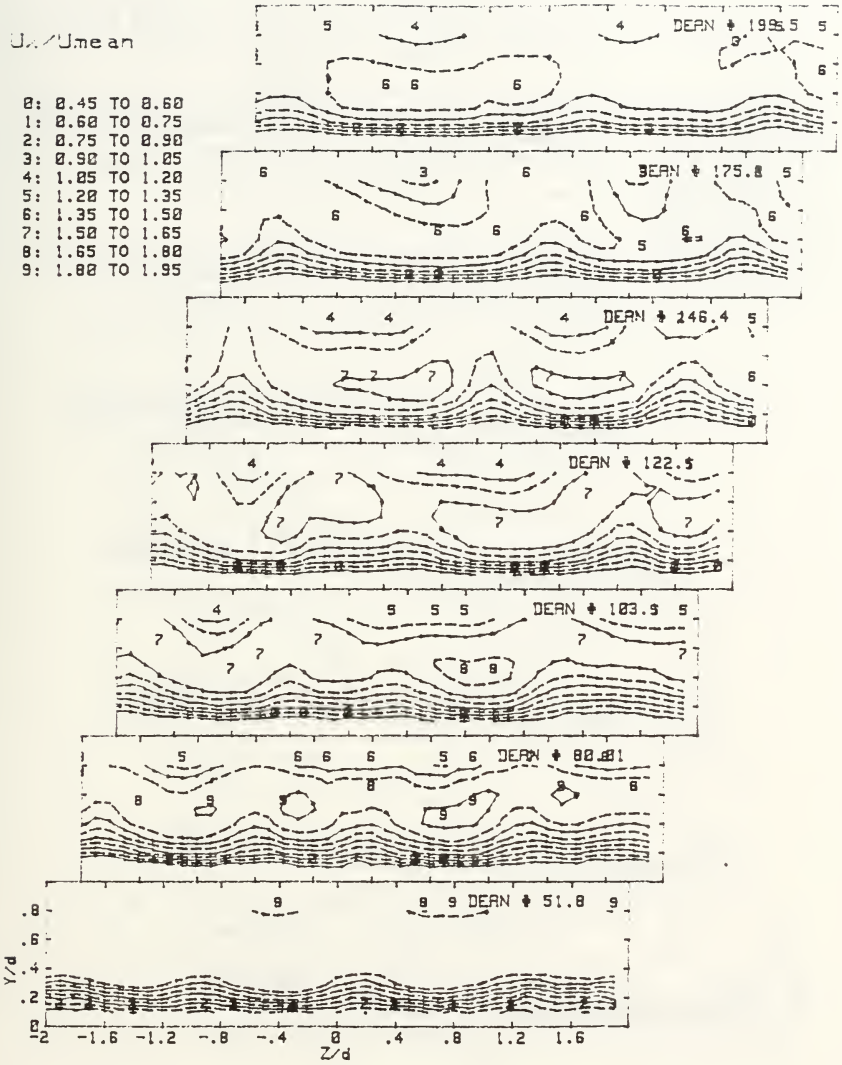

Figure 14. Ux/Umean for De = 50 to 200

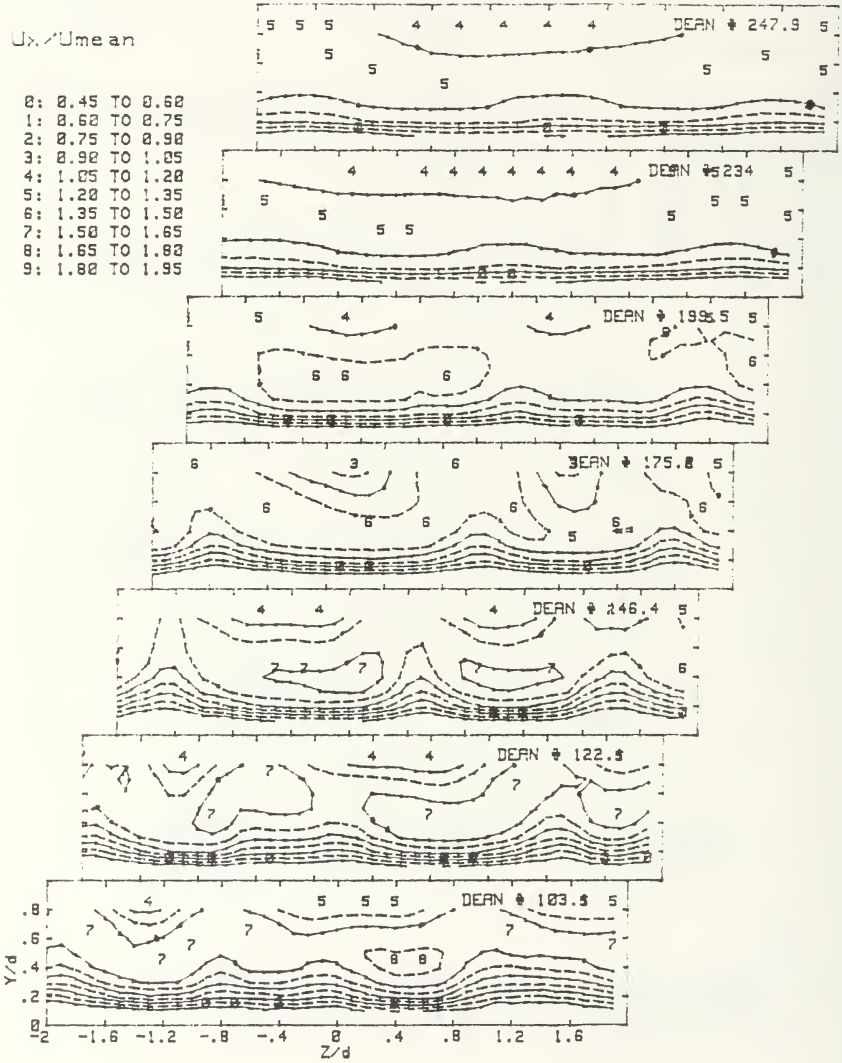

Figure 15. Ux/Umean for De = 100 to 250

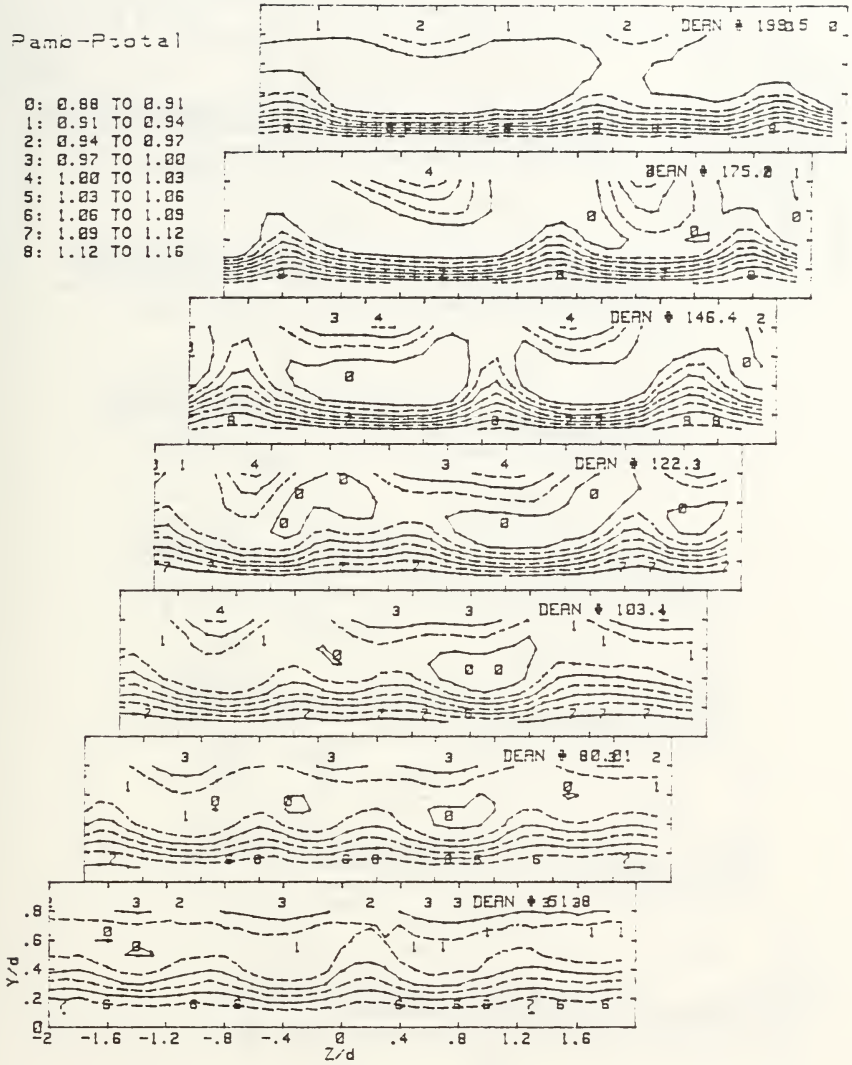

Figure 16. Pamb - Ptot for De = 50 to 200

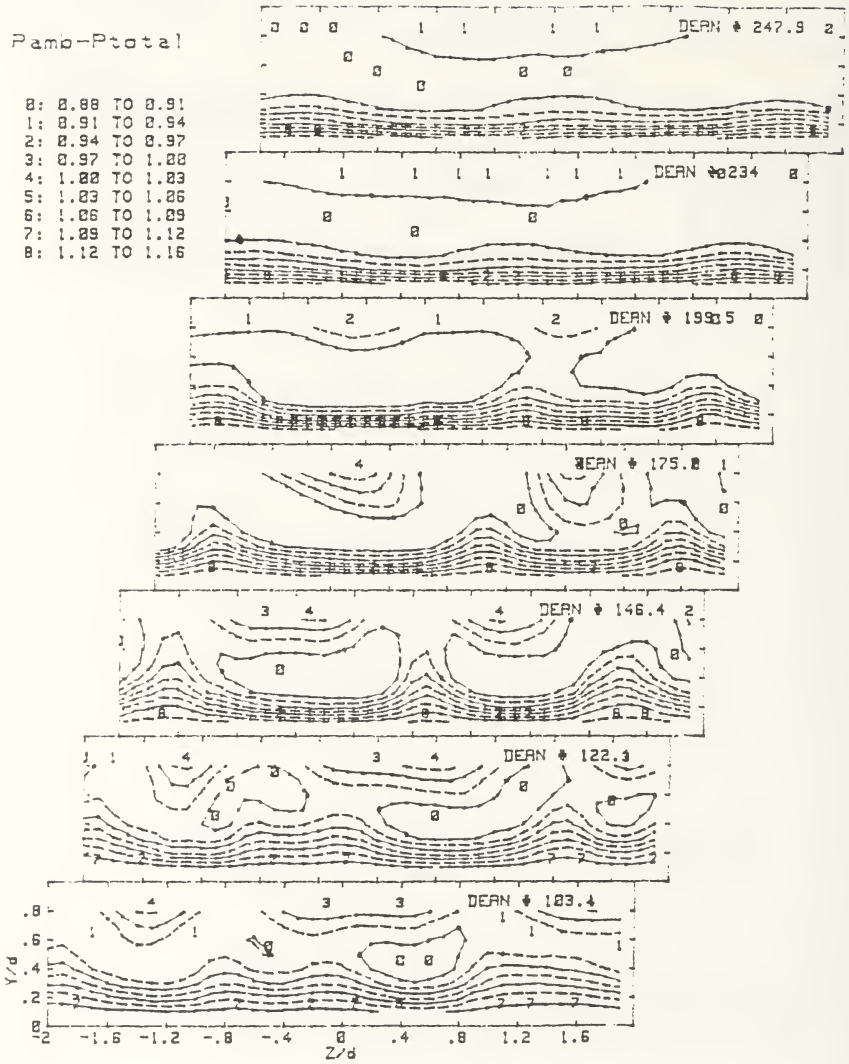

Figure 17. Pamb - Ptot for De = 100 to 250

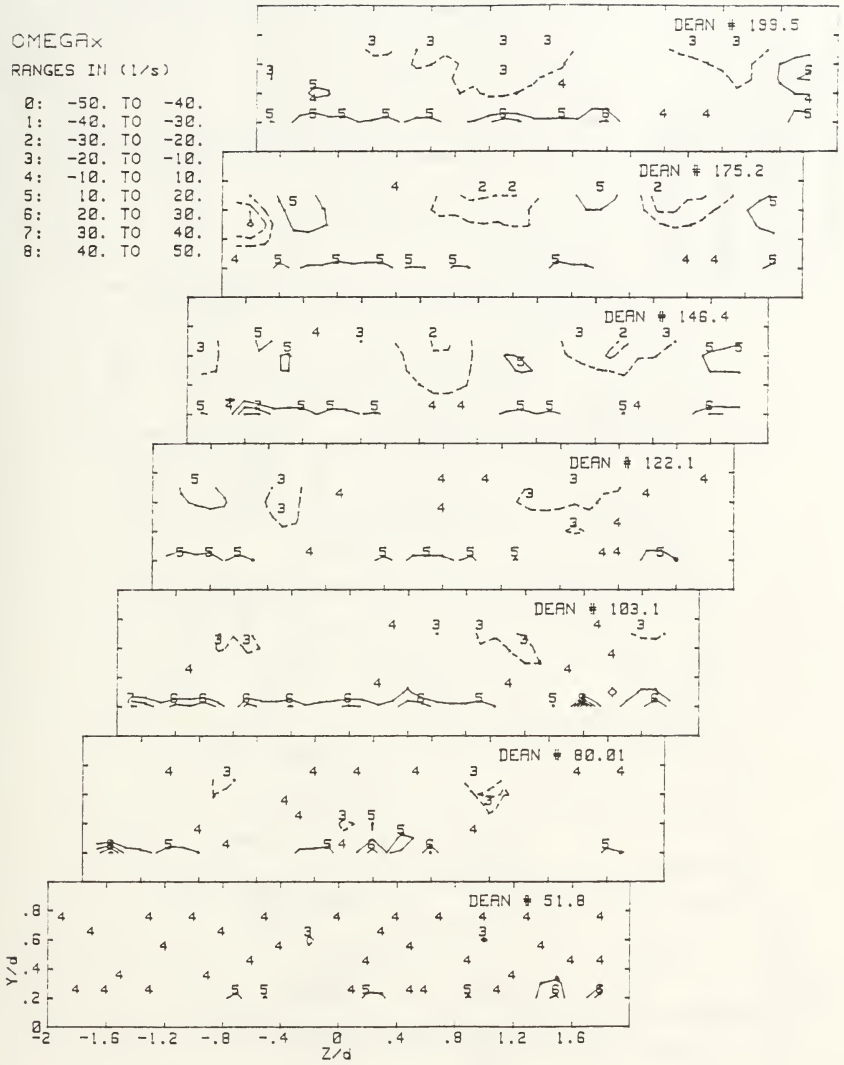

Figure 18. Omegax for De = 50 to 200

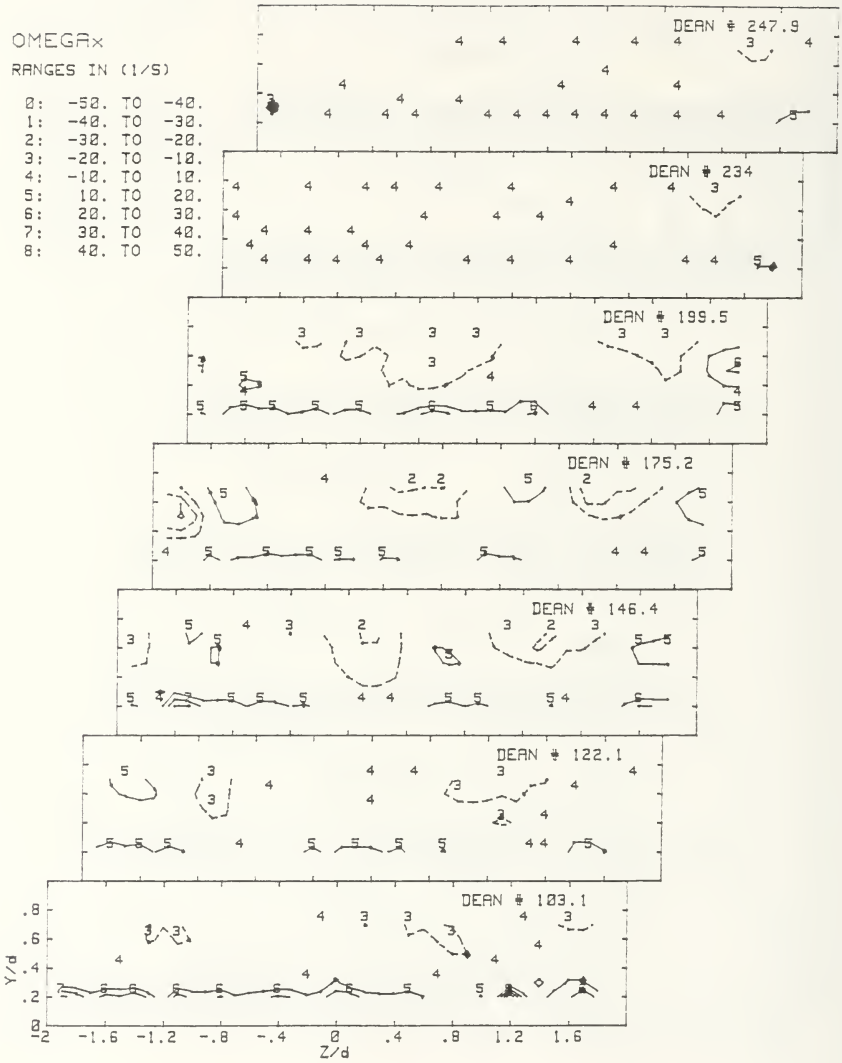

Figure 19. Omegax for De = 100 to 250

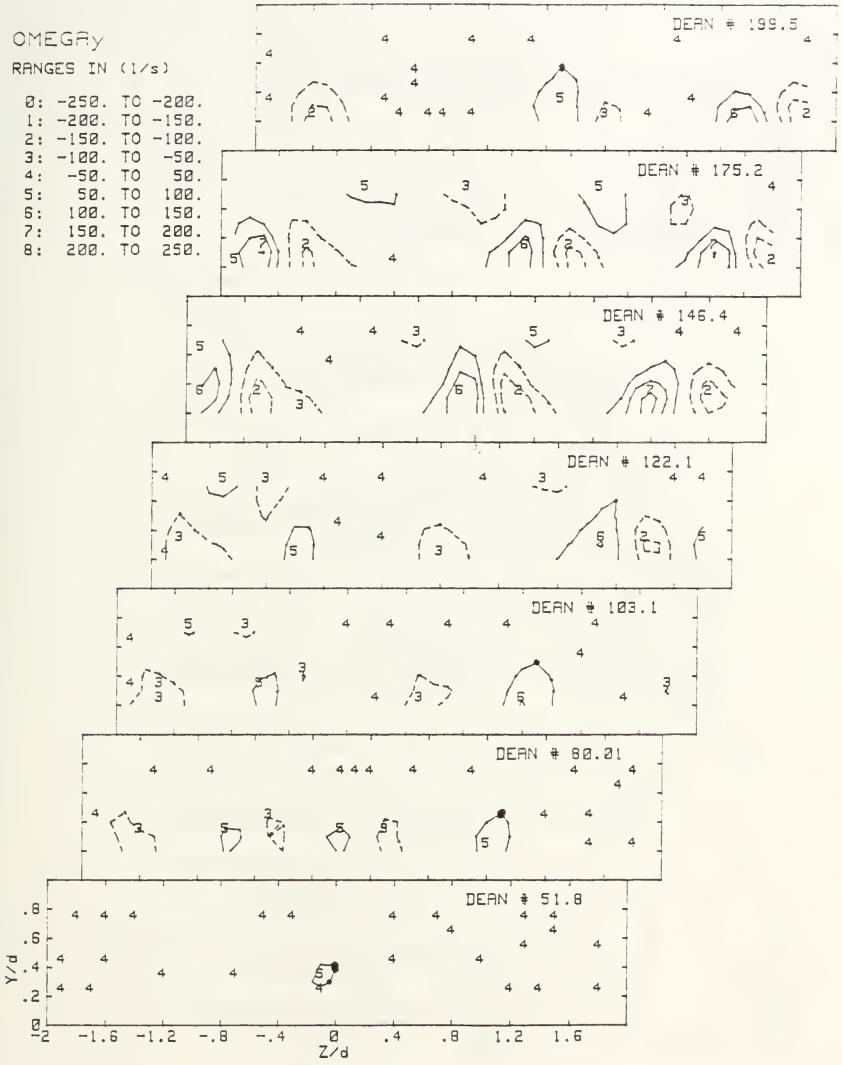

Figure 20. Omegay for De = 50 to 200

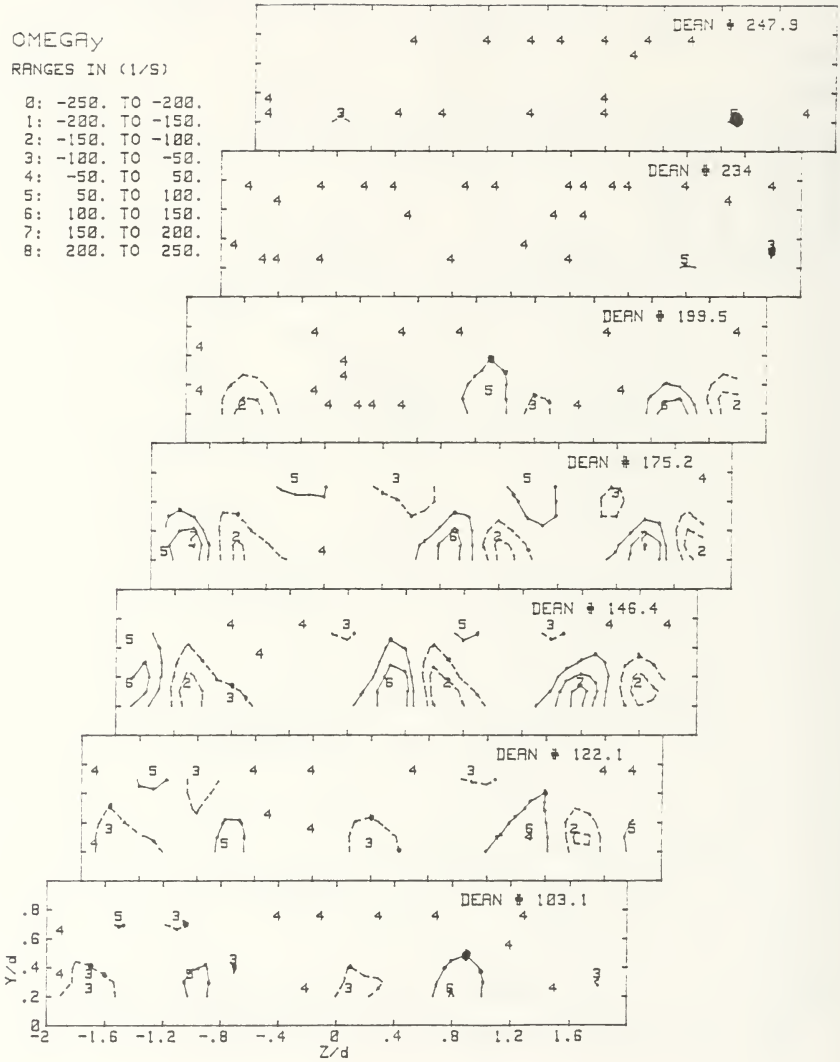

Figure 21. Omegay for De = 100 to 250

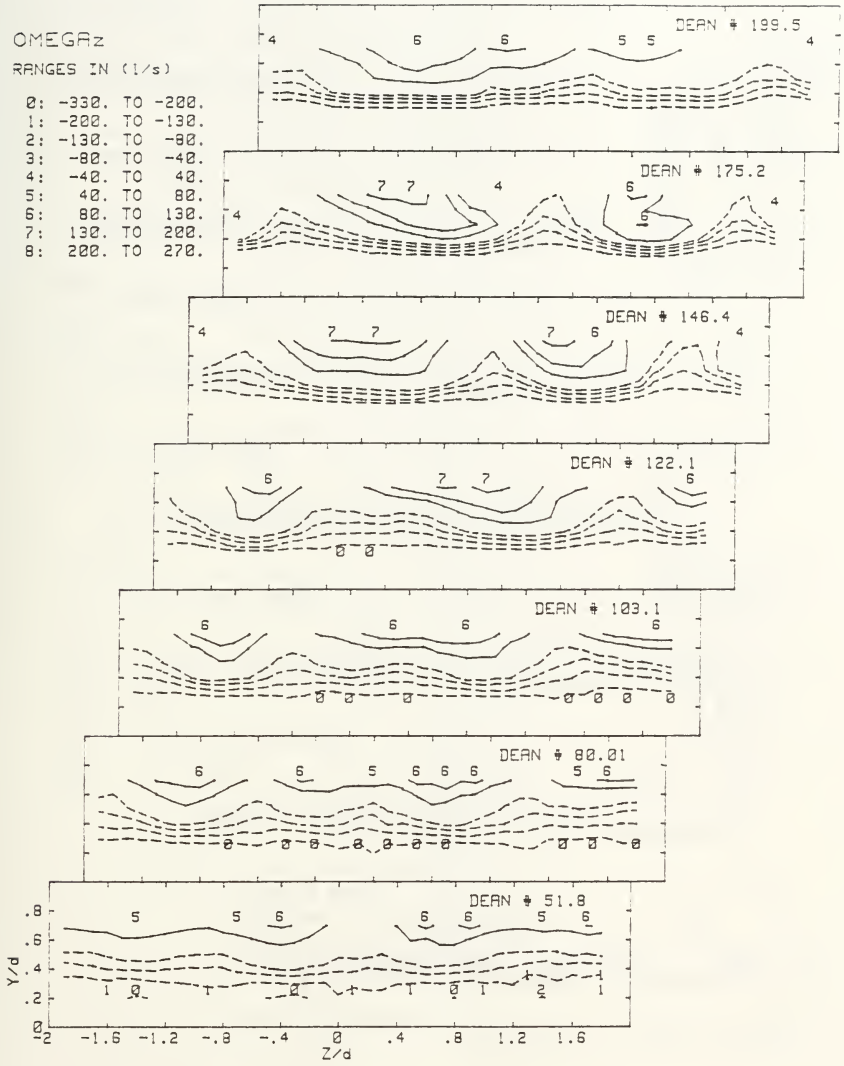

Figure 22. Omegaz for De = 50 to 200

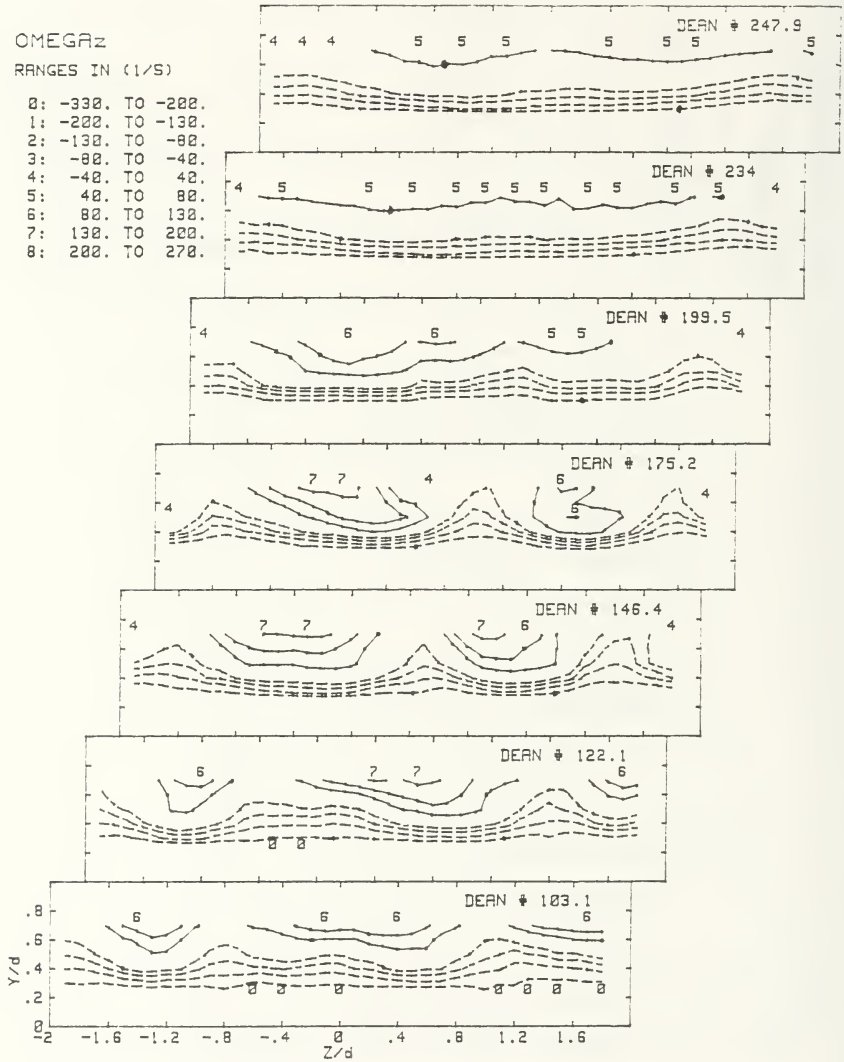

Figure 23. Omegaz for De = 100 to 250

Figure 24. Ux for De = 80

Figure 25. Ux for De = 146

Figure 26. Ux for De = 175

Figure 27. Ux for De = 248

Figure 28. Omegax for De = 80

Figure 29. Omegax for De = 146

Figure 30. Omegax for De = 175

Figure 31. Omegax for De = 248

Figure 32. Omegay for De = 80

Figure 33. Omegay for De = 146

Figure 34. Omegay for De = 175

Figure 35. Omegay for De = 248

Figure 36. Omegaz for De = 80

Figure 37. Omegaz for De = 146

Figure 38. Omegaz for De = 175

Figure 39. Omegaz for De = 248

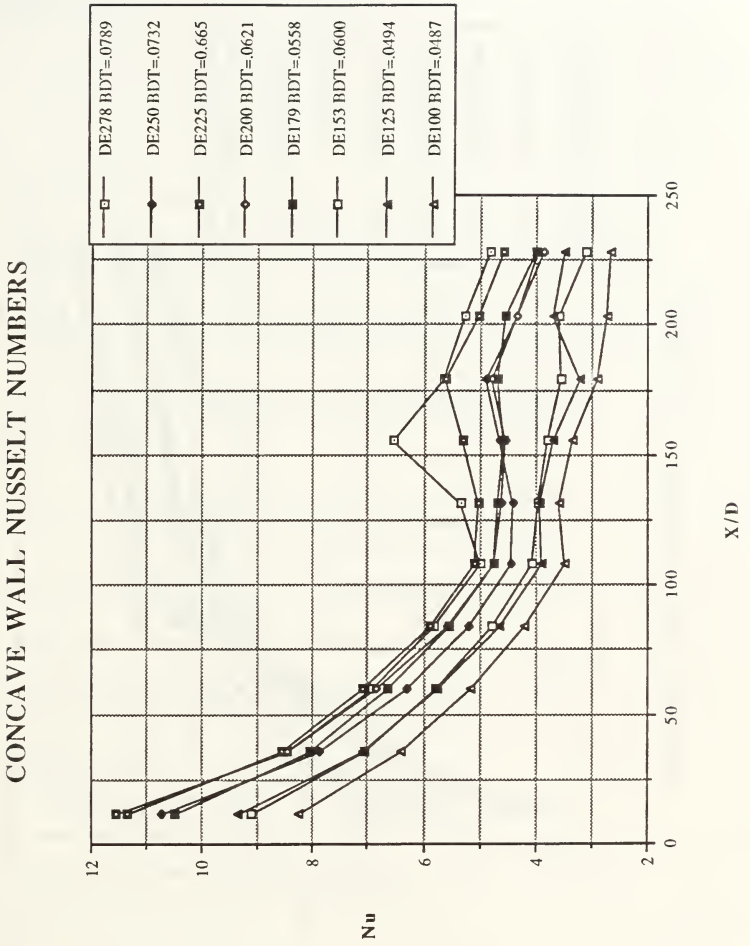

Figure 40. Concave Wall Nusselt Number Versus x/d

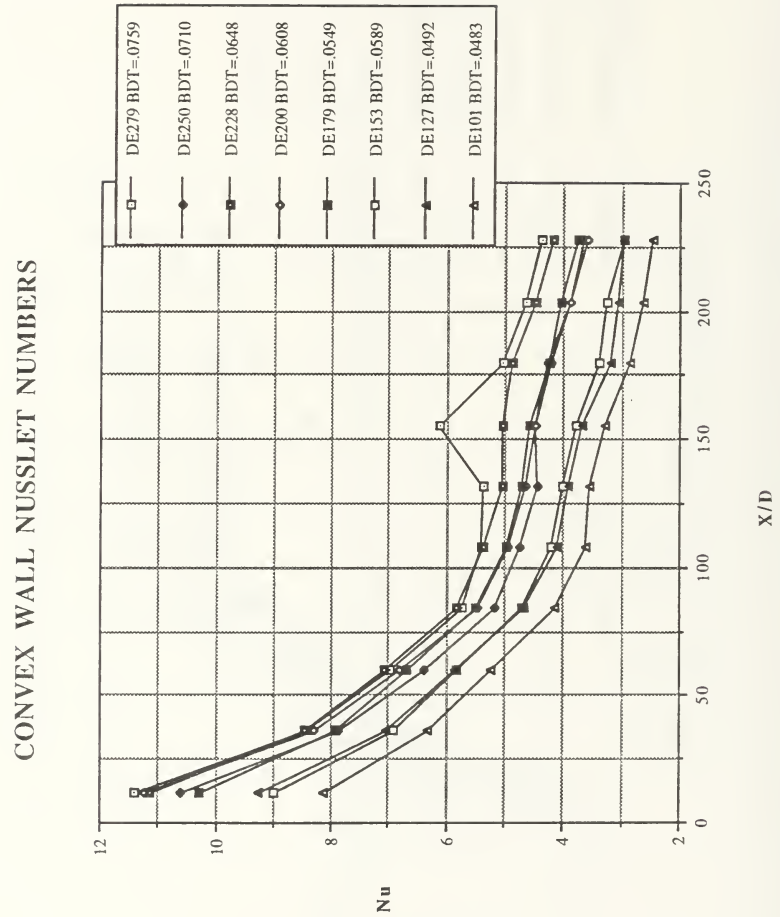

Figure 41. Convex Wall Nusselt Number Versus x/d

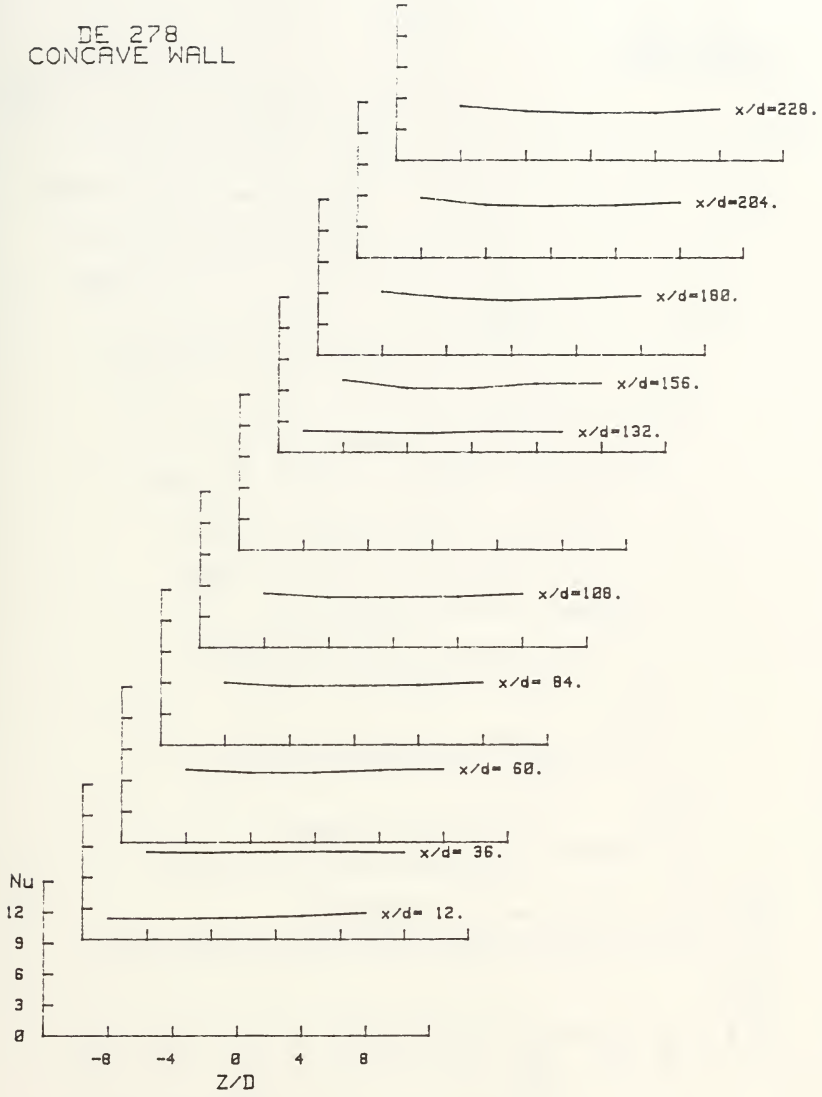

Figure 42. 3D Nusselt Number Distribution for De = 278 Concave Wall

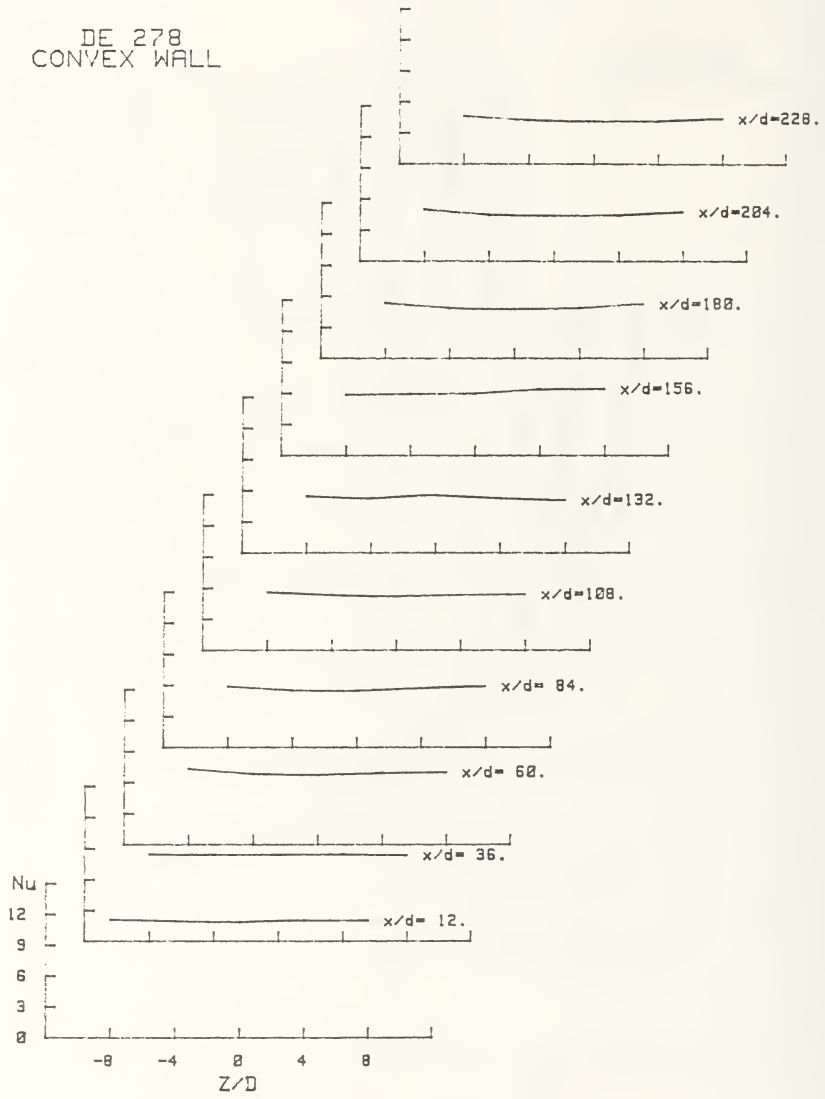

Figure 43. 3D Nusselt Number Distribution for De = 278 Convex Wall

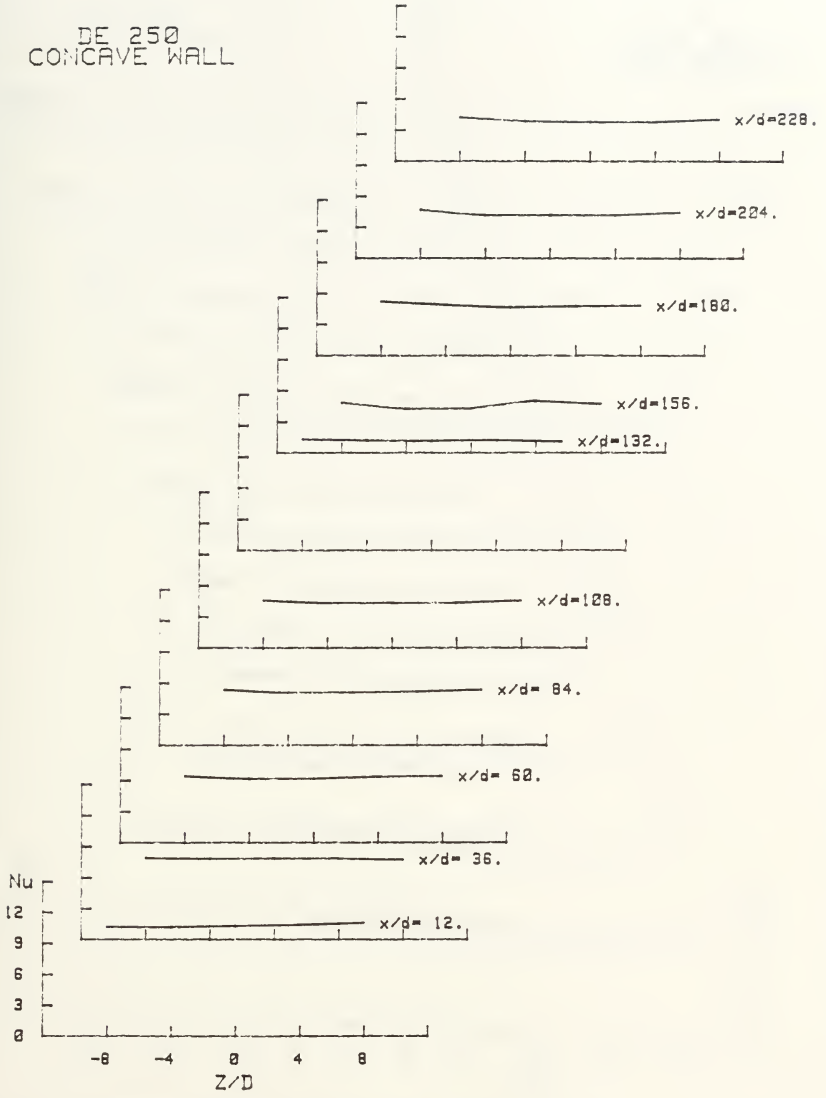

Figure 44. 3D Nusselt Number Distribution for De = 250 Concave Wall

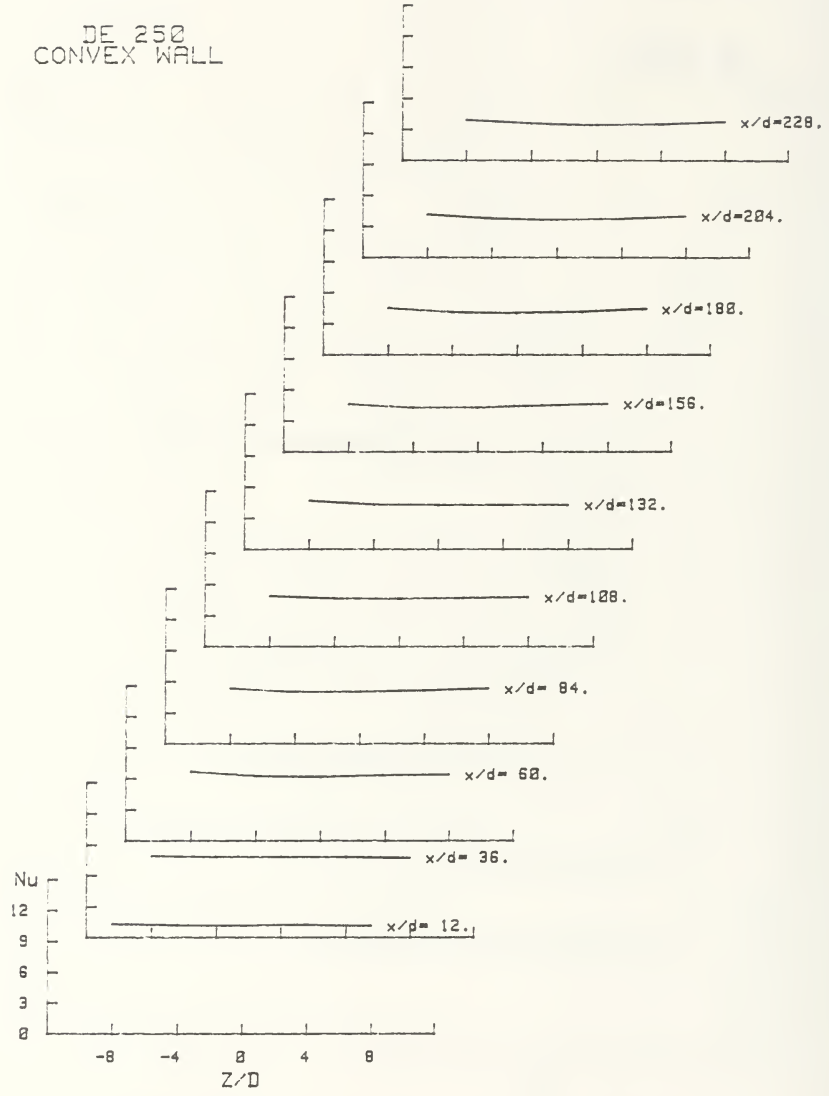

Figure 45. 3D Nusselt Number Distribution for De = 250 Convex Wall

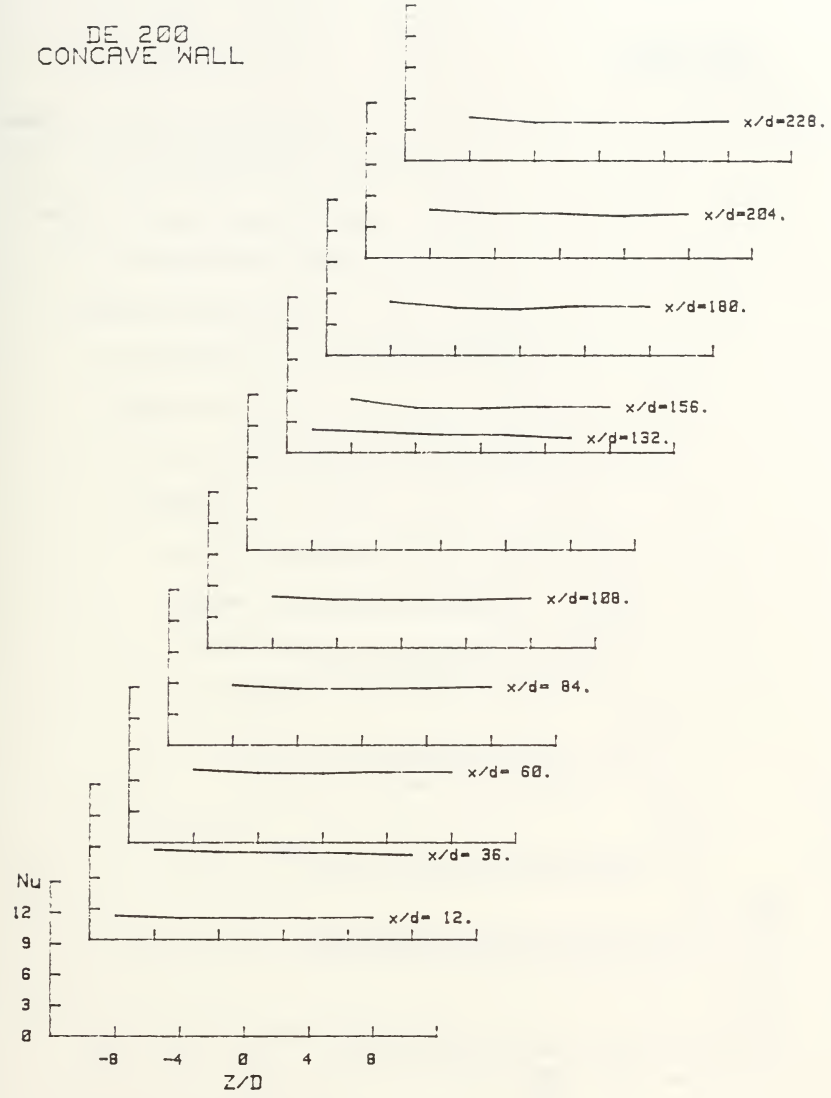

Figure 46. 3D Nusselt Number Distribution for De = 200 Concave Wall

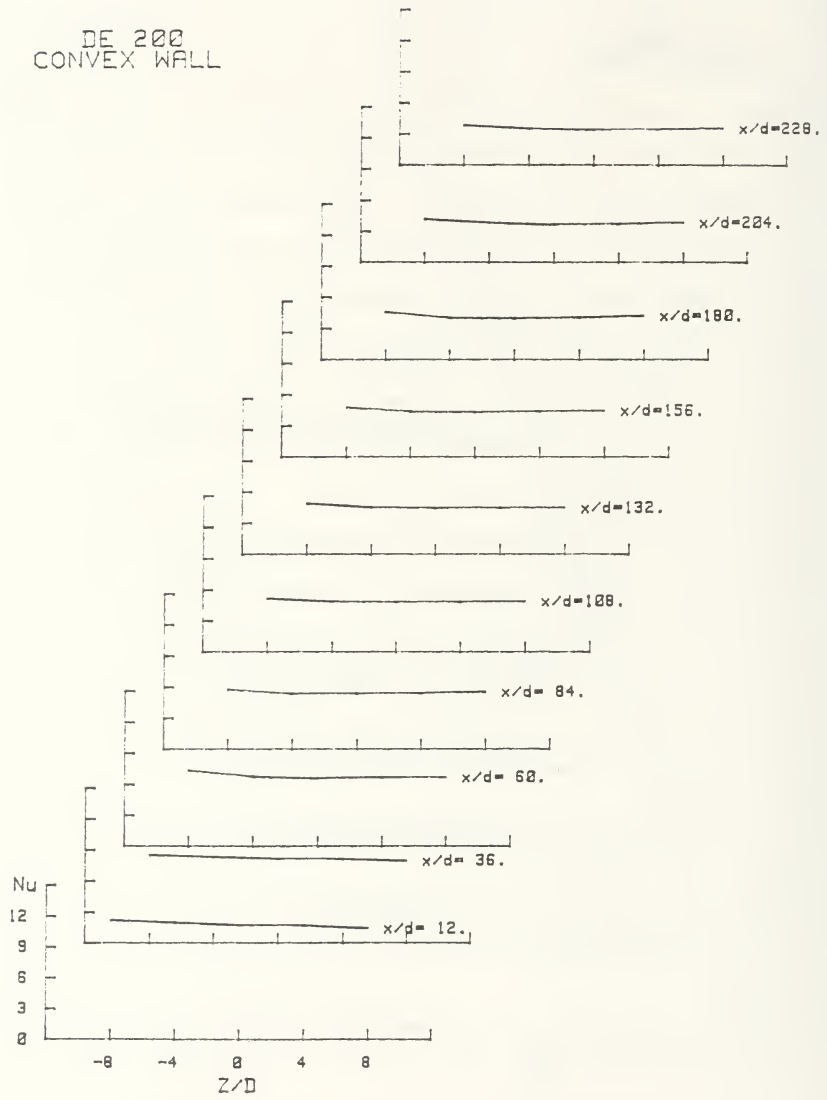

Figure 47. 3D Nusselt Number Distribution for De = 200 Convex Wall

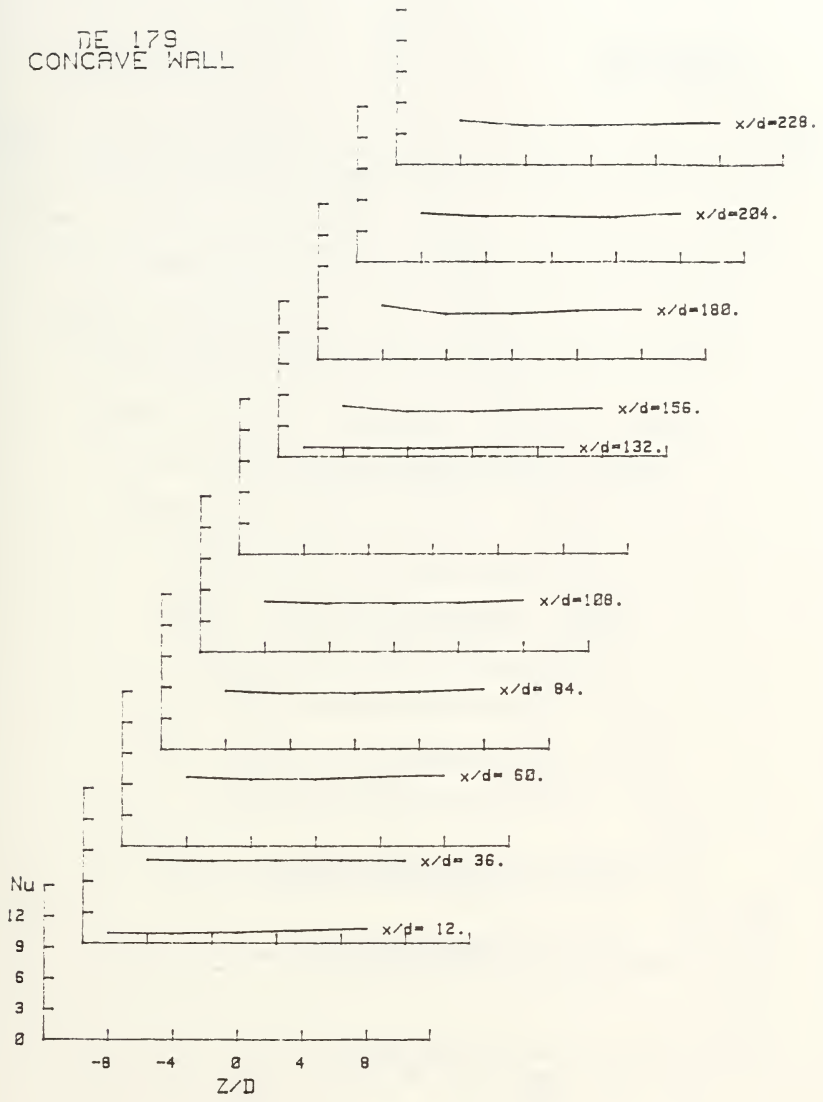

Figure 48. 3D Nusselt Number Distribution for De = 179 Concave Wall

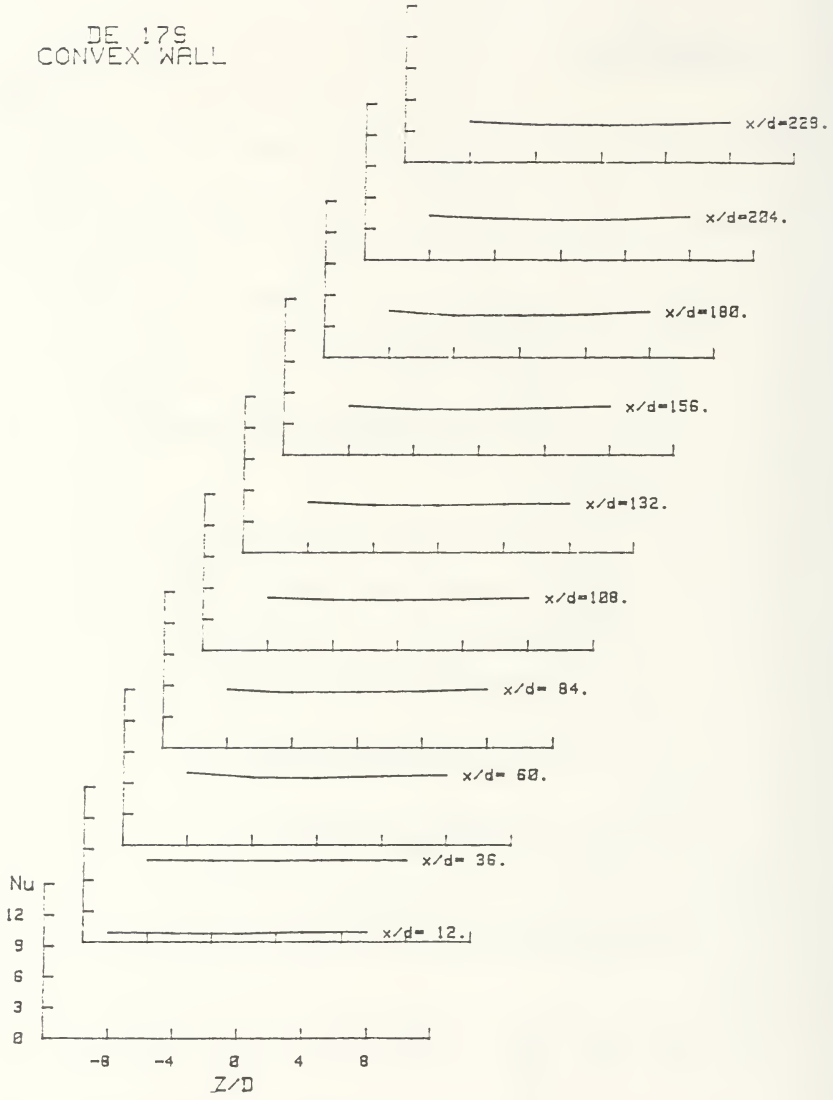

Figure 49. 3D Nusselt Number Distribution for De = 179 Convex Wall

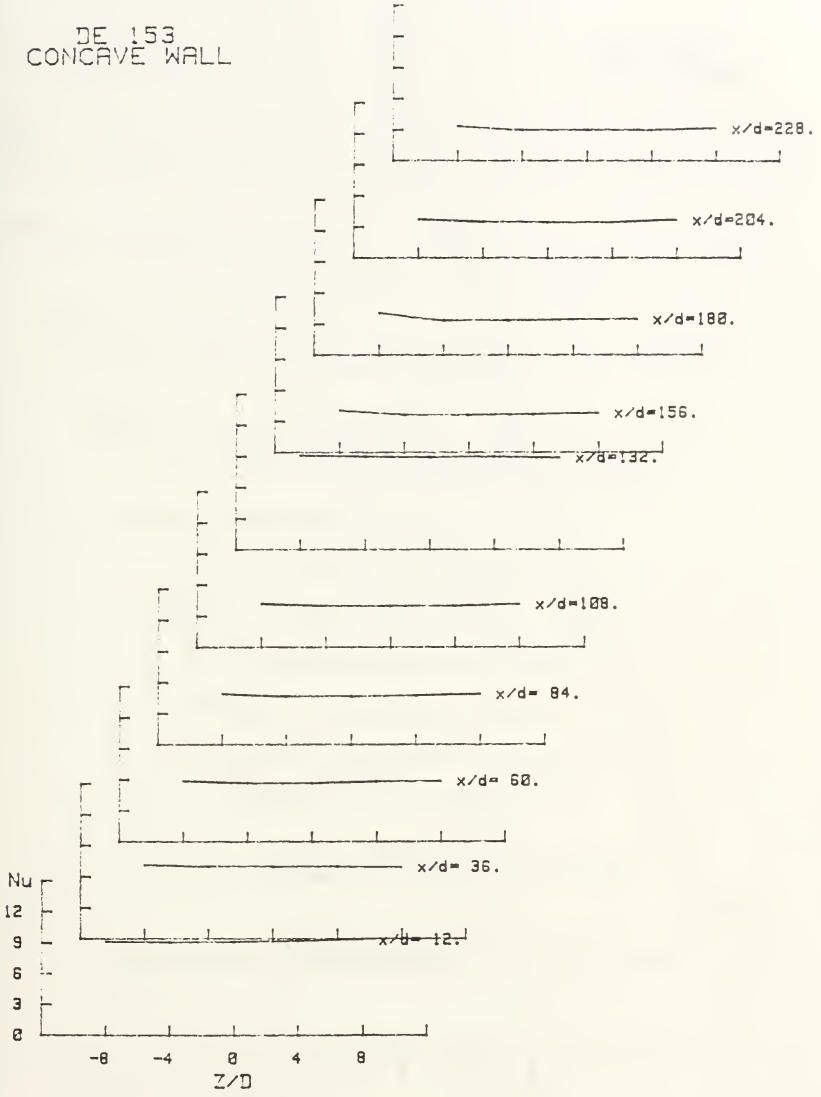

Figure 50. 3D Nusselt Number Distribution for De = 153 Concave Wall

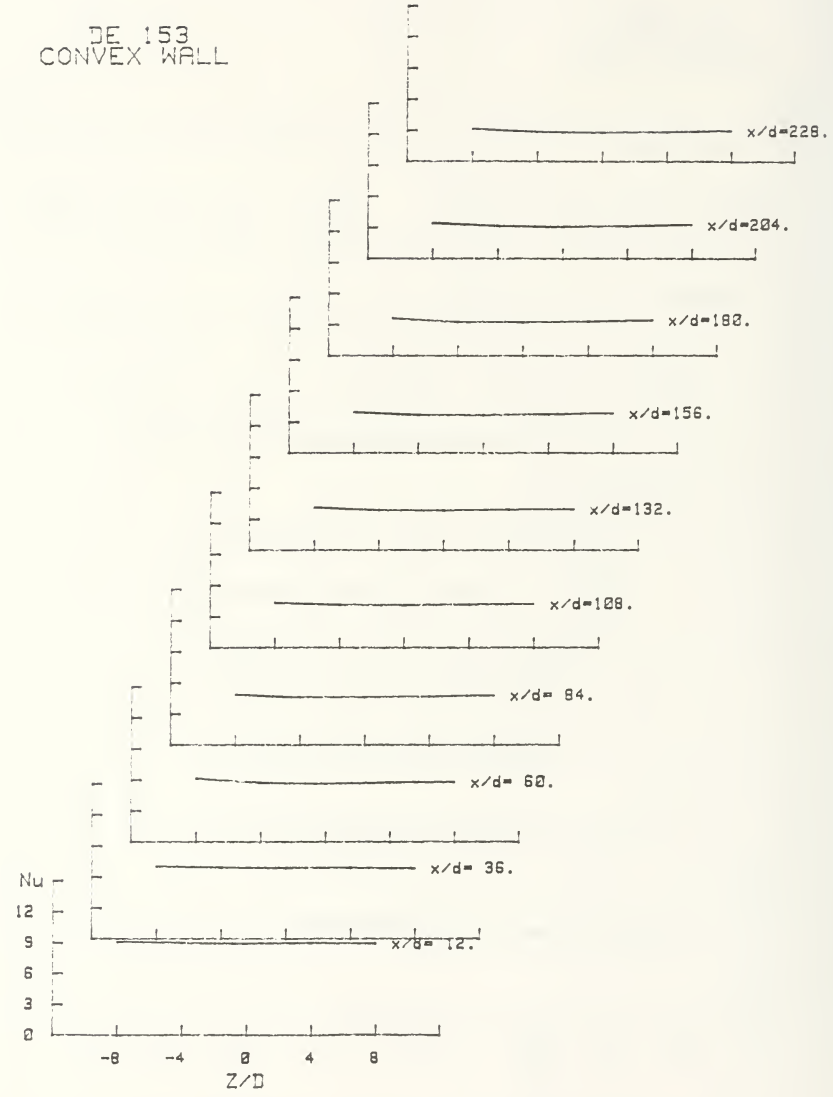

Figure 51. 3D Nusselt Number Distribution for De = 153 Convex Wall

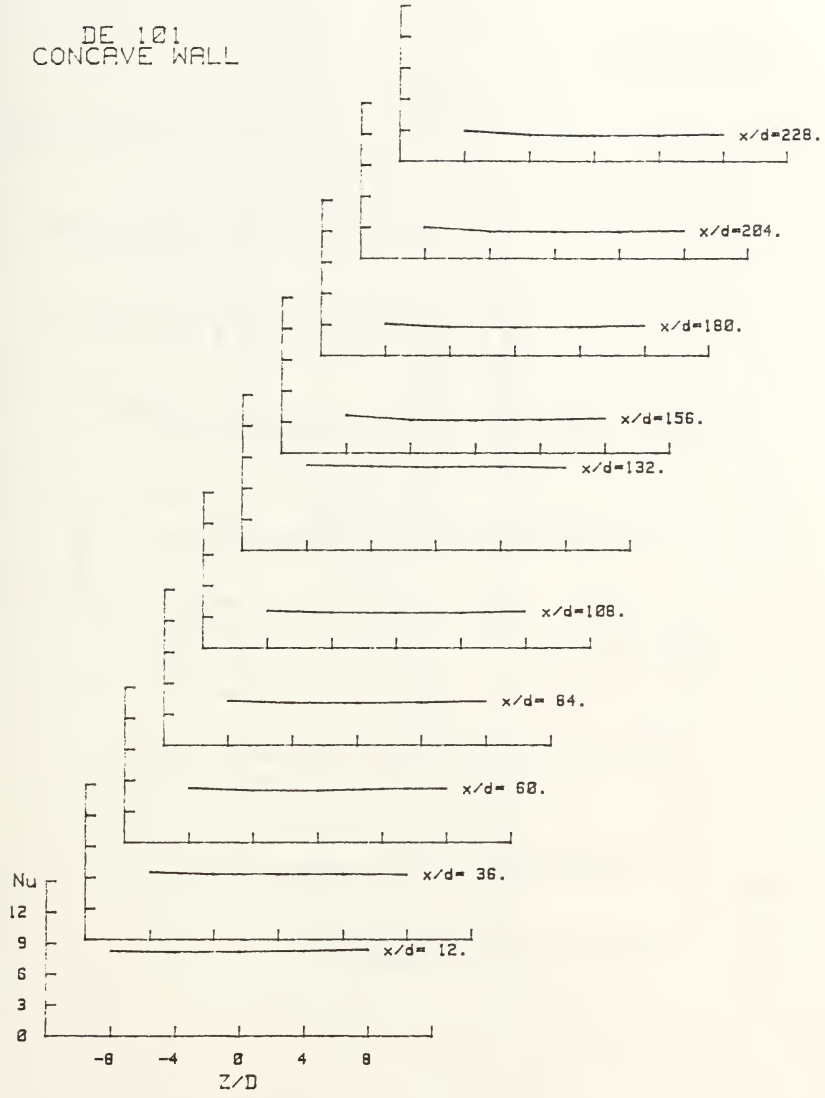

Figure 52. 3D Nusselt Number Distribution for De = 101 Concave Wall

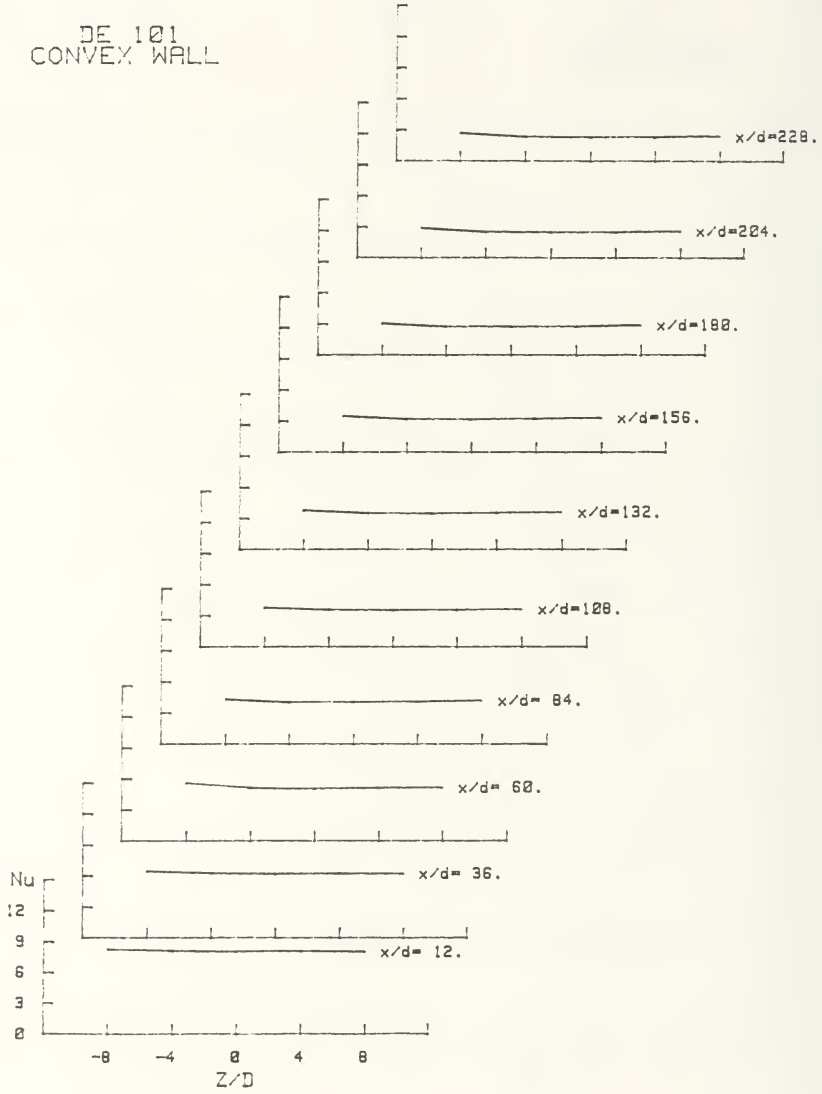

Figure 53. 3D Nusselt Number Distribution for De = 101 Convex Wall

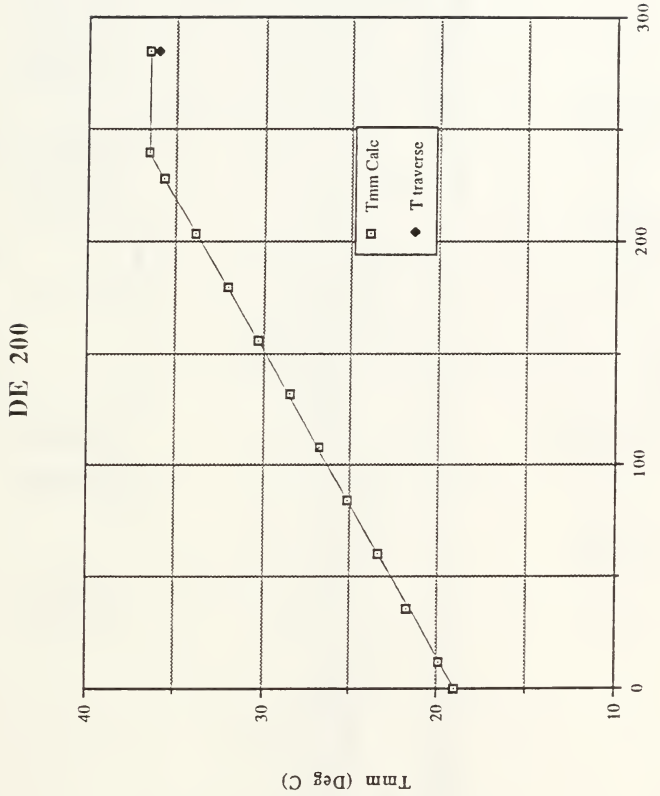

Figure 54. Tmm Versus x/d for De = 200

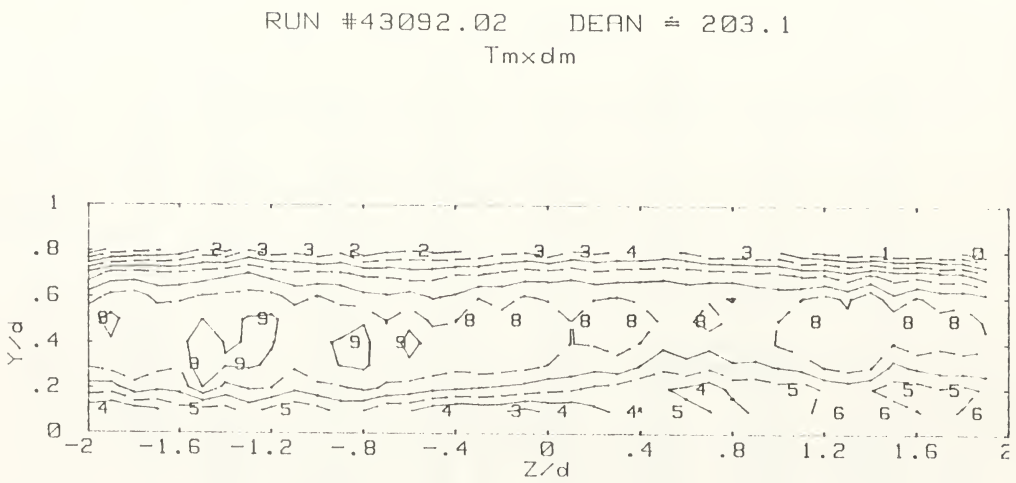

Tmxdm (deg.C) RANGES

0 :	22.68	- 22.95	5 :	24.07	- 24.34
1 :	22.95	- 23.23	6 :	24.34	- 24.62
2 :	23.23	- 23.51	7 :	24.62	- 24.9
3 :	23.51	- 23.79	8 :	24.9	- 25.18
4 :	23.79	- 24.07	9 :	25.18	- 25.46

Figure 55. Tmm Traverse Plot for De = 203

Figure 56. Ux Traverse Plot for De = 200

Figure 57. Tmm * Ux Plot for De = 200

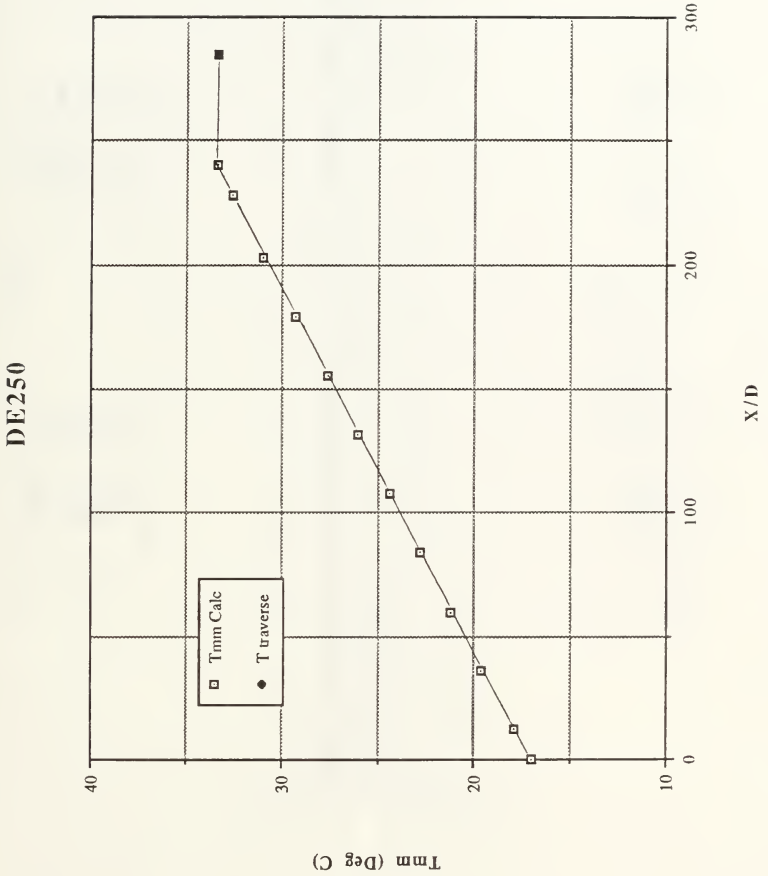

Figure 58. Tmm Versus x/d for De = 250

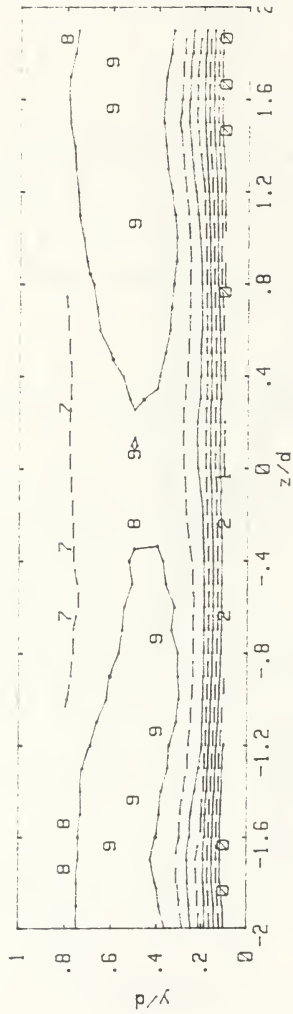

Figure 59. Tmm Traverse Plot for De = 250

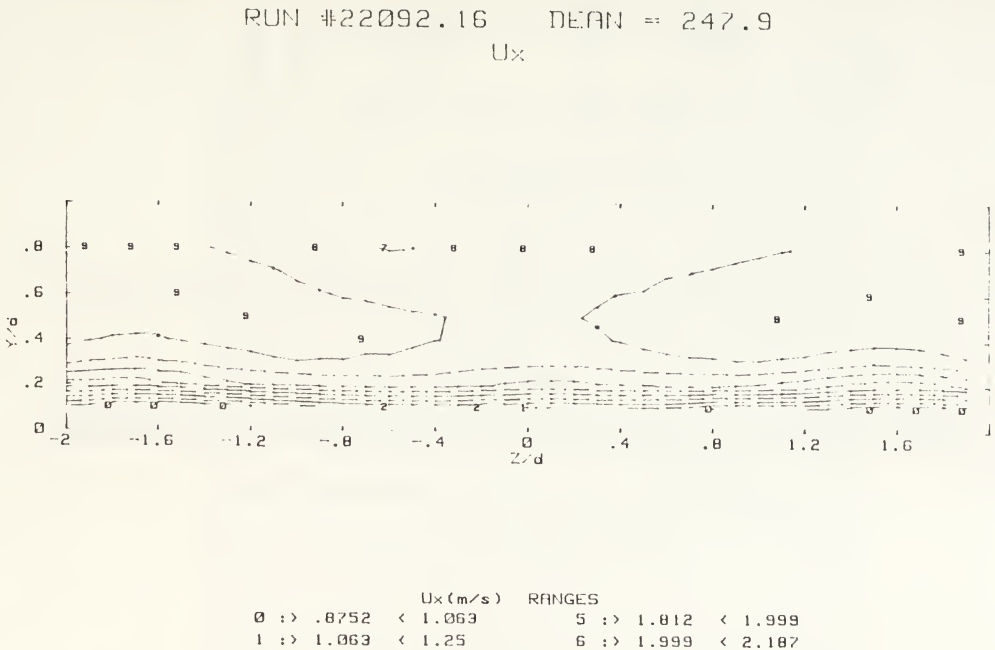

Figure 60. Ux Traverse Plot for De = 250

Figure 61. Tmm * Ux Plot for De = 250

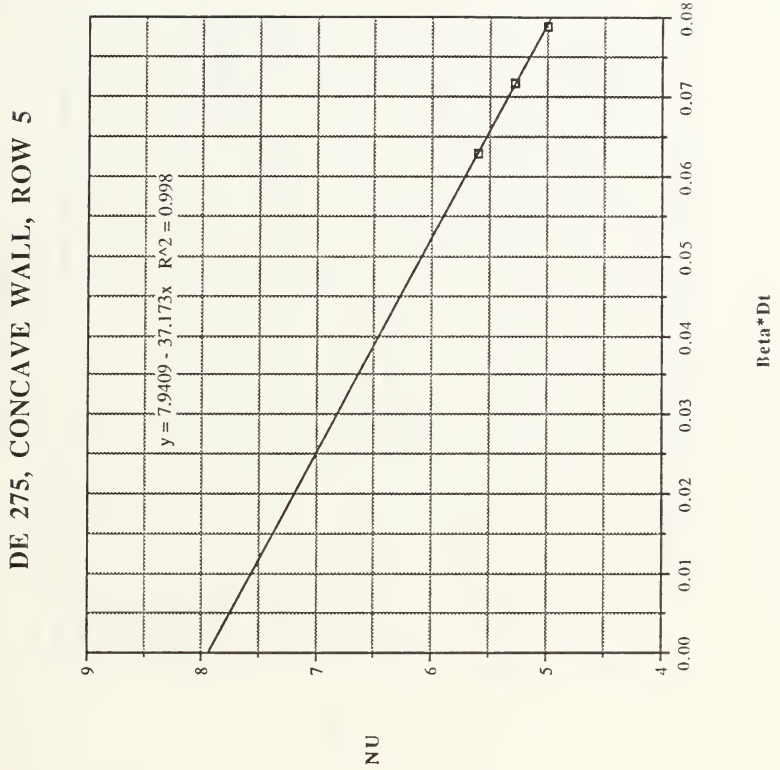

Figure 62. Nusselt Number Versus Beta * Dt for De = 275 Concave Wall

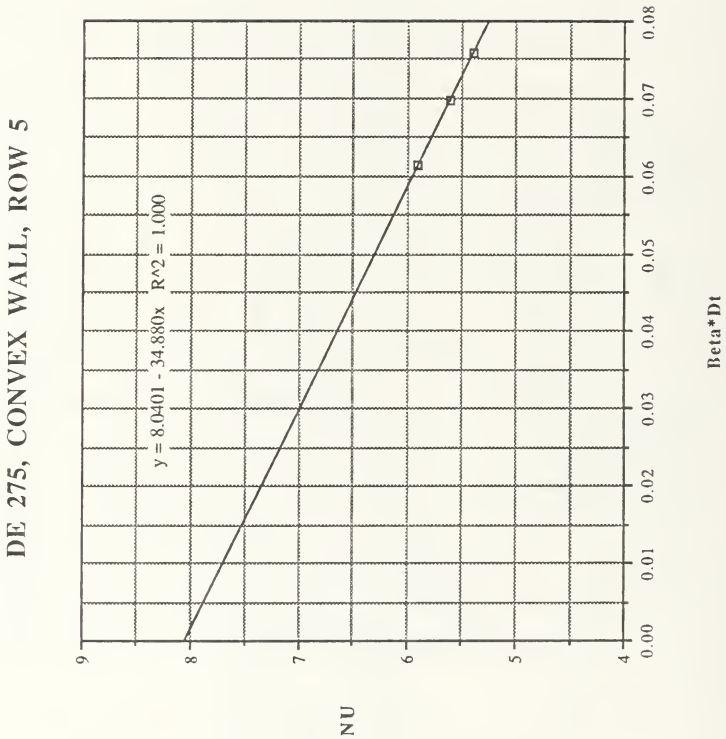

Figure 63. Nusselt Number Versus Beta * Dt for De = 275 Convex Wall

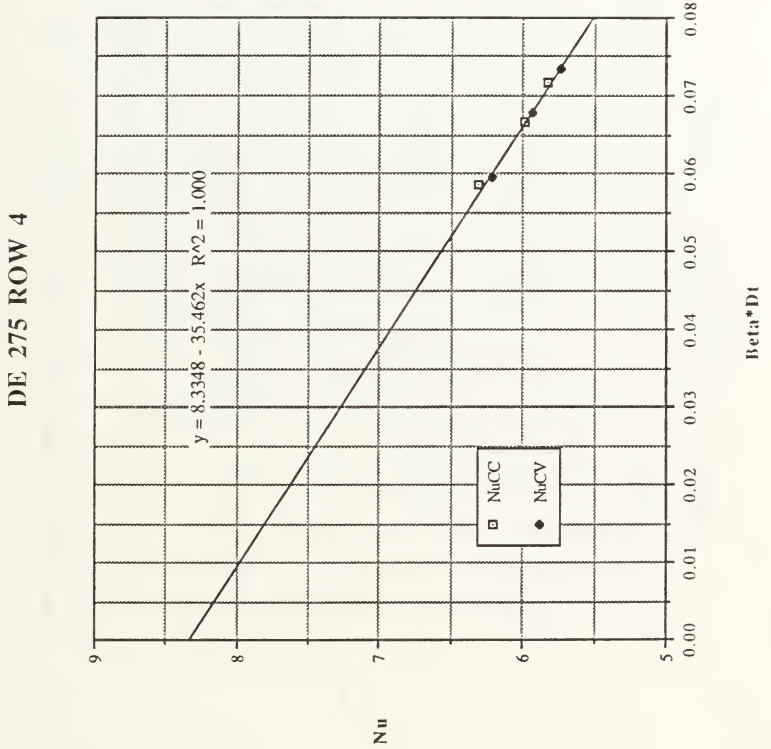

Figure 64. Nusselt Number Versus Beta * Dt for De = 275 Row 4

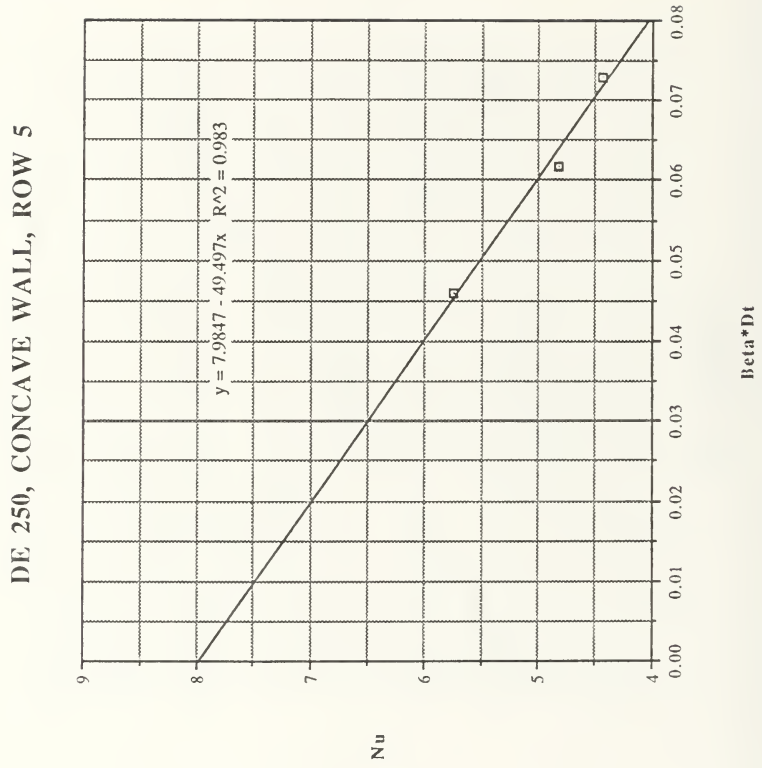

Figure 65. Nusselt Number Versus Beta * Dt for De = 250 Concave Wall for 3 Data Points

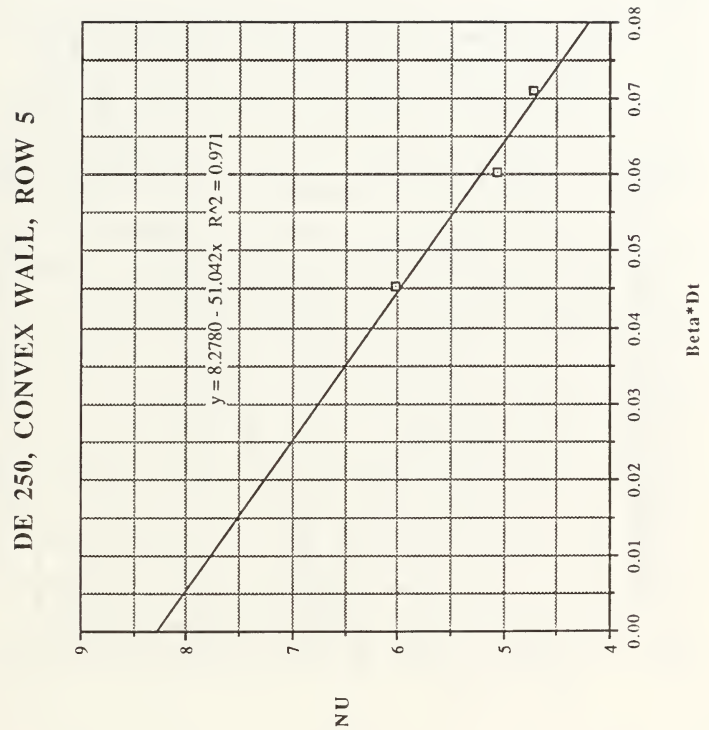

Figure 66. Nusselt Number Versus Beta * Dt for De = 250 Convex Wall for 3 Data Points

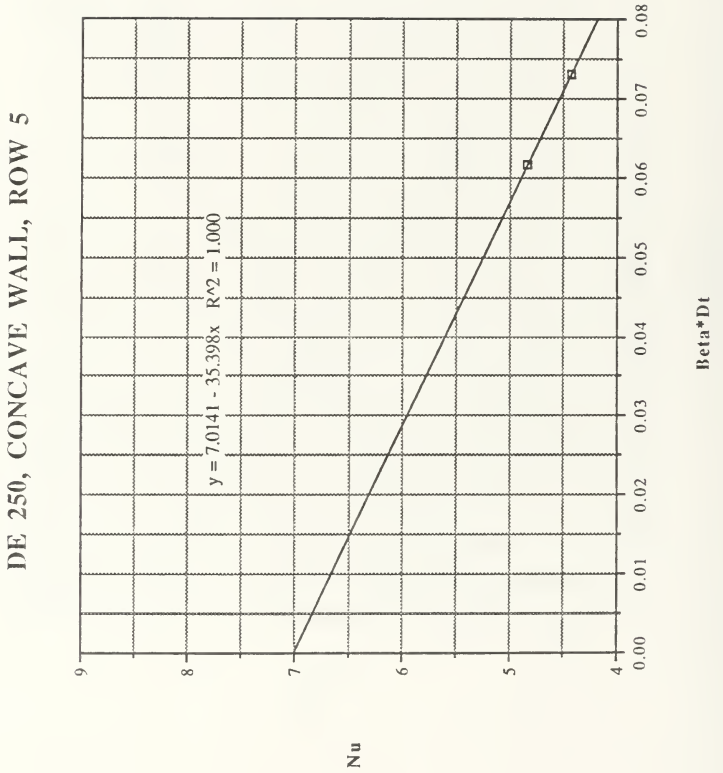

Figure 67. Nusselt Number Versus Beta * Dt for De = 250 Concave Wall for 2 Data Points

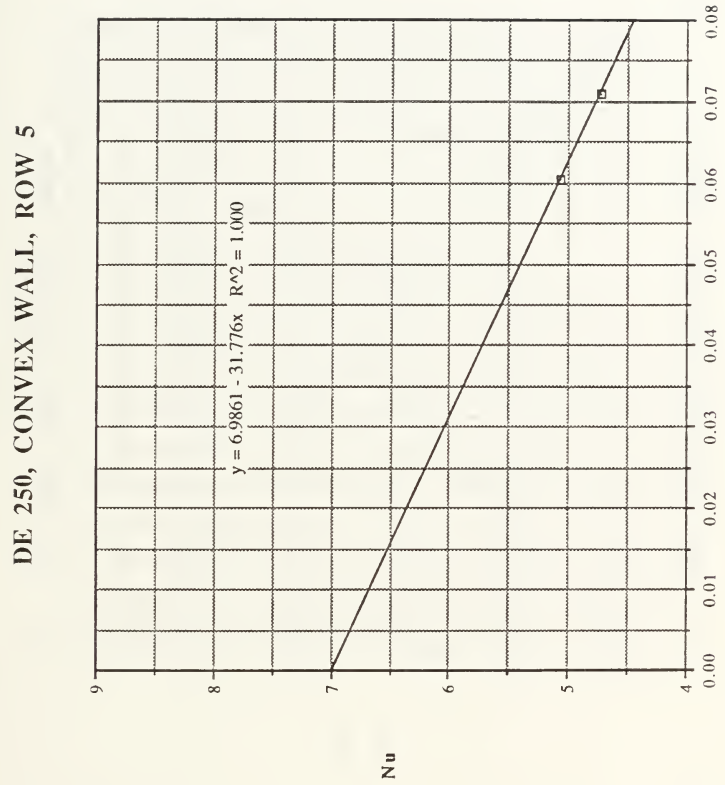

Figure 68. Nusselt Number Versus Beta * Dt for De = 250 Convex Wall for 2 Data Points

Figure 69. Nusselt Number Versus Beta * Dt for De = 250 Concave Wall Row 4

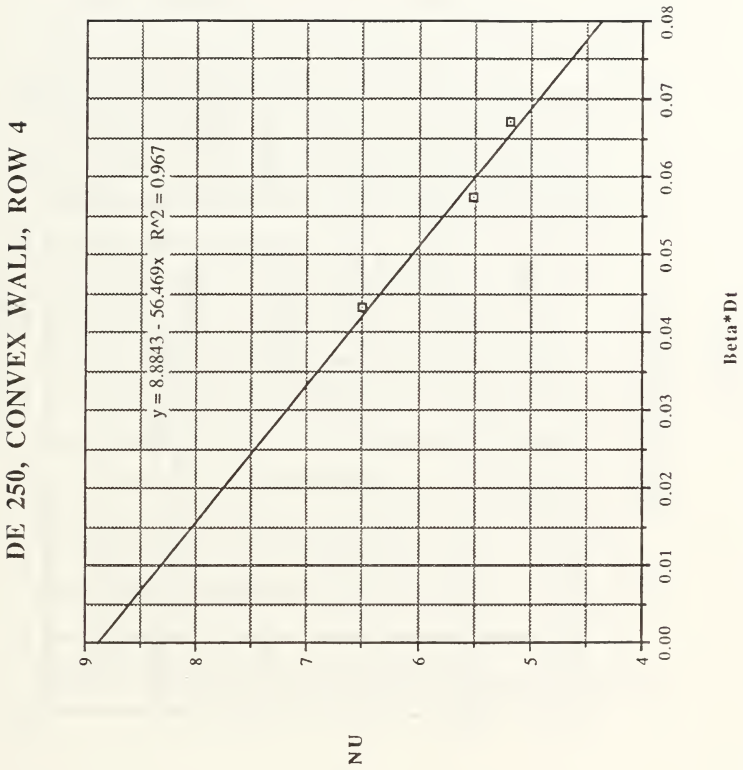

Figure 70. Nusselt Number Versus Beta * Dt for De = 250 Convex Wall Row 4

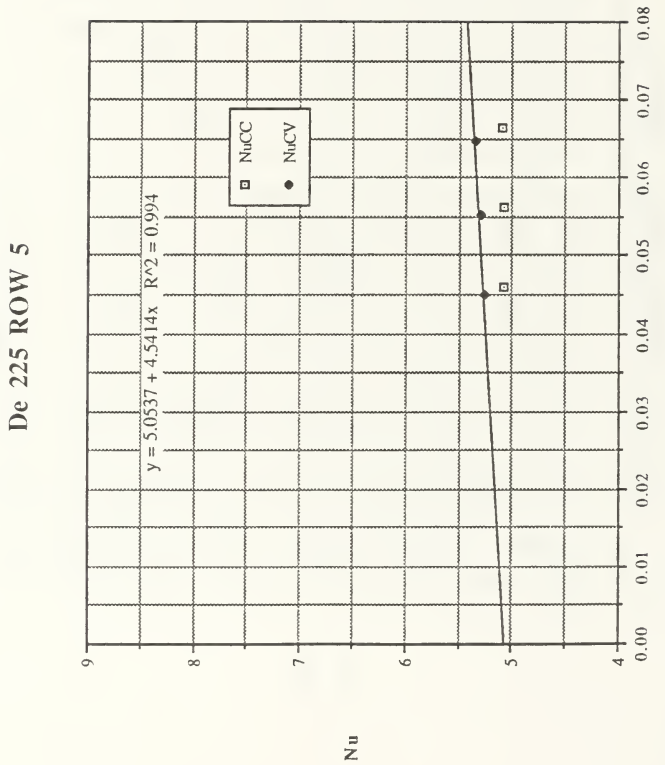

Figure 71. Nusselt Number Versus Beta * Dt for De = 225 Row 5

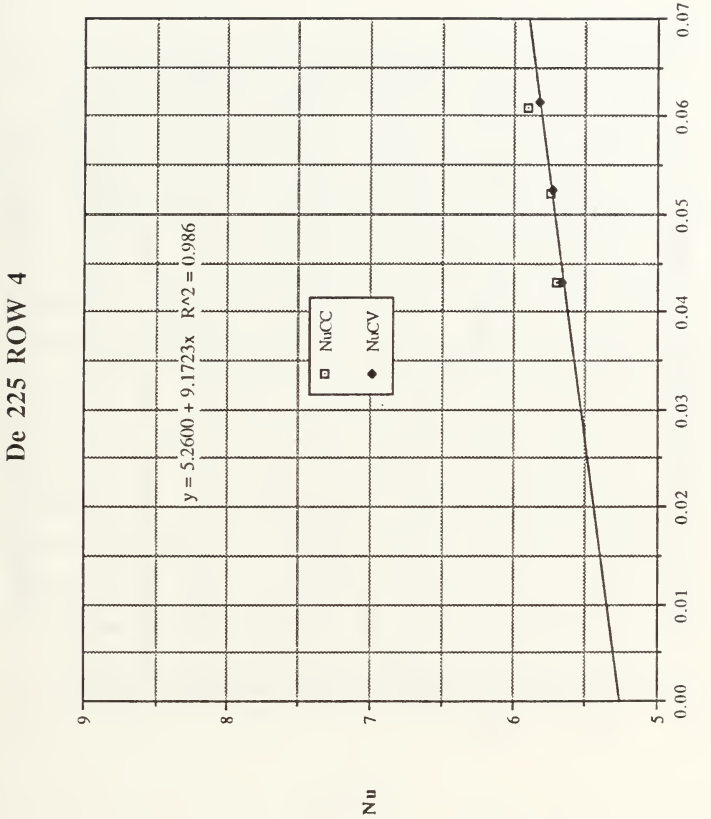

Figure 72. Nusselt Number Versus Beta * Dt for De = 225 Row 4

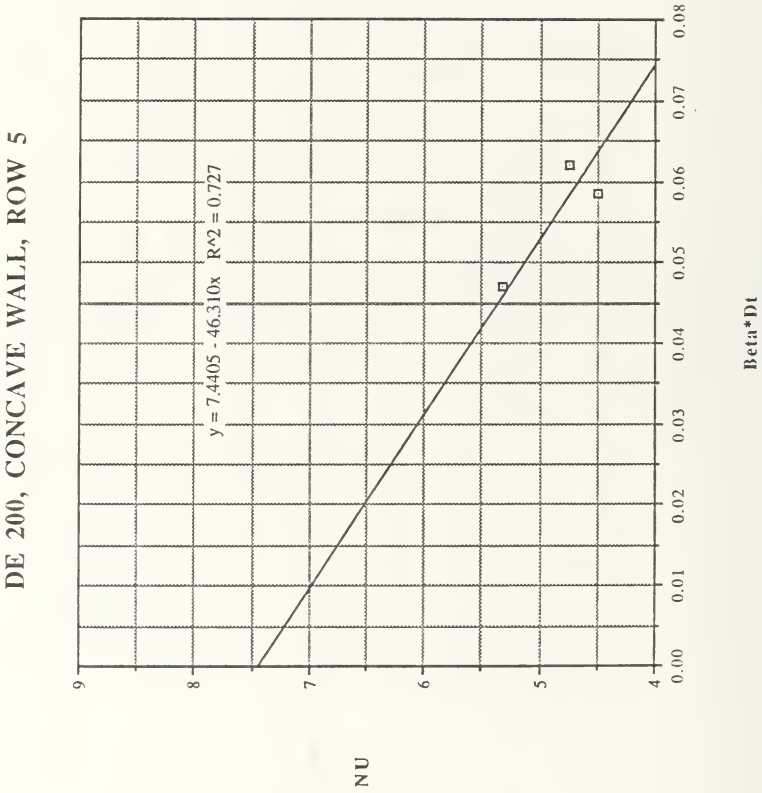

Figure 73. Nusselt Number Versus Beta * Dt for De = 200 Concave Wall

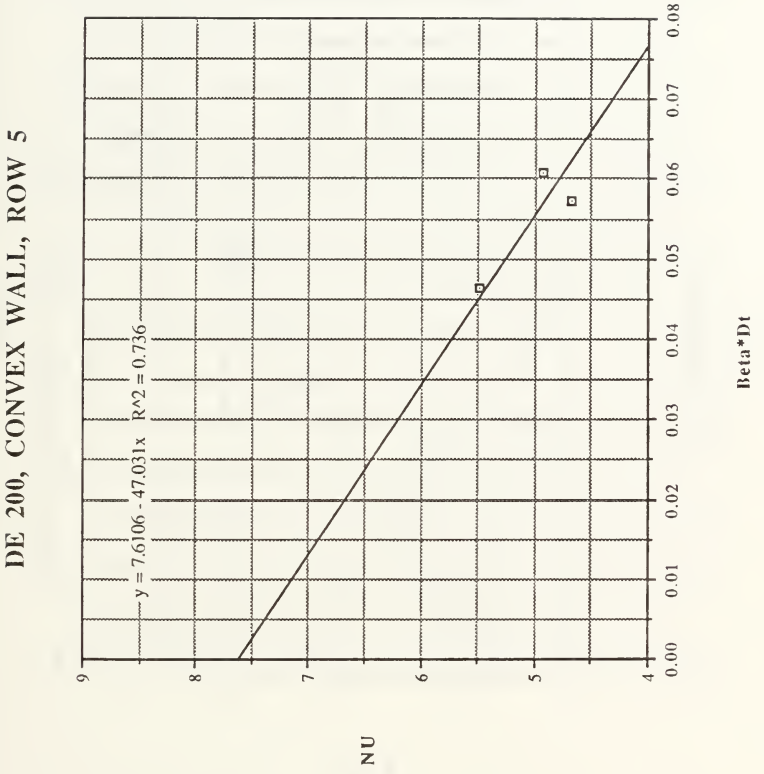

Figure 74. Nusselt Number Versus Beta * Dt for De = 200 Convex Wall

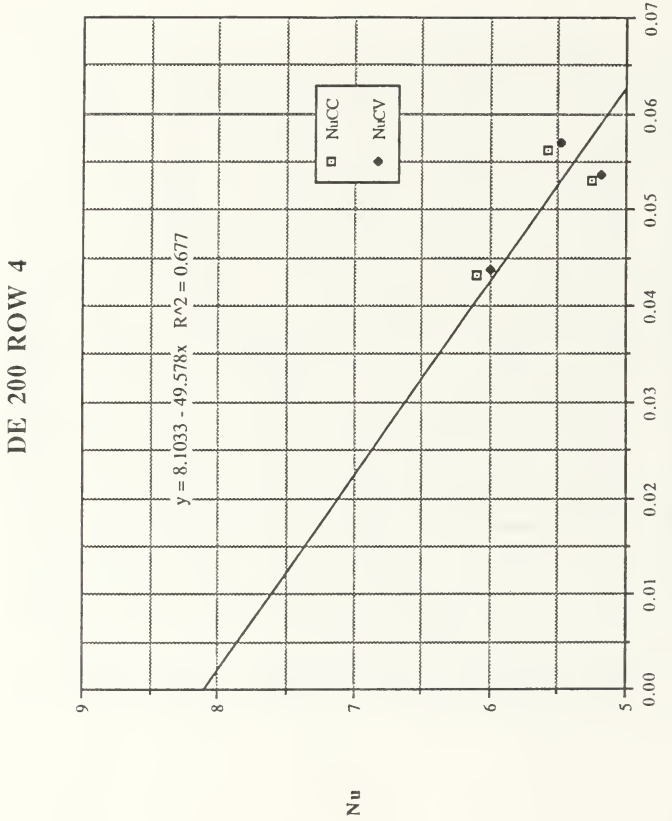

Figure 75. Nusselt Number Versus Beta * Dt for De = 200 Row 4

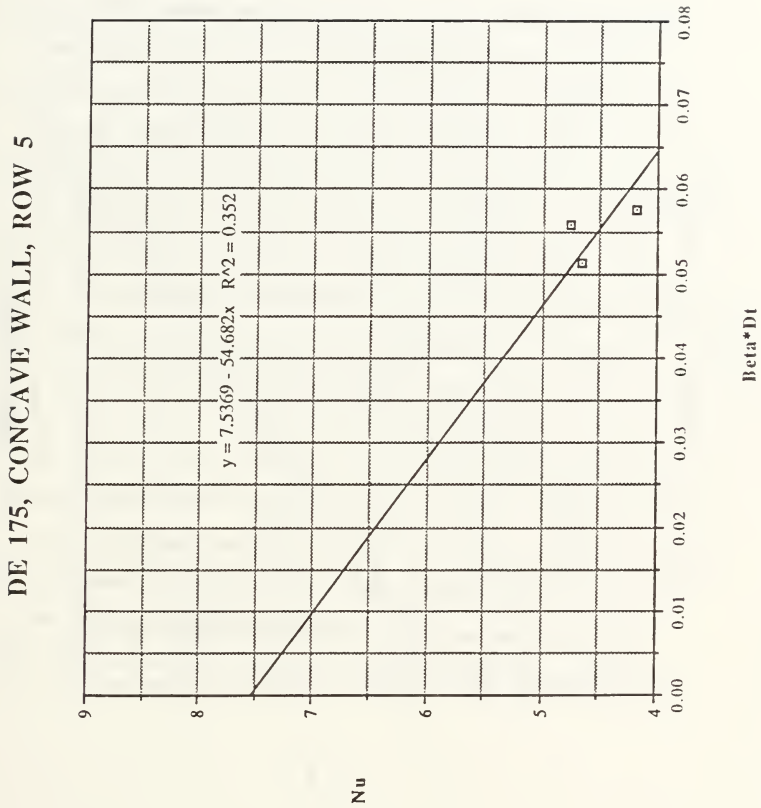

Figure 76. Nusselt Number Versus Beta * Dt for De = 175 Concave Wall

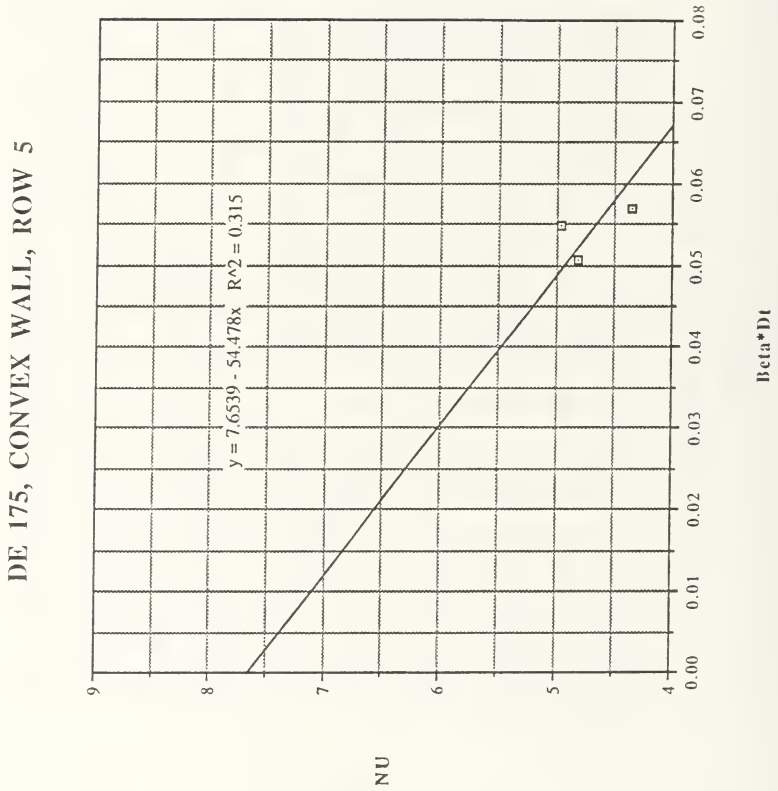

Figure 77. Nusselt Number Versus Beta * Dt for De = 175 Convex Wall

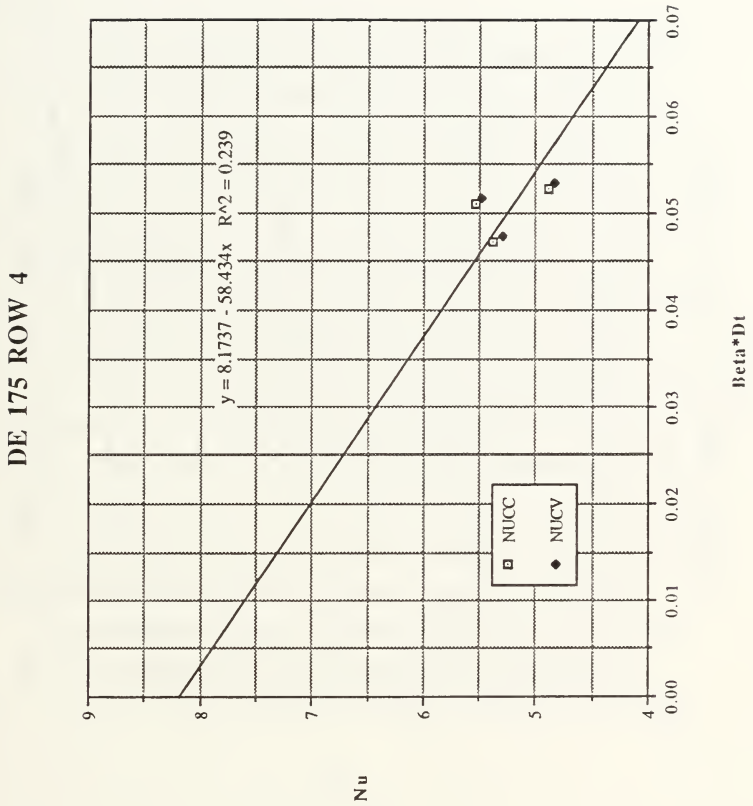

Figure 78. Nusselt Number Versus Beta * Dt for De = 175 Row 4

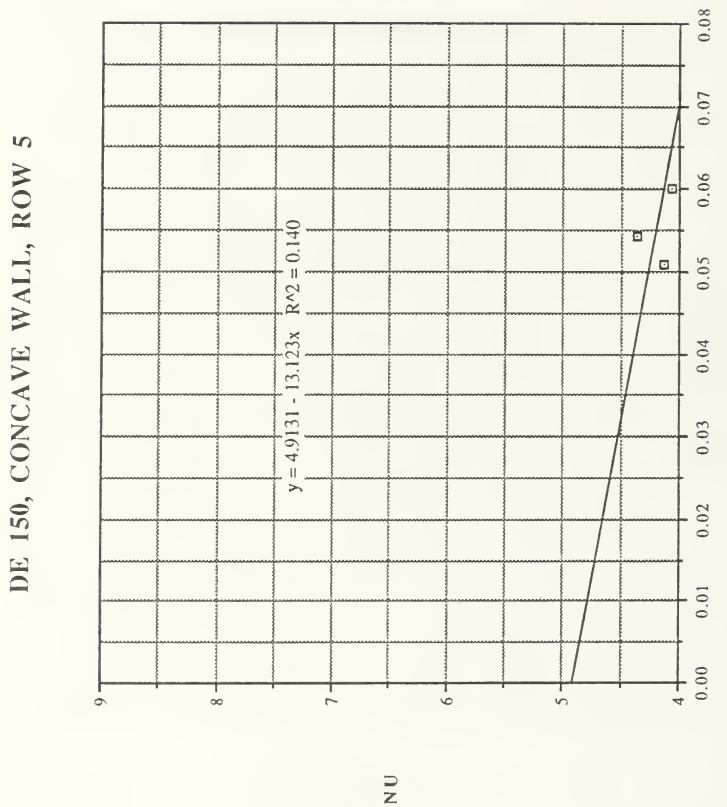

Figure 79. Nusselt Number Versus Beta * Dt for De = 150 Concave Wall

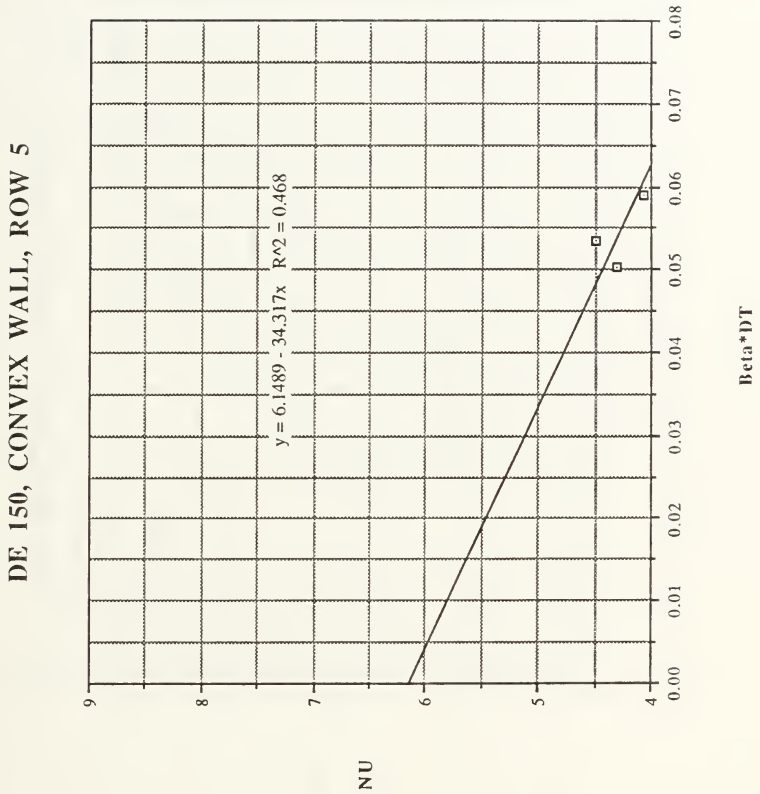

Figure 80. Nusselt Number Versus Beta * Dt for De = 150 Convex Wall

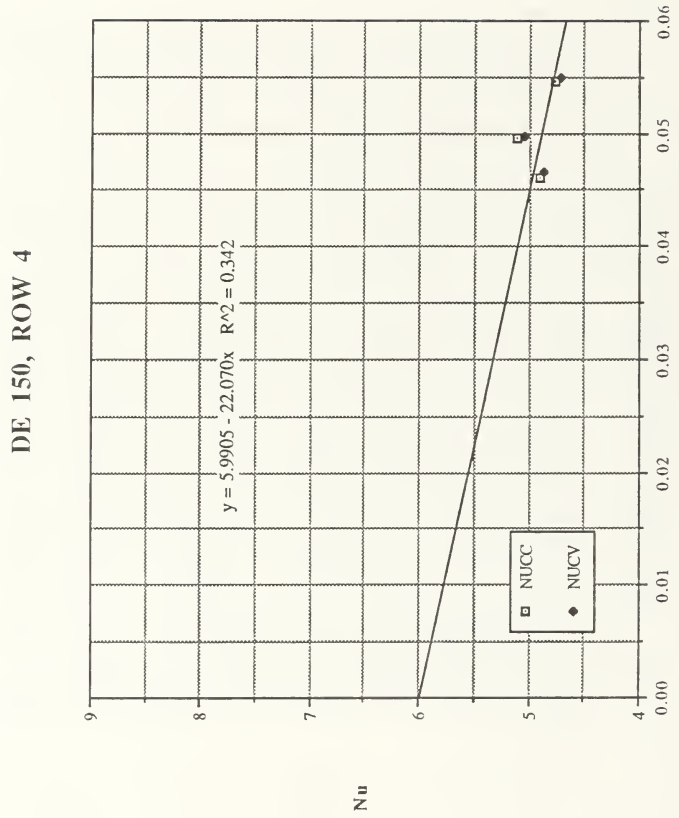

Figure 81. Nusselt Number Versus Beta * Dt for De = 150 Row 4

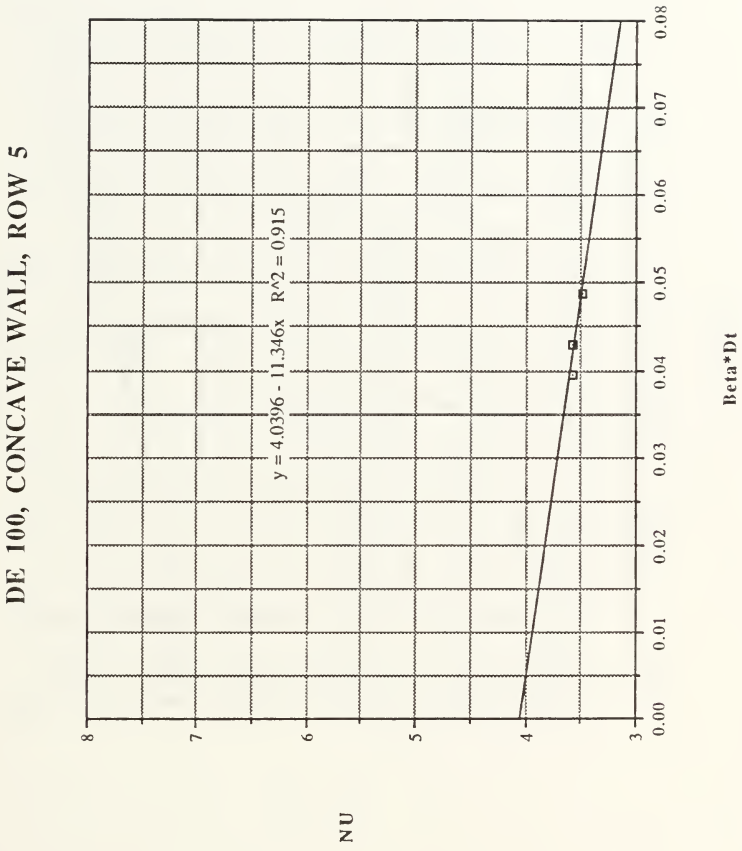

Figure 82. Nusselt Number Versus Beta * Dt for De = 100 Concave Wall

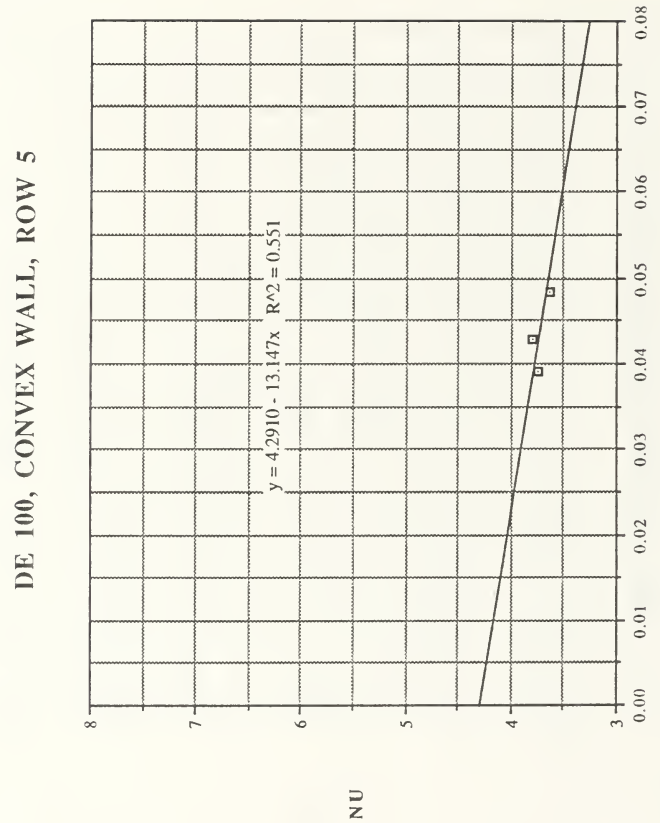

Figure 83. Nusselt Number Versus Beta * Dt for De = 100 Convex Wall

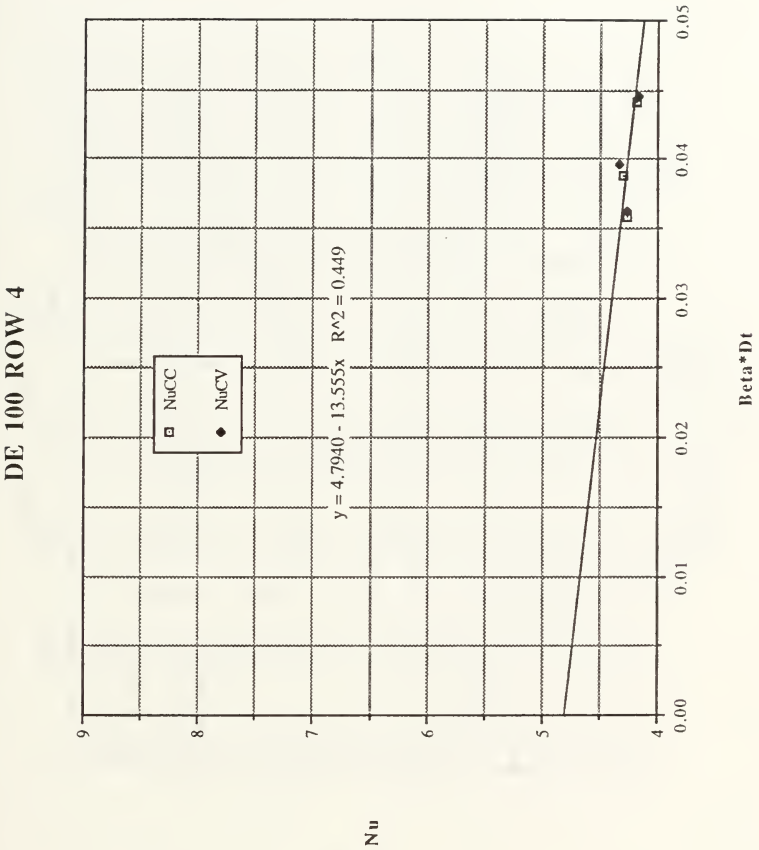

Figure 84. Nusselt Number Versus Beta * Dt for De = 100 Row 4

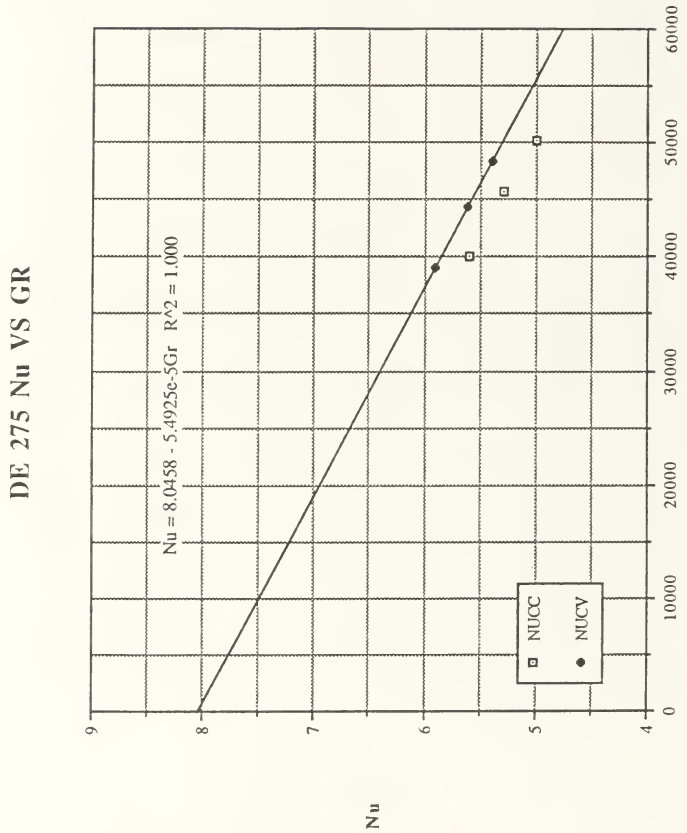

Figure 85. Nusselt Number Versus Grassoff Number for De = 275

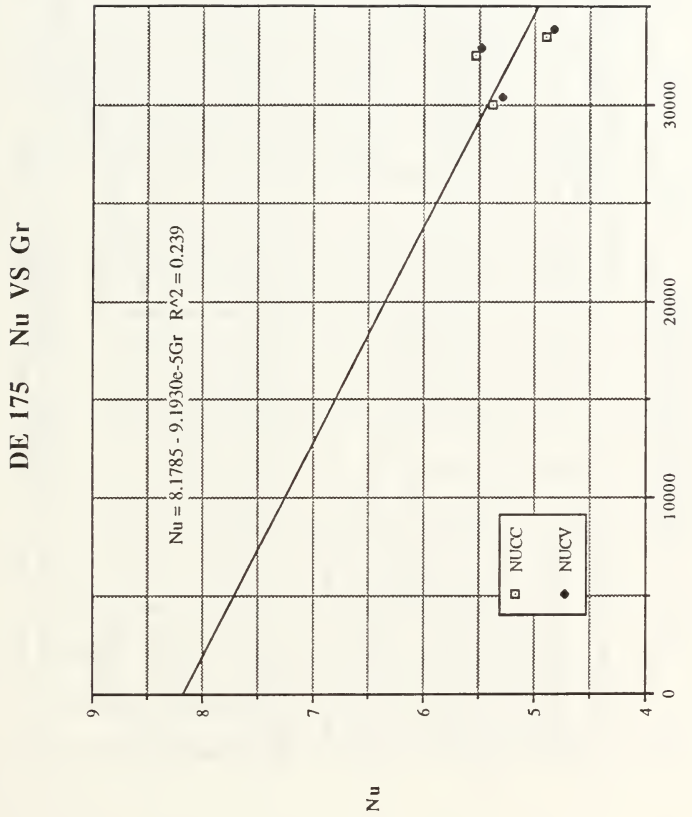

Figure 86. Nusselt Number Versus Grassoff Number for De = 175

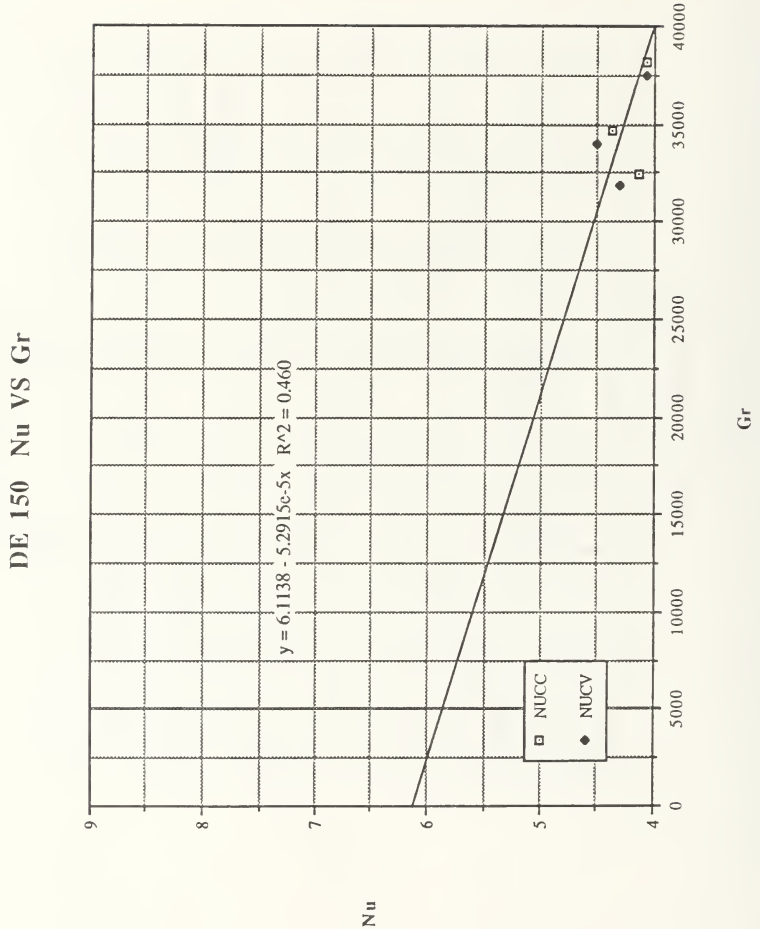

Figure 87. Nusselt Number Versus Grassoff Number for De = 150

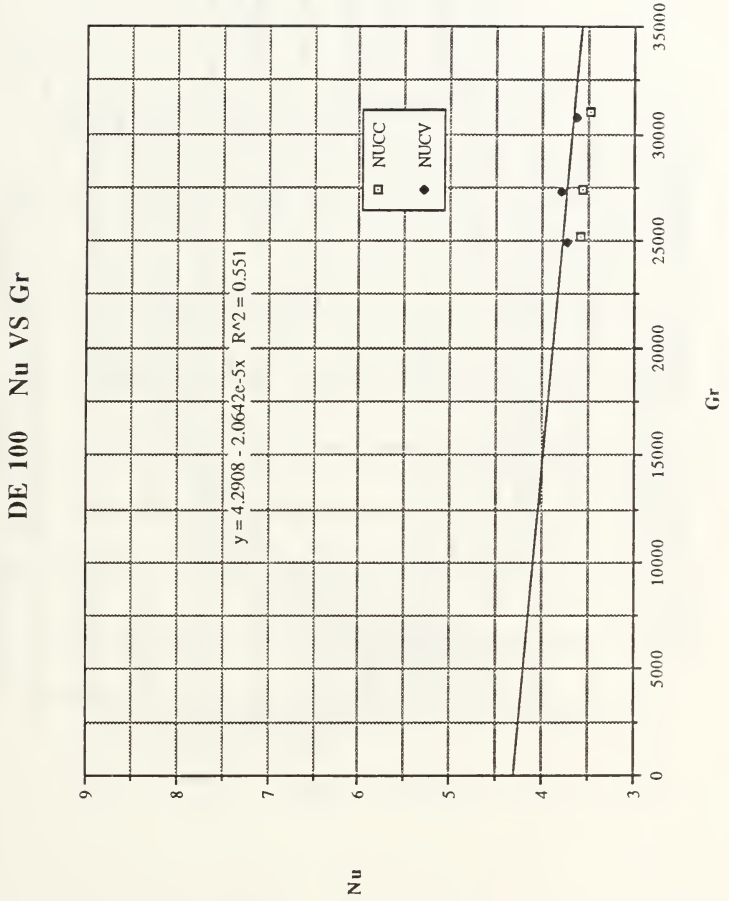

Figure 88. Nusselt Number Versus Grassoff Number for De = 100

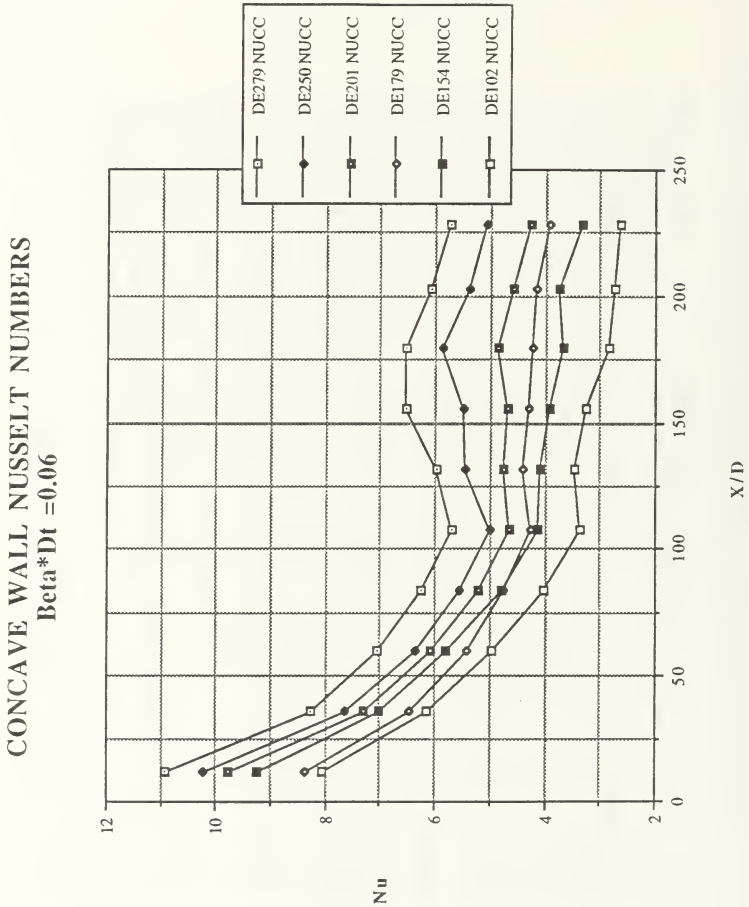

Figure 89. Concave Wall Nusselt Numbers Beta * Dt = 0.06

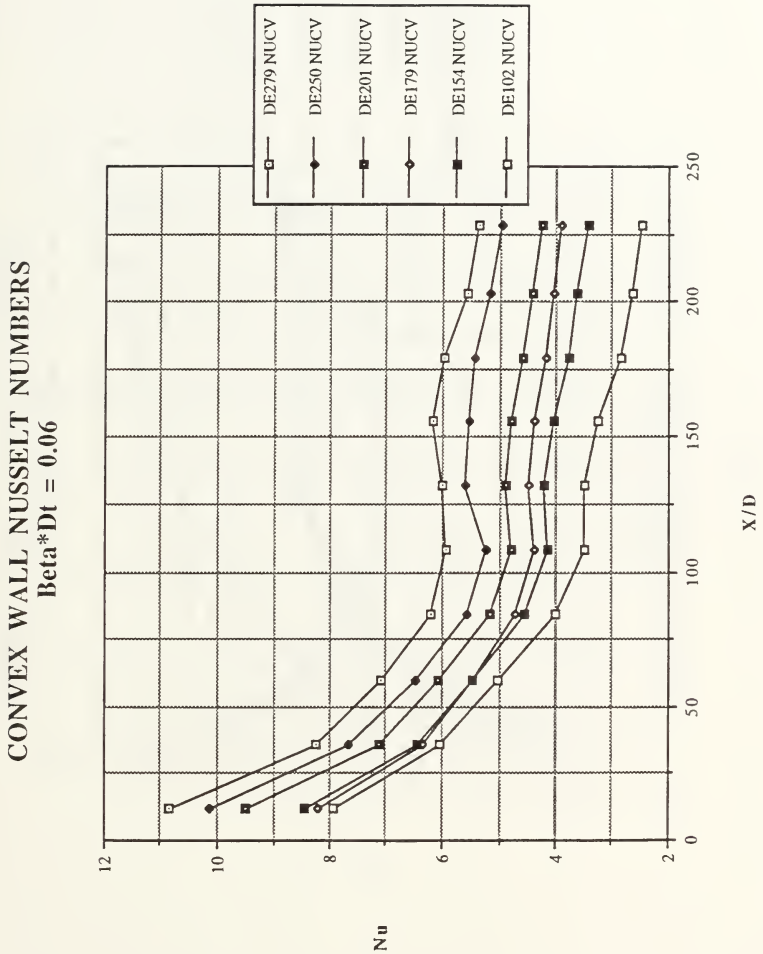

Figure 90. Convex Wall Nusselt Numbers Beta * Dt = 0.06

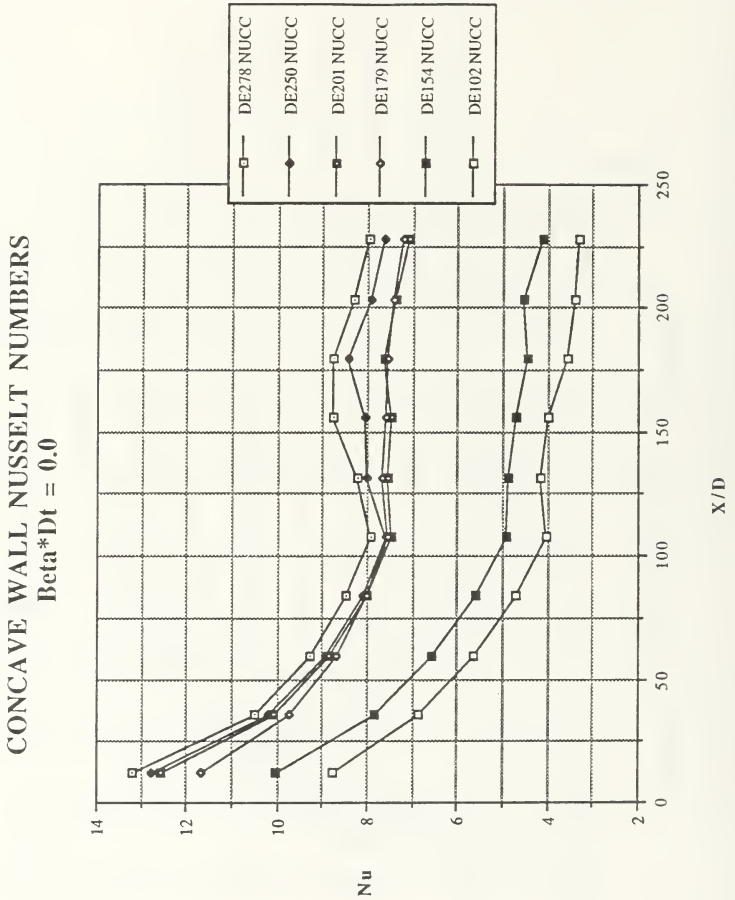

Figure 91. Concave Wall Nusselt Numbers Beta * Dt = 0.0

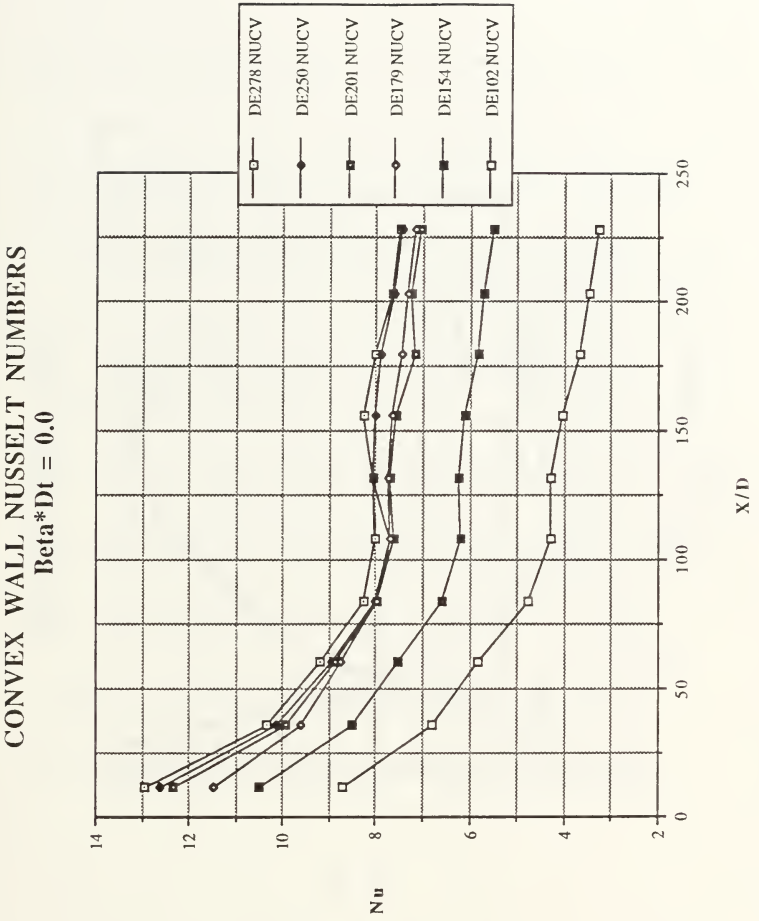

Figure 92. Convex Wall Nusselt Numbers Beta * Dt = 0.0

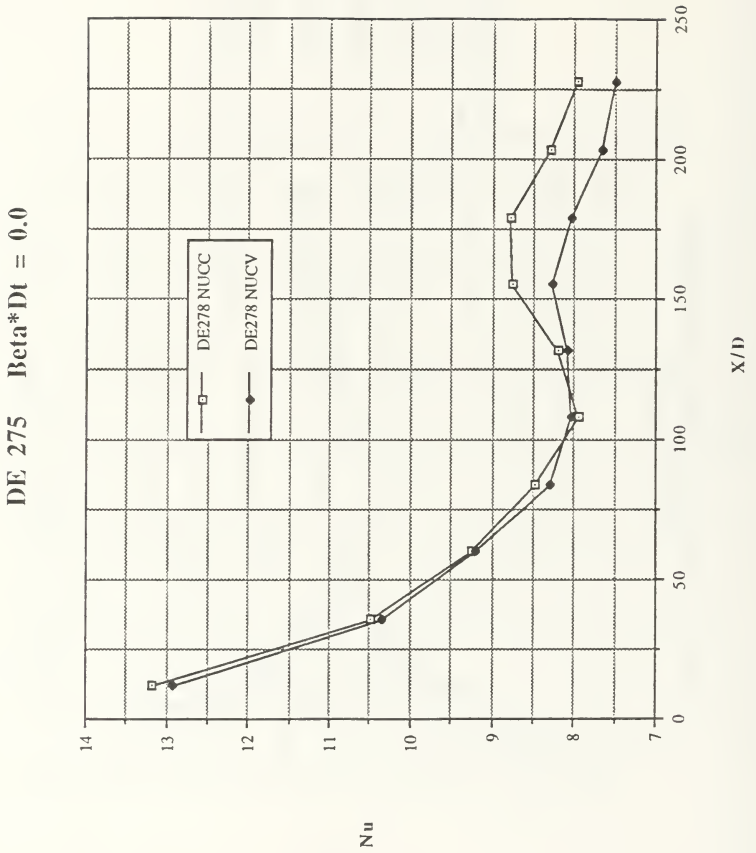

Figure 93. Nusselt Number Versus x/d for De = 275

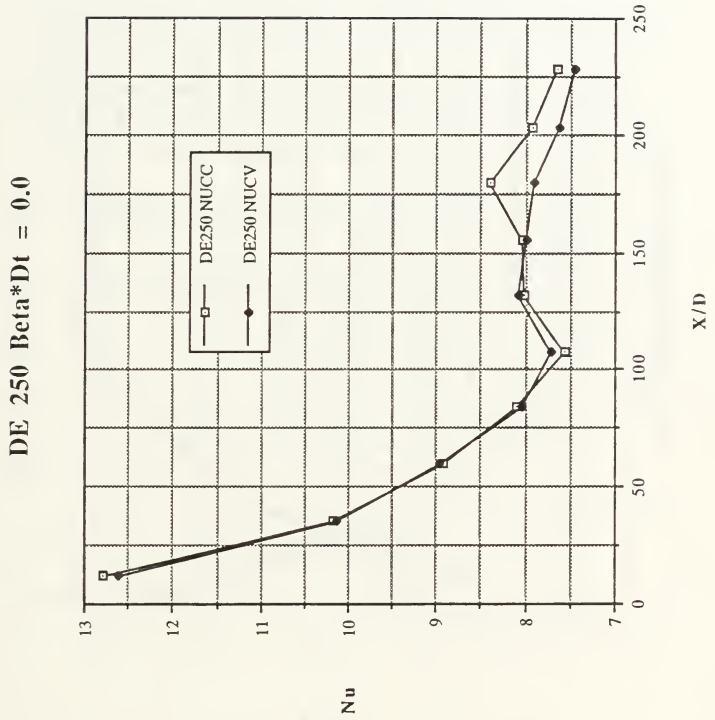

Figure 94. Nusselt Number Versus x/d for De = 250

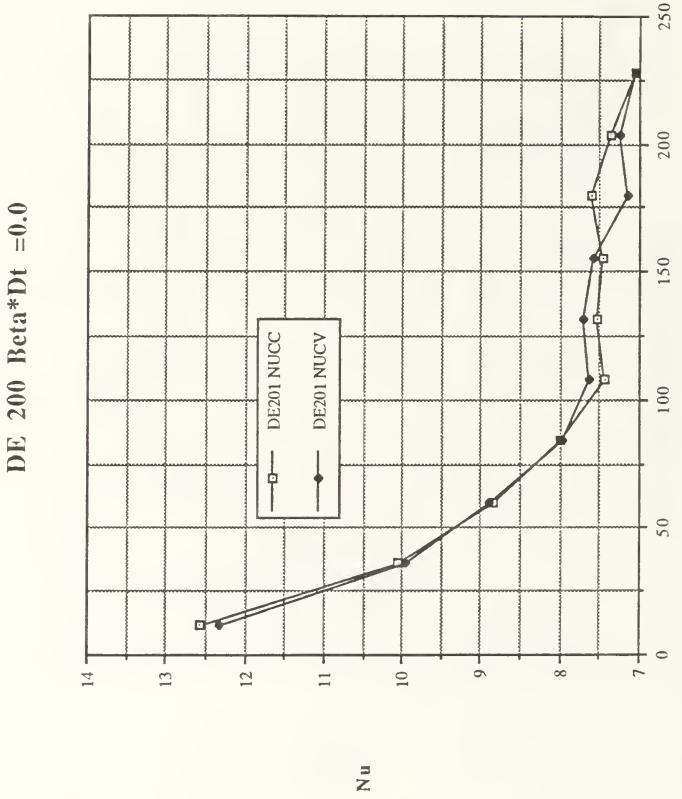

Figure 95. Nusselt Number Versus x/d for De = 200

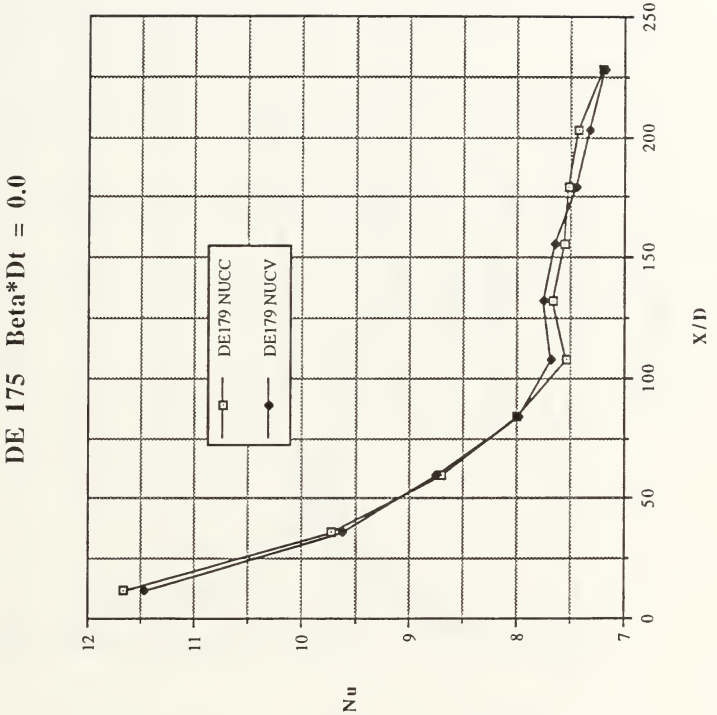

Figure 96. Nusselt Number Versus x/d for De = 175

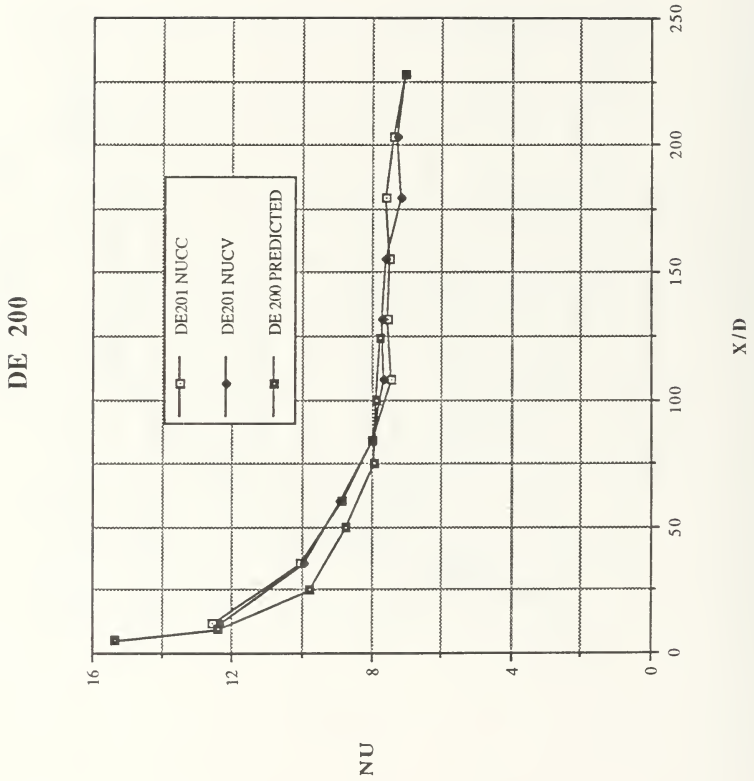

Figure 97. Predicted Nusselt Number & Measured Nusselt Number Versus x/d for De = 200

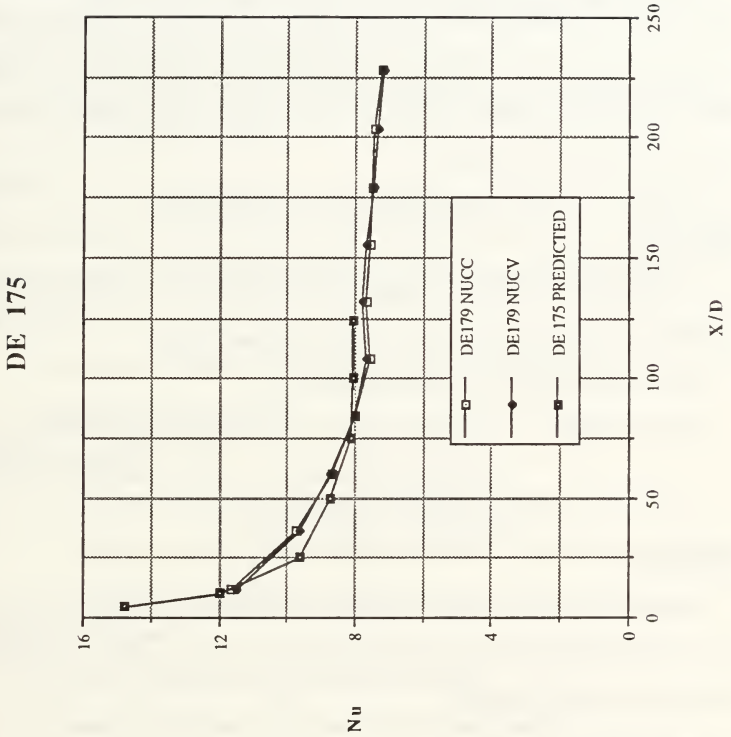

Figure 98. Predicted Nusselt Number & Measured Nusselt Number Versus x/d for De = 175

APPENDIX B
SOFTWARE DIRECTORY

This Appendix gives a listing of the various programs used in this thesis. Each program listing contains a summary of how the program is used, user inputs, program outputs and any additional features. Programs are listed in two groups; Nusselt number distributions and exit mixed-mean temperature measurement. All programs were written in BASIC 4.0 for use on the HP9836S computer.

I. NUSSELT NUMBER DISTRIBUTION PROGRAMS

TCHECK:

This program acquires multiple channel thermocouple data and performs temperature calibration equations to provide measurements in Degrees Celsius.

user inputs: thermocouple voltage readings, X

program output: provides monitor summary of thermocouple number, data acquisition channel number, voltage reading and corresponding temperature reading in Deg. C.

TEMCURV:

This program acquires multiple channel thermocouple data and creates two files to be used in other programs for the curved heating channel. Primary purpose is to supply data for Nusselt number calculations.

user inputs:

a) thermocouple voltage readings.

b) run number.

c) voltages across shunts for all four heaters, mvolts.

d) voltages across heaters, volts.

e) ambient pressure, inches of mercury.

f) pressure drop across orifice plate, inches of water.

program outputs:

a) data file, Idata, provides data required to determine heat input, conduction loss and Dean number; Runno, Amp1, Amp2, Amp3, Amp4, Vh1, Vh2, Vh3, Vh4, Pamb, Deltap, Tmi, Ro.

b) data file, Tdata, provides temperature data in Deg. C for determination of local Nusselt numbers.

NUCURV2:

This program determines heat transfer coefficients and Nusselt numbers by conducting surface energy balance. Heat flux inputs and conducted heat losses are determined.

user inputs:

a) reads data files Tdata and Idata from program TEMCURV.

b) estimated Dean number.

program outputs:

a) data file, Hdata, of heat transfer coefficients, local Nusselt numbers streamwise and spanwise locations, measured and corrected temperatures as follows; H, Nus, X2, Z, T1 and T.

additional features:

a) provides spanwise-averaged Nusselt numbers.

b) using energy balance, calculates local mean temperatures.

c) with estimated Dean number, performs iteration process to determine actual Dean number.

3DNU:

This program reads the Hdata data file created by the NUCURV2 program and plots spanwise variations of Nusselt numbers by rows for either wall of the channel.

user inputs:

a) local Nusselt numbers along with corresponding streamwise and spanwise distances (output data file, Hdata, from program NUCURV2).

b) Dean number and which wall to plot

program outputs: Nusselt number distribution contours

II. EXIT MIXED-MEAN TEMPERATURE MEASUREMENT

TEMTRAV:

Program for control of temperature traverse probe positioning and data acquisition in the curved heating channel. Interfaces with MITAS controller to control the probe position. Provides temperature difference between exit temperature and ambient inlet temperature.

user inputs:

a) estimate of Dean number

b) initial position of pressure probe.

c) number of y and z points to take data at.

d) resolution of data.

e) ambient inlet temperature channel number.

f) temperature probe channel number.

g) ambient pressure.

h) pressure drop across orifice plate.

i) delay time to start the taking data.

program outputs:

a) data file, Temp, provides position and temperature data as follows: Y, Z, temperature, inlet temperature, temperature difference.

b) provides actual Dean number through iteration process.

TMXDMPLOT:

Program to plot time averaged traverses of temperature probe measurements.

user input: a) temperature data file, TEMP (output from program TEMTRAV).

program output: temperature traverse plot

TMXDM:

Modified version of TMXDMEAN used by Skogerboe [Ref. 21] to plot traverse of mean temperature, mean velocity products. Program has been modified to determine exit mixed-mean temperature using process described in Chapter 3, Section C, part 2.

user inputs:

a) temperature data file, TEMP (output from program TEMTRAV).

b) velocity data file, VEL (output from program VELOCITY).

program output:

a) mean temperature, mean velocity traverse plot.

b) monitor output of exit mixed-mean temperature.

III. FIVE-HOLE PRESSURE PROBE PROGRAMS

ALIGN:

This program aligns the five hole pressure probe in the curved channel at zero yaw and zero pitch. It also interfaces with the MITAS controller to position the probe at the desired location and repositions the to the original position upon completion of the program.

user inputs:

a) number of samples per channel

b) number of standard deviations

c) ambient pressure

d) transducer calibration coefficients

e) original position of probe

f) desired position of probe

program output:

a) mean velocity

b) P_1, P_2, P_3, P_4, P_5

c) C_{py}, C_{pp}

additional features:

a) allows the user to realign the probe between measurement sequences

b) allows the user to calibrate transducers or input their calibration coefficients

PADJUST:

This program implements the spatial resolution correction as described by Ligrani et al. [Ref. 6].

user input:

a) distance between port 1 and the center of the other pressure ports, ylen and zlen. For the miniature five hole probe both are 0.018.

b) data file of the raw pressure data as output by the program FIVHOLE.

program output:

a) file of corrected pressure coefficients: y, z, C_{py}, C_{pp}, P, De

additional features:

a) can be used with a survey of one spanwise location, i.e., a profile.

VELOCITY1:

This program computes the three mean velocity components from the pressure data that has been corrected for spatial resolution.

user input:

a) data files of calibration coefficients and pressure data as output from program PROCAL this data file was made by Fields [Ref. 25]

b) number of yaw points

c) number of pitch points

d) data file of pressure coefficients as output by program PADJUST

e) values of y and z direction downwash velocity correction, dely and delz. In this study, a value of 0.011 is used for both dely and delz.

program output:

a) data file of pressures and velocities for each measurement location: y, z, P_t, U, U_0, U_r, U_z.

additional features:

a) can be used with a survey of one spanwise location, i.e., a profile.

VORTICITY:

This program calculates the three mean components of vorticity at each measurement location.

user input:

a) data file of velocities created by the program VELOCITY1.

program output:

a) data file of vorticity as follows: y, z, $omega_0$, $omega_r$, $omega_z$.

APPENDIX C
DATA FILE LISTING

A Summary of the data files and corresponding experimental parameters is given in two parts, the first of which involves the determination of all Nusselt number results and the second with the calculation of the measured exit mixed-mean temperature results.

A. NUSSELT NUMBER RESULTS.

The following lists of data were used for the determination of all Nusselt number data presented in this thesis. This includes both the spanwise-averaged Nusselt data and the local spanwise Nusselt number distributions.

experimental parameters:

Dean number	102	153	179	201	225	250	279
Pressure drop (in water)	.095	0.22	0.30	0.38	0.50	0.60	0.75
Heat flux/CC1 & CV1 (watts)	41.5	56.9	61.0	67.3	76.7	75.2	82.7
Heat flux/CC2 & CV2 (watts)	48.2	62.4	67.0	73.4	82.3	81.4	82.7
Max. surface temp. (TC#98, ^{O}C)	59.5	62.1	60.2	61.0	60.8	62.9	61.8

data file listings:

Data file numbers are the estimated Dean number plus the run number at that dean number. Example: The files for the third run at an estimated Dean number of 150 are all numbered 153.

B. MEASURED MIXED-MEAN TEMPERATURE RESULTS

The following list of data provides the data information used in calculating the measured exit mixed-mean temperature and the plotting of the temperature traverse contours.

experimental parameters:

Dean number	102	153	179	201	225	250	279
Pressure drop (in water)	.095	0.22	0.30	0.38	0.50	0.60	0.75
Heat flux/CC1 & CV1 (watts)	41.5	56.9	61.0	67.3	76.7	75.2	82.7
Heat flux/CC2 & CV2 (watts)	48.2	62.4	67.0	73.4	82.3	81.4	82.7
Max. surface temp. (TC#98, ^{O}C)	59.5	62.1	60.2	61.0	60.8	62.9	61.8

data file listing:

Data file numbers are the estimated Dean number plus the run number at that dean number. Example: The files for the third run at an estimated Dean number of 150 are all numbered 153.

LIST OF REFERENCES

1. Ghia, K. N., Sokhey, J. S., "Laminar Incompressible Viscous Flow in Curved Ducts of Rectangular Cross-Sections," Transactions of The ASME Journal of Fluids Engineering, pp. 640-648, December 1977.

2. Komiyama, Y., "Laminar Forced Convection Heat Transfer in Curved Channels of Rectangular Cross-Section," Transactions of The Journal of The Society of Mechanical Engineers, V. 50,1984, pp.424-434.

3. Iacovides, H., Launder, B. E., and Loizou, P. A., "Numerical Computation of Turbulent Flow Through a Square-Sectioned 90 Degree Bend," Heat and Fluid Flow, V. 8, December 1987, pp. 320-325.

4. Humphrey, J. A. C., Taylor, A. M. K., and Whitelaw, J. H., "Laminar Flow in a Square Duct of Strong Curvature," Journal of Fluid Mechanics, V. 83, 1977, pp. 509-527.

5. Ligrani, P. M. and Niver, R. D., "Flow Visualization of Dean Vortices in a Curved Channel With 40 to 1 Aspect Ratio," The Physics of Fluids, V. 31, pp. 3605-3617, 1988.

6. Ligrani, P. M., Finlay, W. H., Fields, W.A., Fuqua, S. J., and Subramanian, C. S., "Features of Way Vortices in a Curved Channel From Experimental and Numerical Studies," Physics of Fluids A, V.4, pp. 695-709, April, 1992.

7. Ligrani, P. M., Fields, W. A., and Baun, L. R., "Time-averaged Features of Dean Vortices," Submitted to Physics of Fluids A, 1992.

8. Ligrani, P. M., Longest, J. E., Kendall, M. R., and Fields, W. A., "Splitting, Merging and Spanwise Wavenumber Selection of Dean Vortex Pairs During Their Initial Development in a Curved Rectangular Channel," Submitted to Physics of Fluids A, 1992.

9. Yee, G., Chilukuri, R., and Humphrey, J. A. C., "Developing Flow and Heat Transfer in Strongly Curved Ducts of Rectangular Cross Section," Transactions of The ASME Journal of Heat Transfer, pp. 285-291, May 1980.

10. Iacovides,H., and Launder, B. E., "ASM Predictions of Turbulent Momentum and Heat Transfer in Coils and U-bends," Proc 4th International Conference On Numerical Methods In Laminar and Turbulent Flow," Swansea, 1985.

11. Mori, Y., Ucjida, Y., and Ukon, T., "Forced Convection Heat Transfer in a Curved Channel With a Square Cross Section," Journal of Heat Mass Transfer, V. 14, 1971, pp 1787-1805.

12. Johnson, R. W. and Launder, B. E., "Local Heat Transfer Behavior in Turbulent Flow Around a 180 deg Bend of Square Cross Section," The American Society of Mechanical Engineers, Presented at the 30th International Gas Turbine Conference and Exhibit, Paper No. 85-GT-68, 1985.

13. Chang, S. M., Humphrey, J. A. C., Johnson, R. W., and Launder, B. E., "Turbulent Momentum and Heat Transfer in Flow Through a 180 deg Bend of Square Cross Section," Proc. 4th Turbulent Shear Flow Symposium, University of Karlsruhe, Karlsruhe, FRG, 1983.

14. Brinch, P. F., and Graham, R. W., "Flow and Heat Transfer in a Curved Channel," National Aeronautics and Space Administration, Technical Note D-8464, May 1977.

15. Gibson, M. M., Verriopoulos, C. A., and Nagano, Y., "Measurements in the Heated Turbulent Boundary Layer on a Mildly Convex Surface," Turbulent Shear Flows, V. 3, 1982, p. 80.

16. Simon, T. J., and Moffat, R. J., "Heat Transfer Through Turbulent Boundary Layers-The Effects of Introduction and Recovery From Convex Curvature," ASME Paper No. 79-WA/GT-10, 1979.

17. Chang, S. M., Humphrey, J. A. C., and Modavi, A., "Turbulent Flow in a Strongly Curved U-Bend and Downstream Tangent of Square Cross Section," Physico-Chemical Hydrodynamics, Vol. 4, 1983, p. 243.

18. Iacovides, H., and Launder, B. E., "Prediction of Turbulent Flow and Heat Transfer in a 180 Degree Bend of Square Cross Section," Second UK National Conference On Heat Transfer, University of Strathclyde, Glasgow, 1988.

19. Cheng, K. C. and Akiyama, M., "Laminar Forced Convection Heat Transfer in Curved Rectangular Channels," Journal of Heat Mass Transfer, V. 13, 1970, pp. 471-490.

20. Chilukuri, R., and Humphrey, J. A. C., "Numerical Computation of Buoyancy Induced Recirculation in a Curved Square Duct With Laminar Flow," Journal of Heat Mass Transfer, V. 24, 1981, pp. 305-314.

21. Skogerboe, P. E., Locally and Spatially Averaged Heat Transfer Distributions in a Curved Channel With 40 to 1 Aspect Ratio For Dean Numbers From 50 to 200, Master's Thesis, Naval Postgraduate School, Monterey, CA., March 1990.

22. Hughes, R. E., Development, Qualification and Measurements in Two Curved Channels with 40 to 1 Aspect Ratio, Master's Thesis, Naval Postgraduate School, Monterey, CA., September 1989.

23. Payne, B. W., A Study of Spatially-Averaged Nusselt Number Distributions in a Curved Channel with 40 to 1 Aspect Ratio For Dean Numbers From 175 to 375, Master's Thesis, Naval Postgraduate School, Monterey, CA., September 1991.

24. Fuqua, S. J., Study of the Transition to Turbulence within a Curved Rectangular Channel with 40 to 1 Aspect Ratio, Master's Thesis, Naval Postgraduate School, Monterey, CA., September 1991.

25. Fields, W. A., Study of the Effects of Centrifugal Instabilities on Flow in a 40 to 1 Aspect Ratio Rectangular Curved Channel, For Dean Numbers from 35 to Fully Turbulent Conditions, Master's Thesis, Naval Postgraduate School, Monterey, CA., December 1990.

26. Kendall, M. R., Effects of Centrifugal Instabilities on Laminar/Turbulent Transition in Curved Channels with 40 to 1 Aspect Ratios, Master's Thesis, Naval Postgraduate School, Monterey, CA., June 1991.

27. Baun, L. R., The Development and Structural Characteristics of Dean Vortices in a Curved Rectangular Channel, Master's and Engineer's Thesis, Naval Postgraduate School, Monterey, CA., September 1988.

28. Longest, J. M., Flow Visualization Studies in (1) a Curved Rectangular Channel With 40 to 1 Aspect Ratio and (2) a Straight Channel With Bulk Flow Unsteadiness, Master's Thesis, Naval Postgraduate School, Monterey, CA., June 1989.

29. Niver, R. D., Structural Characteristics of Dean Vortices in a Curved Channel, Master's Thesis, Naval Postgraduate School, Monterey, CA., June 1987.

30. Incropera, F. P., and De Witt, D. P., Introduction to Heat Transfer, Second Edition, pp. 429-434, John Wiley & Sons, 1990.

31. Schwartz, G. E., Control of Embedded Vortices Using Wall Jets, Master's Thesis, Naval Postgraduate School, Monterey, CA., September 1988.

32. ASME Power Test Committee, ASME Power Test Codes.(Supplement on Instruments and Apparatus), part 5, Chapter 4, p. 25, American Society of Mechanical Engineers, 1959.

33. Bella, D. W., Flow Visualization of Time-Varying Structural Characteristics of Dean Vortices in a Curved Channel, Master's Thesis, Naval Postgraduate School, Monterey, CA., September 1988.

34. Kays, W. M. and Crawford, M. E., Convective Heat and Mass Transfer, Second Edition, p. 103, McGraw-Hill Book Company, 1980.

INITIAL DISTRIBUTION LIST

		No. Copies
1.	Library, Code 052 Naval Postgraduate School Monterey, CA 93943-5002	2
2.	Professor Phillip M. Ligrani Code ME/Li Department of Mechanical Engineering Naval Postgraduate School Monterey, CA 93943-5000	4
3.	Department Chairman, Code ME Department of Mechanical Engineering Naval Postgraduate School Monterey, CA 93943-5004	1
4.	Lt Anthony R Schallert 6760 Princevalle St Gilroy, CA 95020	1
5.	Naval Engineering Curricular Officer, Code 34 Department of Mechanical Engineering Naval Postgraduate School Monterey, CA 93943-5004	1
6.	Dr. K. Civinskas Propulsion Systems Division Deputy Branch Chief Turbomachinery Technology Branch M.S. 77-6 U.S. Army Aviation Res. and Technology Activity AVSCOM NASA-Lewis Research Center Cleveland, OH 45433	4

Thesis
S24764 Schallert
c.1 A study of Nusselt
number distributions
in a curved channel.